5. SITE 626: STRAITS OF FLORIDA[1]

Shipboard Scientific Party[2]

HOLE 626A

Date occupied: 31 January 1985, 2205 EST (beacon drop)

Date departed: 1 February 1985, 2230 EST (cleared mud line)

Time on hole: 1 day, 25 min

Position: 25°36.00-08′N, 79°32.81′W

Water depth (sea level; corrected m, echo-sounding): 846.8

Water depth (rig floor; corrected m, echo-sounding): 857.3

Bottom felt (m, drill pipe): 858.5

Total depth (m): 871.3

Penetration (m): 12.8

Number of cores: 2

Total length of cored section (m): 11.40

Total core recovered (m): 5.01

Core recovery (%): 44

Oldest sediment cored:
Depth sub-bottom (m): 11.40
Nature: lime sand and rubble
Age: Pleistocene

HOLE 626B

Date occupied: 1 February 1985, 2230 EST (cleared mud line at A)

Date departed: 3 February 1985, 0715 EST

Time on hole: 1 day, 8 hr, 45 min

Position: 25°36.04′N, 79°32.81′W

Water depth (sea level; corrected m, echo-sounding): 848.0

Water depth (rig floor; corrected m, echo-sounding): 858.50

Bottom felt (m, drill pipe): 858.50

Total depth (m): 1044.04

Penetration (m): 185.5

Number of cores: 5

Total length of cored section (m): 47.5

Total core recovered (m): 13.96

Core recovery (%): 29.4

Oldest sediment cored:
Depth sub-bottom (m): 185.5
Nature: unlithified grainstone and packstone
Age: early Miocene

HOLE 626C

Date occupied: 3 February 1985, 0715 EST

Date departed: 4 February 1985, 2300 EST

Time on hole: 1 day, 15 hr, 45 min

Position: 25°36.02′N, 79°32.80′W

Water depth (sea level; corrected m, echo-sounding): 843.5

Water depth (rig floor; corrected m, echo-sounding): 854

Bottom felt (m, drill pipe): 855

Total depth (m): 1034.3

Penetration (m): 179.3

Number of cores: 19

Total length of cored section (m): 179.3

Total core recovered (m): 66.3

Core recovery (%): 37

Oldest sediment cored:
Depth sub-bottom (m): 179.3
Nature: sandy carbonate ooze
Age: earliest middle Miocene

HOLE 626D

Date occupied: 4 February 1985, 2300 EST

Date departed: 9 February 1985, 0800 EST

Time on hole: 4 days, 9 hr

Position: 25°36.02′N, 79°32.81′W

Water depth (sea level; corrected m, echo-sounding): 843.5

---

[1] Austin, J. A., Jr., Schlager, W., Palmer, A. A., et al., 1986. *Proc. Init. Repts. (Pt. A), ODP*, 101.

[2] James A. Austin Jr. (Co-Chief Scientist), Institute for Geophysics, University of Texas at Austin, Austin, TX 78751; Wolfgang Schlager (Co-Chief Scientist), Rosenstiel School of Marine and Atmospheric Sciences, Miami, FL 33149 (current address: Vrije Universiteit, Instituut v. Aardwetenschappen, Postbus 7161, 1007 MC Amsterdam, Netherlands); Amanda A. Palmer, Staff Scientist, Ocean Drilling Program, Texas A&M University, College Station, TX 77843; Paul A. Comet, The University, Newcastle-Upon-Tyne, Newcastle, United Kingdom (current address: Core Labs Singapore, 24A-Lim Teck Boo Rd., Singapore 1953); André Droxler, Rosenstiel School of Marine and Atmospheric Sciences, Miami, FL 33149 (current address: Department of Geology, University of South Carolina, Columbia, SC 29208); Gregor Eberli, Geologisches Institut, ETH-Zentrum, Zürich, Switzerland (current address: Fisher Island Station, University of Miami, Miami, FL 33139); Eric Fourcade, Laboratoire de Stratigraphie, Université Pierre et Marie Curie, 4 Place Jussieu 75230, Paris Cedex 05, France; Raymond Freeman-Lynde, Department of Geology, University of Georgia, Athens, GA 30602; Craig S. Fulthorpe, Department of Geological Sciences, Northwestern University, Evanston, IL 60201; Gill Harwood, Department of Geology, The University, Newcastle-Upon-Tyne, NE1 7RU United Kingdom; Gerhard Kuhn, Geologisches Institut Göttingen, Federal Republic of Germany (current address: Alfred Wegener Institut für Polarforschung, Columbus Center, D-2850 Bremerhaven, West Germany); Dawn Lavoie, NORDA Code 363, Seafloor Geosciences Division, NSTL, MS 39529; Mark Leckie, Woods Hole Oceanographic Institution, Woods Hole, MA 02543 (current address: Department of Geology and Geography, University of Massachusetts, Amherst, MA 01003); Allan J. Melillo, Department of Geological Sciences, Rutgers University, New Brunswick, NJ 08903 (current address: Chevron U.S.A., New Orleans, LA 70114); Arthur Moore, Marathon Oil Company, P.O. Box 269, Littleton, CO 80160; Henry T. Mullins, Department of Geology, Syracuse University, Syracuse, NY 13210; Christian Ravenne, Institut Français du Pétrole, B.P. 311, 92506 Rueil Malmaison Cedex, France; William W. Sager, Department of Oceanography, Texas A&M University, College Station, TX 77843; Peter Swart, Fisher Island Station, University of Miami, Miami, FL 33139 (current address: Marine Geology and Geophysics, Rosenstiel School of Marine and Atmospheric Sciences, Miami, FL 33149); Joost W. Verbeek, Dutch Geological Survey, P.O. Box 157, 2000 A.D. Haarlem, Netherlands; David K. Watkins, Department of Geology, University of Nebraska, Lincoln, NE 68588; Colin Williams, Borehole Research Group, Lamont-Doherty Geological Observatory, Palisades, NY 10964.

Water depth (rig floor; corrected m, echo-sounding): 854.0

Bottom felt (m, drill pipe): 854

Total depth (m): 1310.3

Penetration (m): 456.3

Number of cores: 28

Total length of cored section (m): 276.9

Total core recovered (m): 9.36

Core recovery (%): 3.4

Oldest sediment cored:
Depth sub-bottom (m): 446.8
Nature: limestone
Age: undated
Measured velocity (km/s): 5, Hamilton Frame

Principal results: The *JOIDES Resolution* occupied Site 626 (BAH-1-C) in the Straits of Florida from 31 January to 9 February 1985. Four holes were drilled, of which Holes 626C and 626D were scientifically important. Both are located at 25°36.02′N, 79°32.80.5′W, water depth 854 m. Hole 626C was continuously cored with hydraulic-piston-core/extended-core-barrel (HPC/XCB) techniques from 0 to 179 m sub-bottom with 37% recovery. Hole 626D was washed to 179 m sub-bottom and continuously rotary cored from 179 to 456 m sub-bottom; recovery was 3.4%. Quicksands in both holes were responsible for the low recovery and for the loss of Hole 626D.

Together, Holes 626C and 626D penetrated the following sequence: (1) 0–122 m sub-bottom; carbonate contourite sand (planktonic-foraminifer and neritic material), middle Miocene to Pleistocene in age; (2) 122-170 m sub-bottom; debris flows and turbidites, middle Miocene in age; and (3) 170–447 m sub-bottom; carbonate sand and calcarenitic limestone (all contourites), late Oligocene to middle Miocene in age.

Even though we did not reach the Cretaceous target, the site produced some significant results:

1. Several hundred meters of winnowed sand indicate that the Gulf Stream has changed little in vigor and position since the Oligocene. Throughout this time interval the Gulf Stream was able to winnow almost completely the carbonate mud and rework the turbidites with neritic material.
2. Middle Miocene debris flows and turbidites are coeval with similar deposits in the Blake Basin (DSDP Sites 391 and 534), suggesting a common tectonic or environmental trigger.
3. Diagenesis in the carbonate deposits is less advanced than in coeval deep-sea carbonates. This surprising trend remains currently unexplained.
4. Borehole stratigraphy provides adequate ties with seismic reflectors of the site surveys.
5. Comparison of Site 626 with the Great Isaac 1 well on Great Bahama Bank provides strong arguments in favor of the "megabank" hypothesis, which proposes that Florida and the Bahama Banks formed one large, unsegmented platform until mid-Cretaceous time. Oligocene–Miocene facies in the two wells are similar, and time lines between them nearly horizontal. The present relief between the two areas apparently developed during the late Miocene–Pliocene, when the margin of Great Bahama Bank prograded westward to its current position. Mid-Miocene and older rocks at Sites 626 and Great Isaac seem to be connected without significant vertical offset. Therefore, by inference, the untested target reflector at Site 626 corresponds to the top of mid-Cretaceous platform carbonates drilled at Great Isaac.

BACKGROUND AND OBJECTIVES

Background

Operations at Site 626 represented the first attempt to drill on the Bahama Platform since 1971. Until Leg 101, only five other deep stratigraphic tests had ever been conducted. Of these, four were efforts by the oil industry: Andros 1, to a total depth of 4446 m, by Chevron-Gulf in 1947; Cay Sal IV-1, 5763 m, by Chevron-Gulf in 1959; Long Island 1, 5351 m, by Chevron-Gulf in 1970; and Great Isaac 1, 5440 m, by Chevron in 1971 (Paulus, 1972; Tator and Hatfield, 1975). Only the Great Isaac 1 well penetrated beneath the carbonate section to sample Upper Triassic(?) volcaniclastics. All of the others bottomed in Upper Jurassic–Lower Cretaceous carbonates or anhydrite. The fifth borehole is Deep Sea Drilling Project (DSDP) Site 98 near the axis of the Northeast Providence Channel. In 1970, DSDP Site 98 sampled approximately 350 m of a deep-water-carbonate section before terminating in calciturbidites of early Campanian age (Hollister, Ewing, et al., 1972).

Bahamian stratigraphy has been further developed by means of dredging and submersible sampling, but these efforts have been confined primarily to the precipitous Bahama Escarpment, which forms the northeastern limit of the carbonate province and its modern boundary with the western North Atlantic Basin. Examples of these studies are the detailed section of Lower Cretaceous–Cenomanian platform carbonates overlain by Maestrichtian and middle Eocene pelagic limestones measured by the *DSRV Alvin* north of Cat Island (Freeman-Lynde et al., 1981), and the detailed correlation of dredged Valanginian–Cenomanian deep-water chalks and limestones with a crossing multichannel seismic-reflection line in the Samana Reentrant of the Bahama Platform south of San Salvador (Schlager, Austin, et al., 1984).

Apart from the nature of the basement, the most intriguing question in Bahamian geology is the origin of the present pattern of banks and basins. Some viewed these features as extremely long-lived and rooted in the structure (Talwani et al., 1960; Mullins and Lynts, 1977) or topography (Hess *in* Talwani et al., 1960) of the Triassic–Lias rift system of this continental margin. Others proposed that banks and basins formed much later on top of a large carbonate bank that stretched from the eastern Bahamas to the Gulf of Mexico and northern Cuba (Paulus, 1972; Meyerhoff and Hatten, 1974; Sheridan, 1974; Schlager and Ginsburg, 1981; Sheridan et al., 1981).

Two predominant hypotheses have emerged as a result of these studies (Fig. 1). The *graben hypothesis*, as advanced by Mullins and Lynts (1977), postulates that the present topographic configuration of the Bahamas reflects underlying horsts and grabens developed during the separation of Africa and North America in the Late Triassic–Early Jurassic. These authors used their concept to explain both the apparent overlap of the Bahamas with Africa in plate reconstructions of the North Atlantic and the arkosic "graben-fill" recovered at the bottom of the Great Isaac 1 well. The broad implication of the graben hypothesis is that deep-water-carbonate facies should consistently characterize the stratigraphic successions beneath troughs, while shallower water facies persist beneath the intervening banks. While available well control on the banks supports the notion that the present bank-trough configuration has been generally stable since the Late Cretaceous (Schlager and Ginsburg, 1981), the Great Isaac 1 well indicates tens of kilometers of progradation of the northwestern part of Great Bahama Bank since the Miocene (see "Summary and Conclusions," this chapter). This suggests migration of bank edges over time regardless of the nature of underlying crustal structure.

The *megabank hypothesis* proposes shallow roots for the bank–basin pattern. Sheridan et al. (1981) used multifold seismic-reflection profiles and sonobuoys to identify a pronounced discontinuity in compressional wave velocity (from 4.2 to 5.2 km/s) beneath the Straits of Florida and the Northwest Providence Channel (Fig. 2). By extrapolation of well control both in Florida and on the Great Bahama Bank, Sheridan and his coauthors correlated this acoustic horizon with the boundary between Aptian–Albian shallow-water limestones and Cenomanian and younger pelagic–hemipelagic carbonates, suggesting a mid-Cretaceous drowning of a larger, previously homogeneous car-

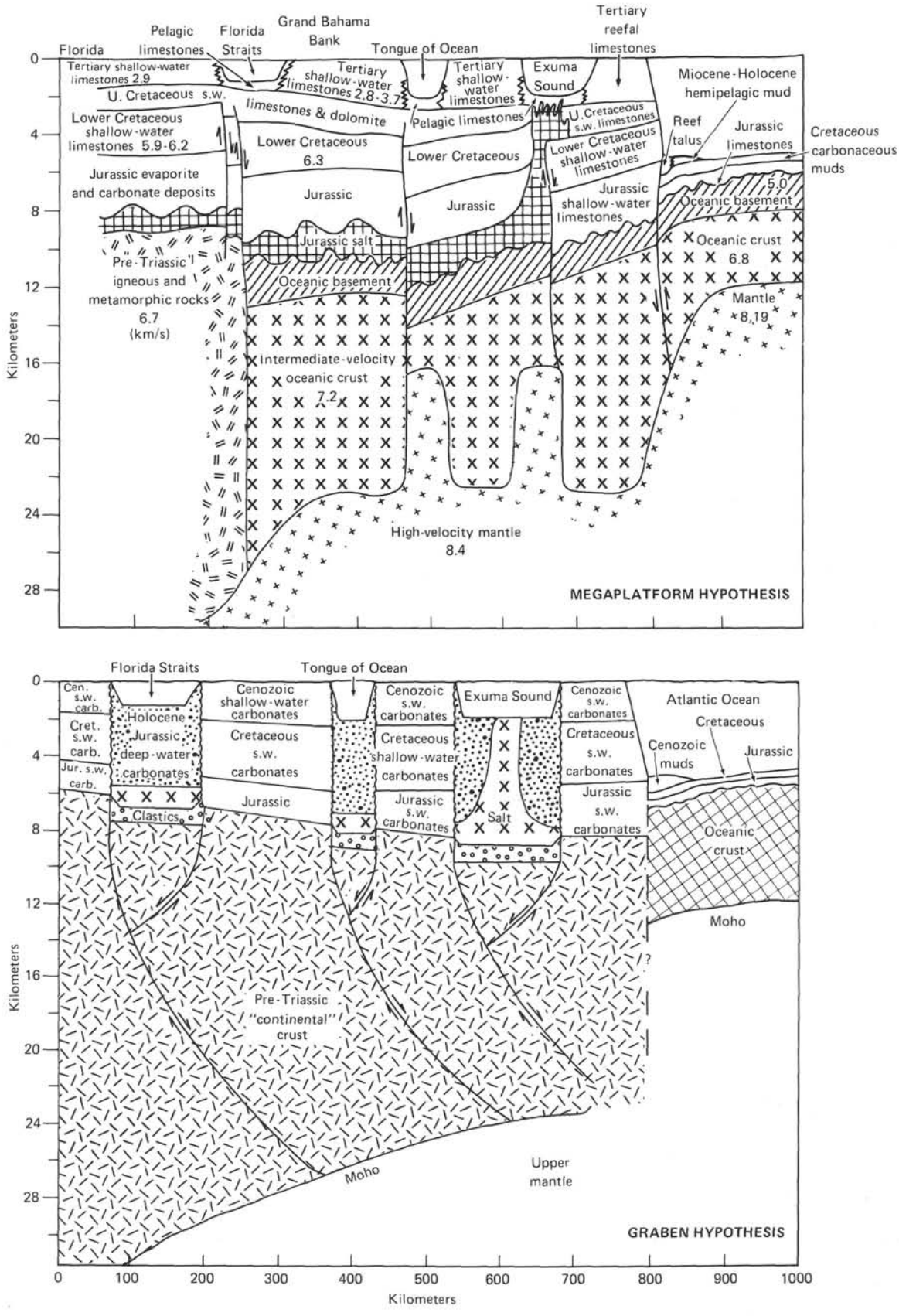

Figure 1. The two currently favored hypotheses concerning the origin and evolution of the Bahamas (after Sheridan et al., 1981; Mullins and Lynts, 1977).

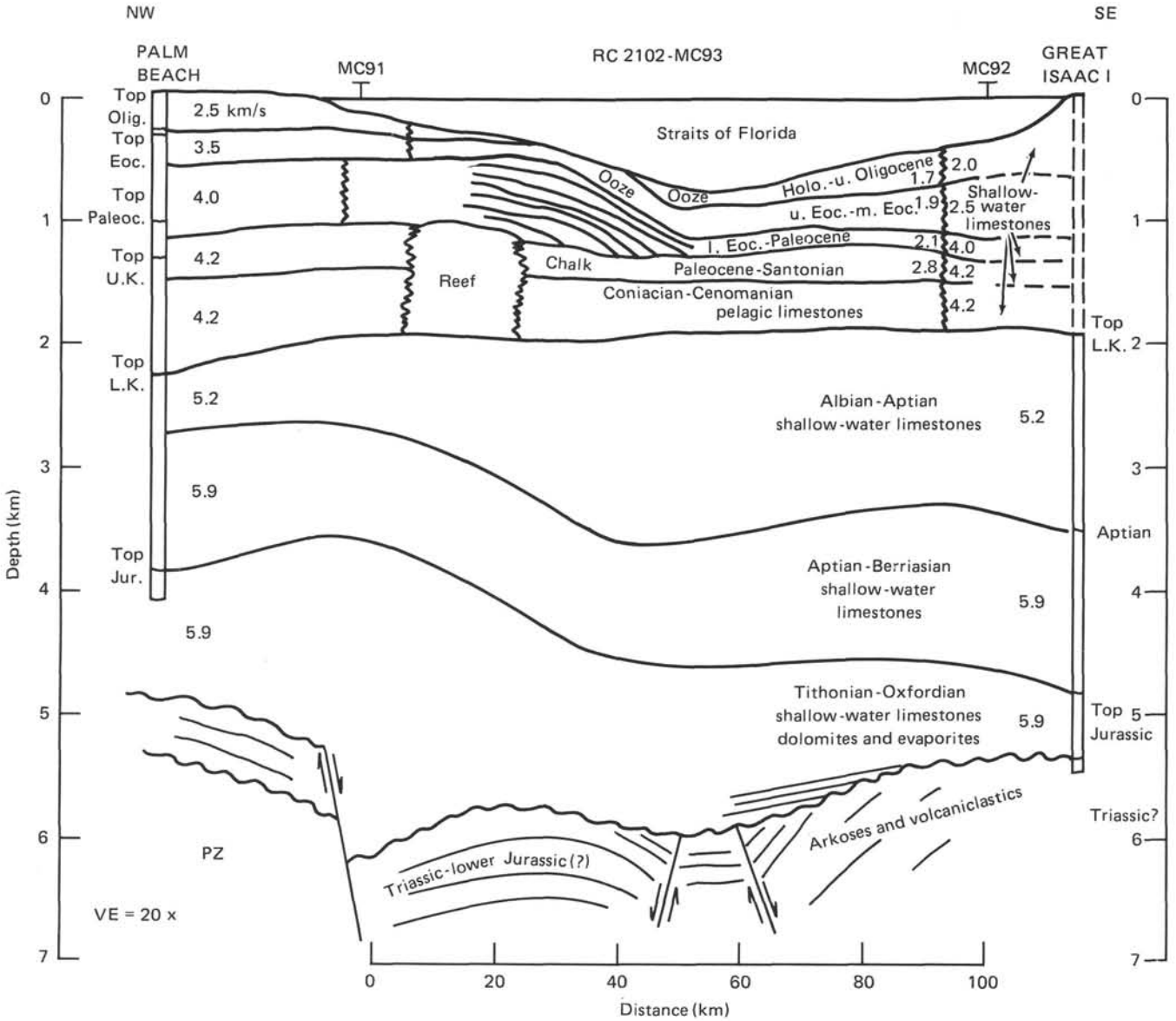

Figure 2. Seismic line RC2102-MC93 in the Straits of Florida from Sheridan et al. (1981), illustrating the acoustic horizon interpreted as the boundary between Aptian–Albian shallow-water limestones and Cenomanian and younger pelagic–hemipelagic carbonates.

bonate platform or "megabank." Using stratigraphic evidence from both the Bahamas and Cuba, Meyerhoff and Hatten (1974) and Schlager and Ginsburg (1981) also concluded that partial drowning of an Early Cretaceous megabank was responsible for the present pattern of Bahamian platforms and troughs.

In contrast to the graben hypothesis, the megabank hypothesis predicts that platform facies should underlie both highs and lows below the unconformity created by the drowning event(s). At the same time, this second hypothesis relates initiation of modern Bahamian relief to a global crisis of carbonate platforms in the mid-Cretaceous. The postulated timing also correlates neatly with a major seismic unconformity in the deep Gulf of Mexico termed the mid-Cretaceous unconformity (MCU) by Buffler et al. (1981). The MCU signals a major stratigraphic turning point that coincides with the drowning of carbonate platforms rimming the Gulf (Schlager et al., 1984). The MCU was interpreted by Buffler (1984) as a response to a rapid fall in Cenomanian sea level (the postulated 98 Ma lowstand of Vail et al., 1977), with consequent erosion, followed by a sea-level rise and associated initiation of deep-water clastic deposition. It remains undetermined whether the sequence boundary is shaped primarily by erosion during a lowstand of sea level or by platform drowning and backstepping during a sea-level rise.

In an attempt to provide additional seismic data needed for three-dimensional structural control prior to drilling, both regional and site-specific geophysical surveys were conducted in several areas of the Bahamas by a consortium of universities led by the University of Texas Institute for Geophysics. High-resolution, 12-fold water-gun reflection and sonobuoy refraction profiles were collected. The survey in the Straits of Florida consisted of a 250-nautical-mile (n. mi) grid (see "Operations Summary," this chapter). These profiles were processed and interpreted in the manner of Vail et al. (1977), and both the pronounced velocity discontinuity of Sheridan et al. (1981) and a number of younger seismic-sequence boundaries were identified and mapped (Fig. 3).

Site 626 (BAH-1-C) lies approximately 61 km east-southeast of Miami, Florida, and 28 km west-southwest of the island of

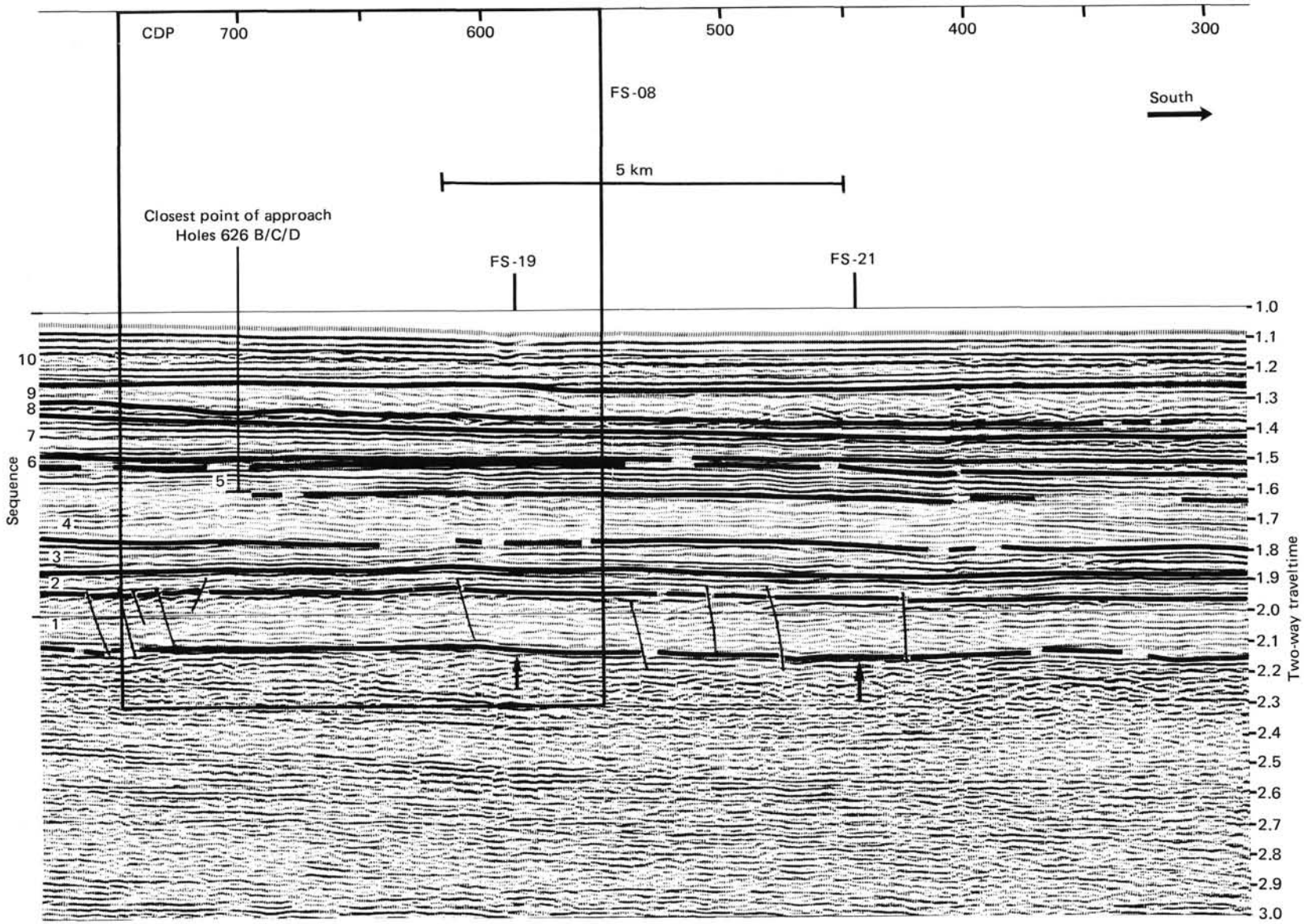

Figure 3. Interpreted copy of survey line FS-08. The target horizon is indicated by arrows. This is the pronounced velocity discontinuity of Sheridan et al. (1981). Younger sequence boundaries and faults are also indicated. Box indicates portion of FS-08 detailed in Figure 19.

Bimini in the Bahamas (Fig. 4). This location is just east of the axis of the Straits of Florida and the present thalweg of the Gulf Stream. On 3.5-kHz profiles collected during the site surveys, bottom returns in the vicinity of the site are reverberant, of high amplitude, and characterized by up to 7 m of local relief. Water depths in this part of the Straits generally exceed 800 m.

Objectives

Based on analysis of the site-survey results in the Straits, the depth to the velocity discontinuity and sequence boundary of Sheridan et al. (1981) was estimated to be approximately 1200 m sub-bottom at Site 626. Recovery of a continuous section above that surface, and sampling of it, were considered to be important in providing answers to the following scientific questions:

1. What is the nature of the basal discontinuity? If this discontinuity indeed marks the transition downward from deep-water to shallow-water carbonate facies, the megaplatform hypothesis is proved for the Straits of Florida and, by seismic correlation, for the Northwest Providence Channel. If not, the graben hypothesis remains viable, at least where subsequent bank progradation cannot be proved.

2. What is the depositional record of the Gulf Stream? Did it or its predecessor(s) play a role in the postulated mid-Cretaceous drowning of this carbonate platform? How does it affect the vertical and lateral migration of facies patterns through time?

3. How do the ages of seismic-sequence boundaries identified beneath the Straits compare with the global fluctuations in relative sea levels postulated by Vail et al. (1977)?

4. What is the role of Cuba in supplying clastic sediments to this site, particularly during the Late Cretaceous–Paleogene collision of the Cuban island arc with the Florida–Bahamas carbonate province?

5. Finally, can Straits of Florida stratigraphy be successfully tied to better dated Mesozoic–Cenozoic stratigraphic successions in the deep Gulf of Mexico Basin, on the Blake Plateau, and farther northward along the east coast of the United States and Canada?

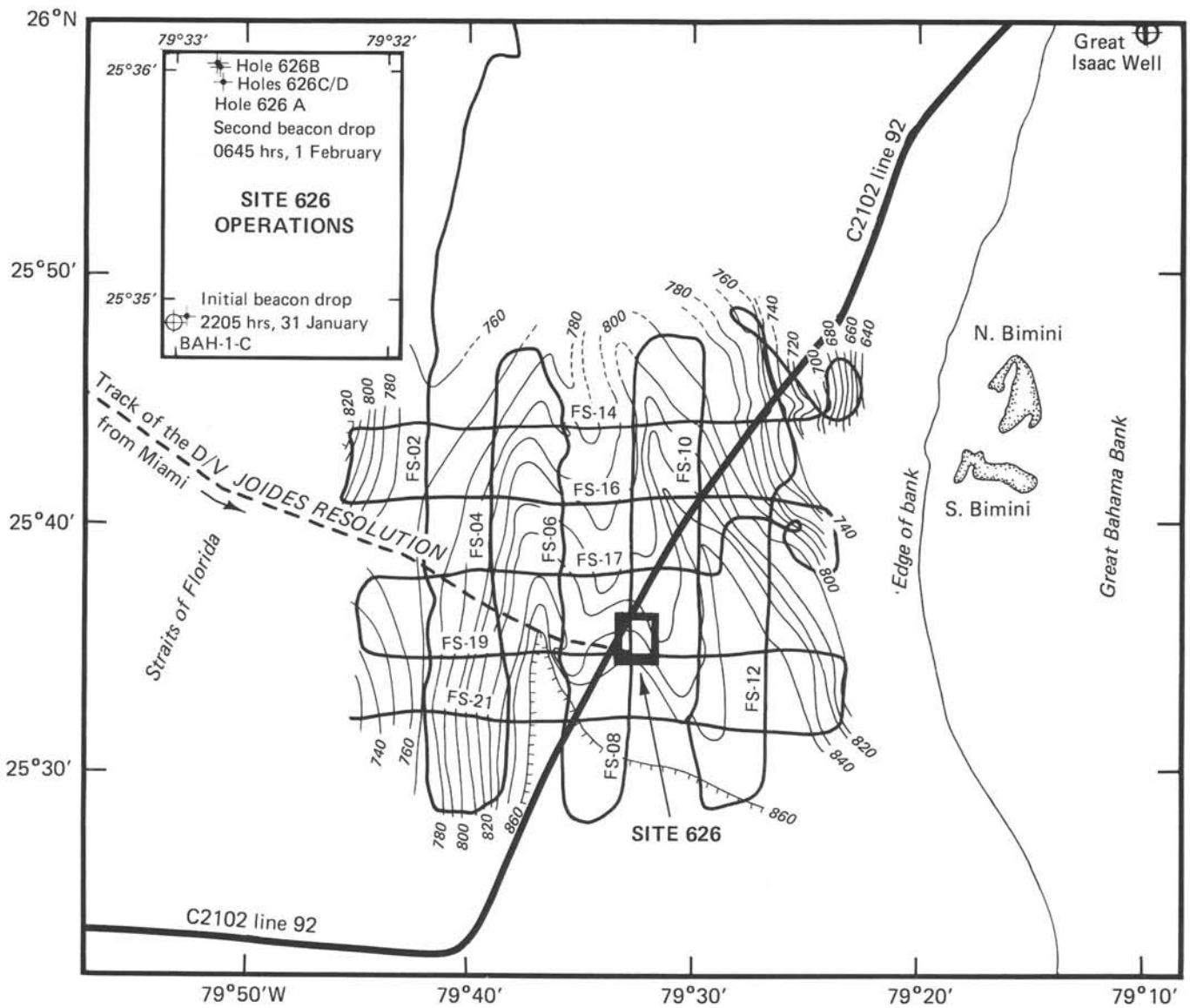

Figure 4. Trackline map (bathymetry shown in meters) for the site-specific survey in the Straits of Florida region (SF). *C* denotes multichannel seismic lines reported by Sheridan et al. (1981). Seismic line 1, ODP Leg 101, is shown by the dashed line. Detail of Site 626 operations appears in inset, upper left.

OPERATIONS SUMMARY

Introduction

During the shakedown cruise of the *JOIDES Resolution*, ODP Leg 100 (22–26 January 1985), attempts were made to drop a reentry cone at designated sites BAH-1-A, BAH-1-B, and BAH-1-C within the Straits of Florida survey grid (Fig. 4). BAH-1-A and BAH-1-B were considered to be the optimum targets for drilling in the Straits. Unfortunately, efforts at both sites were unsuccessful as a result of excessive drill-string vibration caused by Gulf Stream currents. BAH-1-C was then chosen as the best available alternative because it was out of the thalweg of the Gulf Stream, despite indications on 3.5-kHz records of a hard, reverberent bottom there which might make spudding in difficult. Unfortunately, even at BAH-1-C, surface currents proved too strong for deployment of a reentry cone. Consequently, plans for Leg 101 were changed to accommodate a single-bit attempt at that location.

Site 626

Leg 101, the inaugural leg of the new Ocean Drilling Program (ODP), began at 1635 hr (all times given in this report will be Eastern Standard Time) on 31 January 1985, when the *JOIDES Resolution* departed the dock in Miami, Florida, for Site 626 (BAH-1-C) in the Straits of Florida. Geophysical acquisition began approximately an hour later. Data from single-channel seismic-reflection profiling (in both analog and digital formats; see "Underway Geophysics" chapter, this volume), using a Teledyne 100-m streamer and an SSI 400-in.^{3} water gun, 3.5-kHz and 12-kHz precision depth recordings, and continuous magnetometer measurements, were collected on a course of 112° at speeds ranging from 5 to 8 kt. The magnetometer soon failed completely for reasons unknown. Occasional intermittent firing of the water gun was ascribed to a faulty trigger pulse from the lab, which was soon corrected. By 2130 hr, the ship was approaching BAH-1-C from the west-northwest (Fig. 4). A Datasonics 24-day beacon was deployed at 2205 hr on 31 January at 25°34.92′N, 79°32.95′W, less than 0.1 n. mi northeast of the designated site location (the intersection of site-survey lines FS-08 and FS-19; Fig. 4). Figure 5 shows a part of the digital single-channel seismic line recorded on our initial approach to Site 626.

After retrieving the seismic gear, a short delay was encountered in turning back to the site because of a problem with a bow thruster, but ranging on the beacon began shortly before midnight, 31 January. Bottom returns using the 3.5-kHz system were of high amplitude and composed of small diffractions, suggesting local relief of approximately 1 m. The water depth was 847 m (corrected from a 12-kHz reading of 840 m at a hull-mounted transducer 7 m below the water line).

Within the first hour, signals from the beacon to the *Resolution*'s Honeywell dynamic-positioning system became erratic. As a backup, a "taut wire" was deployed off the ship's starboard side. In shallow water, such a device provides a positioning capability by allowing monitoring of wire angles. However, because of the presence of a 1.5–2.0-kt Gulf Stream surface current, this method of ranging was marginally effective. Nonetheless, by 0415 hr on 1 February, the decision was made to run in hole (RIH). Approximately 560 m of pipe was out when the signal for the ranging beacon was lost at 0630 hr. An immediate decision was made to launch a second beacon on a different frequency, which was accomplished at 0645 hr at 25°35.95′N, 79°32.78′W. By this time, the ship had drifted approximately 1.0 n. mi northeast of the original site location but only 0.25 n. mi of the northward continuation of site-survey line FS-08 (Fig. 4, inset). After a short period of ranging on the new beacon, the rest of the pipe was RIH. The bottom-hole assembly (BHA) touched bottom at 858.5 m below the dual elevator stool, in excellent agreement with the 857.3 m predicted by the 12-kHz data.

The first "mud-line" rotary core of Hole 626A was recovered at 1255 hr on 1 February and consisted of 1.44 m of lime sand and rubble. A second rotary core recovered 3.57 m of Pleistocene skeletal lime sand. However, while washing at 15 m sub-bottom, the core barrel jammed and the bit plugged. This core barrel was subsequently retrieved using a second barrel, and circulation was restored. Unfortunately, the signal from the second beacon was lost at approximately 2015 hr during continued washing, forcing a decision to pull out of the hole (POOH) and terminate Hole 626A. Consequently, the bit had to be successfully cleared above the mud line to a depth of 680 m. The consensus of the shipboard engineering staff was that either the beacons were defective or they were being tilted by bottom currents, making their usefulness for surface positioning in the Straits suspect.

The dilemma was resolved as the *Resolution* drifted downcurrent (north-northwest) approximately 360 m and reacquired the signal of the second beacon, proving that this beacon was leaning with the current at approximately a 14° angle. Ranging at the downstream location (25°36.04′N, 79°32.81′W; Fig. 4, inset) was successful, and pipe was RIH for Hole 626B starting at 0115 hr, 2 February.

After encountering the mud line at 858.5 m below the rig floor, the string was successfully washed in to a sub-bottom depth of 80.3 m, where the bit became partly plugged with sediment. In order to restore circulation, the core barrel was retrieved at 1055 hr. The first wash core of Hole 626B recovered 4.1 m of lower Pliocene glauconitic foraminifer–nannofossil sand and lime rubble. Throughout the rest of 2 February, washing and coring continued intermittently. Hole conditions continued to be unstable as a result of unconsolidated sands, and drilling mud was frequently used during coring operations to condition the hole. The oldest sediments recovered down to 185.5 m sub-bottom were latest early Miocene to middle Miocene. At that depth, in the process of trying to retrieve a stuck core barrel, the drill string was over-torqued while reaming and washing to the bottom of the hole. Before any braking could be applied, backlash caused the string to back off, resulting in the loss of the BHA and 19 joints (approximately 170 m) of pipe. Subsequent attempts to screw the two ends of the string together proved futile.

All remaining pipe was POOH at Hole 626B by 0715 hr, 3 February. The decision was made to offset slightly and to use HPC/XCB techniques to sample the section washed through at Hole 626B as Hole 626C. By noon, after making up a new BHA, pipe was RIH at the new location (25°36.02′N, 79°32.80′W; Fig. 4, inset). The mud line was encountered at 855 m below the rig floor, and the first XCB core, recovered at 1645 hr, contained calcareous sand and rubble. Cores continued to come up at the rate of 1/1.5 hr for the next 18 hr down to a sub-bottom depth of 112.1 m. At that point, a switch was made to the HPC for core 13 in an attempt to improve recovery, which was running at only 11% for the XCB. Seven HPC cores were recovered down to a sub-bottom depth of 179.3 m, with average recovery of 79.8%. The predominant lithology was bioclastic foraminiferal sand, and the oldest material recovered was early Miocene. At 2300 hr on 4 February, Hole 626C was terminated in order to begin Hole 626D, a single-bit rotary penetration to the original target horizon identified by the site surveys, essentially a repeat of the prematurely terminated Hole 626B. The Hole 626D location (25°36.02′N, 79°32.81′W; Fig. 4, inset) represented a minimum offset from Hole 626C (less than 50 m).

At 0845 hr on 5 February, pipe was RIH at Hole 626D. The mud line was encountered at 854 m below the rig floor, and the section was washed continuously down to a depth of 179.4 m

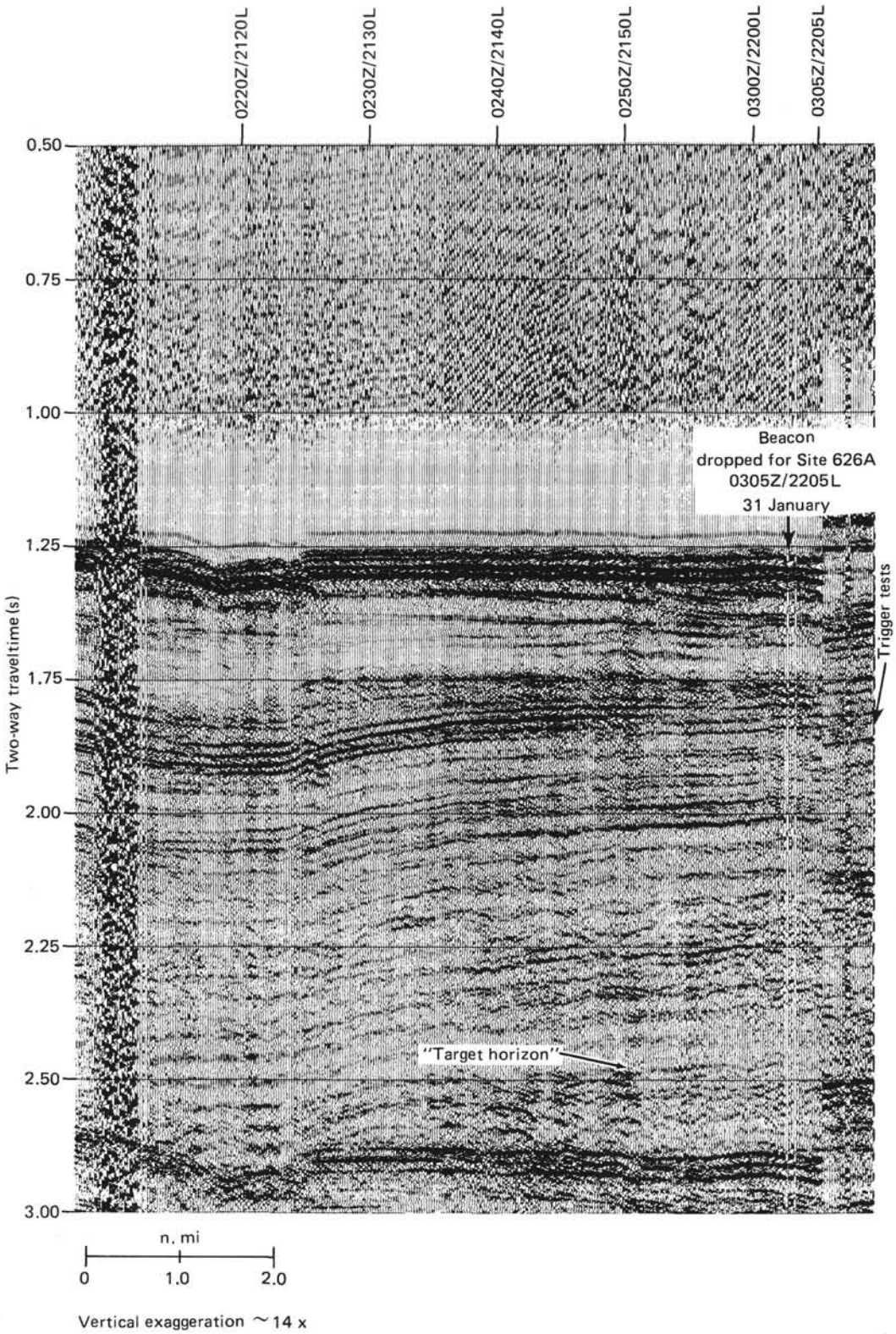

Figure 5. Part of ODP Leg 101 Line 1, approaching Site 626. The data are digital, samples at 1 ms. Sound source was a 400-in.^{3} water gun fired every 12 s. Receiver was 100 m in length, separated from the *JOIDES Resolution* by a 500-m leader.

sub-bottom. The first rotary core was recovered late on 6 February, containing 1.4 m of a partly cemented foraminifer–nannofossil sand with some intergranular fillings of asphalt, which the organic geochemists determined to be completely oxidized and perhaps detrital. Rotary coring continued throughout 6 and 7 February, with both poor recovery (less than 10%) and continuing poor hole conditions as a result of quicksand, necessitating repeated hole conditioning with drilling mud. The oldest sediments recovered, at 437.3 m sub-bottom, were early Oligocene (Core 626D-27R). Core 626D-28R, CC recovered fragments of an undated, well-cemented foraminiferal grainstone. In the process of trying to retrieve Core 626D-29R from approximately 456 m sub-bottom late in the evening of 7 February, both the core barrel and the string became stuck. Apparently sand had penetrated upward around the core barrel, effectively burying it inside the drill pipe. Repeated attempts to reach it using a second core barrel equipped with a hard-formation catcher were unsuccessful, and circulation could not be restored. At 0700 hr on 8 February, the decision was reluctantly made to sever the pipe at 1201.77 m below the rig floor at the top of the third drill collar. No logging personnel from Schlumberger were as yet aboard, so a decision about running logs either below the severed pipe or within the string was postponed.

During the afternoon of 8 February, the drill collar was successfully severed by the first charge. However, the pipe remained stuck, so another charge was prepared for detonation at 1106.21 m below the rig floor. In the meantime, a neutron log was run in the hole inside the pipe by a Schlumberger engineer, who had joined the vessel by helicopter. After the logging was completed, the second charge failed to explode, and a third was prepared for detonation at the same depth. That, too, failed. Finally, at 0500 hr on 9 February, a fourth charge succeeded in severing the string at 1048.69 m below the rig floor. The remaining pipe was POOH successfully by 0800 hr, and the *Resolution* departed Hole 626D immediately thereafter for Site BAH-9-A on the northern slope of Little Bahama Bank.

The coring summary for Site 626 appears in Table 1.

SEDIMENTOLOGY

Introduction

Four holes were drilled at Site 626. Hole 626A penetrated 12.8 m sub-bottom into sediments with 4.9 m of recovery (38%); Hole 626B penetrated 185.5 m sub-bottom with 14.03 m of recovery (8%); Hole 626C penetrated 179.3 m sub-bottom with 66.3 m of recovery (37%); and Hole 626D penetrated 446.8 m sub-bottom, cored from 179.6 to 446.8 m sub-bottom, with 9.36 m of recovery (3.5%).

Sediments recovered are dominantly unlithified, muddy to clean calcareous sands and gravels (packstones, grainstones, floatstones, and rudstones), light gray (2.5Y 8/2) to white (2.5Y 7/2), containing about 1%–5% glauconite. Three dominant kinds of grains, or compositional end-members, compose the sand and gravel fraction of these sediments: planktonic foraminifers and pteropods, skeletal fragments, and clasts. Skeletal fragments include ahermatypic corals, red algae, green algae, echinoderm spines and plates, bivalves, gastropods, pteropods, and benthic foraminifers and are principally of shallow-water origin. Clasts are dominantly lithified skeletal packstones and grainstones. Skeletal fragments in the clasts are principally of shallow-water origin. Proportions of different grain types vary in these sediments, and so in the sediment descriptions below the order of the three compositional end-members has no significance.

Based principally on the continuous coring in Holes 626C and 626D, the section sampled at Site 626 is divided into three lithologic units:

Unit I (0–121.7 m sub-bottom; Cores 626A-1R and 626A-2R; Cores 626C-1X to 626C-13H)

Unit I occurs from 0 to 121.7 m sub-bottom in Hole 626C and consists dominantly of unlithified, glauconitic foraminiferal–skeletal grainstone and packstone, with grain size ranging from medium to coarse sand.

Coarse gravels (clast–skeletal rudstone) were recovered at the seafloor at both Holes 626A and 626C (Fig. 6). We designate these gravels as Subunit IA. These gravels also occurred as downhole contamination in the form of a graded bed at the top of Core 626C-13H. The coarse nature of these deposits is probably the result of winnowing by the Florida Current, which has a present-day average velocity at the bottom in the vicinity of Hole 626A of about 30 cm/s (Brooks, 1979). All of Core 626A-2R and the base of Core 626C-3X contain clasts, in addition to foraminifers and skeletal fragments characteristic of the remainder of this unit. In Hole 626B, Unit I is represented by 4.1 m of unlithified, glauconitic foraminiferal-skeletal grainstone, with grain size ranging from fine to coarse sand, recovered in Core 626B-1W (0–80.2 m sub-bottom), and a few fragments (about 5 cm) of foraminiferal chalk found in the core catcher of Core 626B-2W (80.3–128.1 m sub-bottom). Unlithified foraminiferal packstone was recovered in several cores in Hole 626C. Unit I also contains a volcanic-ash layer (dark grayish brown, 2.5Y 4/2) in the interval between 54.3 and 63.9 m sub-bottom (see Core 626C-7X). The alternation of foraminiferal-skeletal grainstones and packstones in Unit I implies fluctuations in intensity of winnowing by, and therefore changes in velocity of, the Florida Current during deposition of Unit I.

Unit II (121.7–169.6 m sub-bottom; Core 626B-4R; Cores 626C-14H to 626C-18H)

In Hole 626C, Unit II consists of at least three debris flows separated by lithologies similar to those in Unit I and by lithified layers. Unit II extends between 121.7 and 169.6 m sub-bottom in Hole 626C and is dominated by a 35.4-m-thick (124.6–160.0 m sub-bottom) debris flow. This debris flow grades from an unlithified clast–skeletal–foraminiferal floatstone near the base (Fig. 7) to an unlithified clast–foraminiferal–skeletal packstone near the top, which is defined by the last appearance of clasts at the top of Section 6 in Core 626C-14H. Clasts consist dominantly of lithified skeletal grainstone and packstone; skeletal fragments are principally of shallow-water origin. Particularly large skeletal fragments in this debris flow consist of shallow-platform oyster and coral fragments. Clasts range in size from 10 cm at the base to 0.2 cm at the top. Separating this thick debris flow from an overlying (122.2–124.5 m sub-bottom) thinner (2.3-m) debris flow is a 0.1-m-thick layer of foraminifer–nannofossil ooze. The thick debris flow is underlain by a short (2.2-m) interval of unlithified to semilithified, glauconite-rich foraminiferal and foraminiferal–skeletal packstone and a lithified layer of skeletal grainstone (Fig. 8). This grainstone consists entirely of displaced shallow-water-platform debris and may represent a sediment gravity flow, either a turbidite or grainflow. The base of Unit II (162.2–169.6 m sub-bottom) consists of a third debris-flow unit, again grading from unlithified clast–skeletal–foraminiferal floatstone at the base to unlithified clast–foraminiferal–skeletal packstone at the top (Core 626C-18H). Several individual debris flows may constitute this third debris-flow unit.

In Hole 626B, Unit II consists of an interval of unlithified clast–foraminiferal–skeletal floatstone recovered in Core 626B-4R

Table 1. Coring summary, Site 626.

Core no.	Core type[a]	Date (Feb. 1985)	Time	Sub-bottom depths (m)	Length cored (m)	Length recovered (m)	Percentage recovered
Hole 626A							
1	R	1	1255	0–1.4	1.4	1.44	102
2	R	1	1825	1.4–12.8	11.4	3.52	30
Hole 626B							
1	W	2	1055	0–80.2	80.2	4.10	5
2	W	2	1705	80.3–128.1	47.9	0.03	0
3	R	2	1915	128.1–137.7	9.6	0	0
4	R	2	2110	137.7–147.3	9.6	6.97	72
5	W	3	0150	147.3–185.5	38.2	2.88	7
Hole 626C							
1	X	3	1645	0–6.9	6.9	0.04	0
2	X	3	2000	6.9–16.5	9.6	1.61	16
3	X	3	2140	16.5–25.5	9.0	5.10	56
4	X	3	2240	25.5–35.1	9.6	2.72	28
5	X	3	2340	35.1–44.7	9.6	1.09	11
6	X	4	0115	44.7–54.3	9.6	1.33	13
7	X	4	0245	54.3–63.9	9.6	0.05	0
8	X	4	0420	63.9–73.4	9.5	0	0
9	X	4	0530	73.4–83.0	9.6	0.66	6
10	X	4	0730	83.0–92.7	9.7	0	0
11	X	4	0925	92.7–102.4	9.7	0.10	1
12	X	4	1045	102.4–112.1	9.7	0	0
13	H	4	1500	112.1–121.7	9.6	5.13	53
14	H	4	1700	121.7–131.3	9.6	9.30	96
15	H	4	1830	131.3–140.8	9.5	9.75	102
16	H	4	1905	140.8–150.4	9.6	9.77	101
17	H	4	1945	150.4–160.0	9.6	9.64	100
18	H	4	2105	160.0–169.6	9.6	9.31	97
19	H	4	2245	169.6–179.3	9.7	0.74	7
Hole 626D							
1	R	5	2215	179.4–189.0	9.6	1.37	14
2	R	5	2345	189.0–198.6	9.6	0	0
3	R	6	0215	198.6–208.1	9.5	0.57	6
4	R	6	0305	208.1–217.7	9.6	0.24	2
5	R	6	0445	217.7–227.3	9.6	0	0
6	R	6	0710	227.3–236.9	9.6	0.01	0
7	R	6	1045	236.9–245.6	8.7	0	0
8	R	6	1415	245.6–255.2	9.6	0	0
9	R	6	1645	255.2–264.8	9.6	0	0
10	R	6	1845	264.8–274.4	9.6	0	0
11	R	6	1945	274.4–283.7	9.3	1.33	14
12	R	6	2105	283.7–293.2	9.5	0	0
13	R	6	2215	293.2–302.9	9.7	1.45	14
14	R	6	2335	302.9–312.6	9.7	1.15	11
15	R	7	0137	312.6–322.2	9.6	0	0
16	R	7	0405	322.2–331.8	9.6	0.01	0
17	R	7	0645	331.8–341.3	9.5	0.01	0
18	R	7	0835	341.3–351.0	9.7	0	0
19	R	7	1045	351.0–360.7	9.7	0.32	3
20	R	7	1230	360.7–370.4	9.7	0.56	5
21	R	7	1335	370.4–380.1	9.7	0.83	8
22	R	7	1500	380.1–389.6	9.5	0	0
23	R	7	1645	389.6–399.3	9.7	1.06	10
24	R	7	1800	399.3–408.9	9.6	0	0
25	R	7	1925	408.9–418.5	9.6	0	0
26	R	7	1925	418.5–427.7	9.2	0	0
27	R	7	2050	427.7–437.3	9.6	0.47	4
28	R	7	2222	437.3–446.8	9.5	0.01	0

[a] H = hydraulic piston; R = rotary; W = wash; X = extended core barrel.

at 137.7–147.3 m sub-bottom. This unit is interpreted as a debris-flow deposit on the basis of correlation with Hole 626C.

Unit III (169.6–446.8 m sub-bottom; Core 626B-5W; Core 626C-19H; Cores 626D-1R to 626D-28R)

Unit III underlies the mass flow deposits making up Unit II. The uppermost part of Unit III is similar to the sediments in the interval separating the two debris flows in Unit II. A lithified layer of skeletal grainstone containing dead oil lies between unlithified foraminiferal-skeletal packstone. In addition, fragments of lithified skeletal grainstone were recovered in the core catcher of Core 626D-1R. These lithified grainstones may represent mass gravity flows, similar to the lithified grainstone separating the two debris flows of Unit II. The packstone represents partly winnowed perennial sediment.

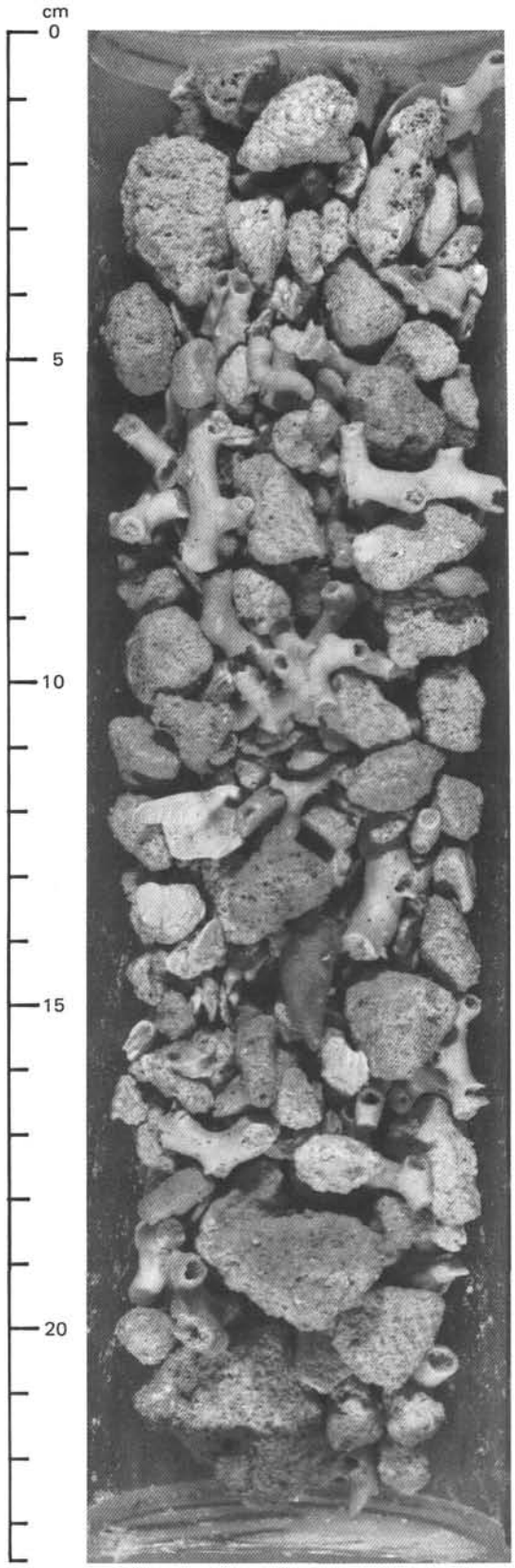

Figure 6. Coarse gravel (clast-skeletal rudstone) recovered from the seafloor at Hole 626A. Skeletal fragments are dominantly pieces of ahermatypic coral, with subordinant amounts of whole and broken bivalves, bryozoans, and echinoid spines. Clasts are lithified skeletal grainstones, with the skeletal component principally of shallow-water origin. Section 626A-1R, CC, Unit IA.

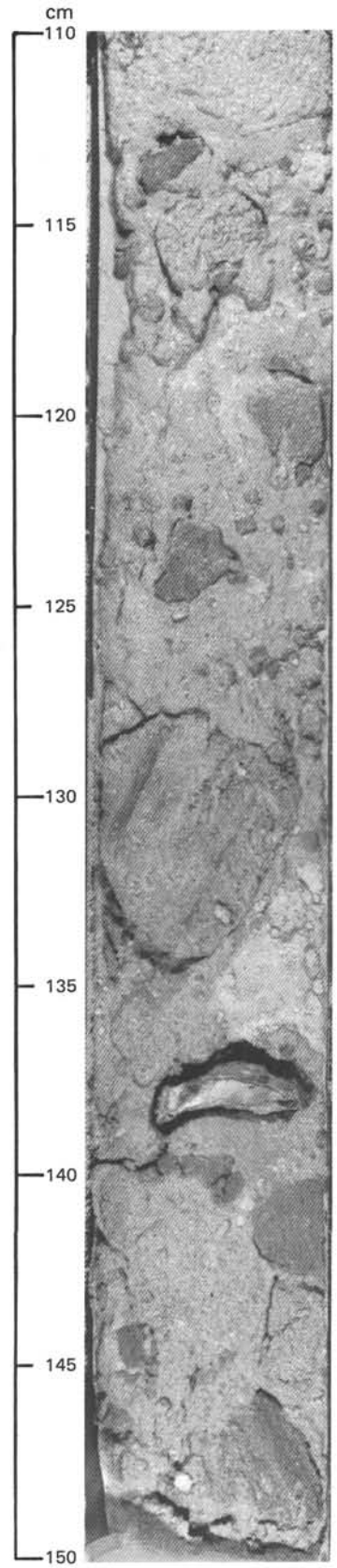

Figure 7. Part of upper debris flow (unlithified clast-skeletal-foraminiferal floatstone), showing large (5-cm) clasts and a skeletal fragment (oyster) in a matrix of foraminifers, skeletal fragments, and micrite. Section 626C-17H-3, 110–150 cm, 154.5–154.9 m sub-bottom, Unit II.

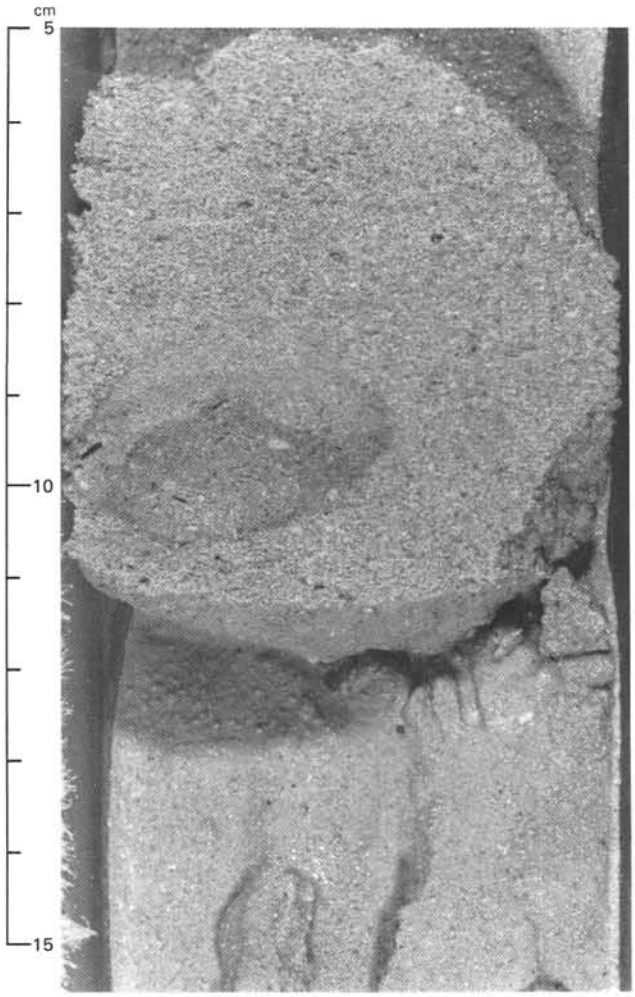

Figure 8. Lithified layer of skeletal grainstone separating debris flows. Skeletal fragments are principally of shallow-water origin. Layer is laminated except for an oval-shaped burrow. Sample 626C-18H-1, 5–15 cm, 160 m sub-bottom, Unit II.

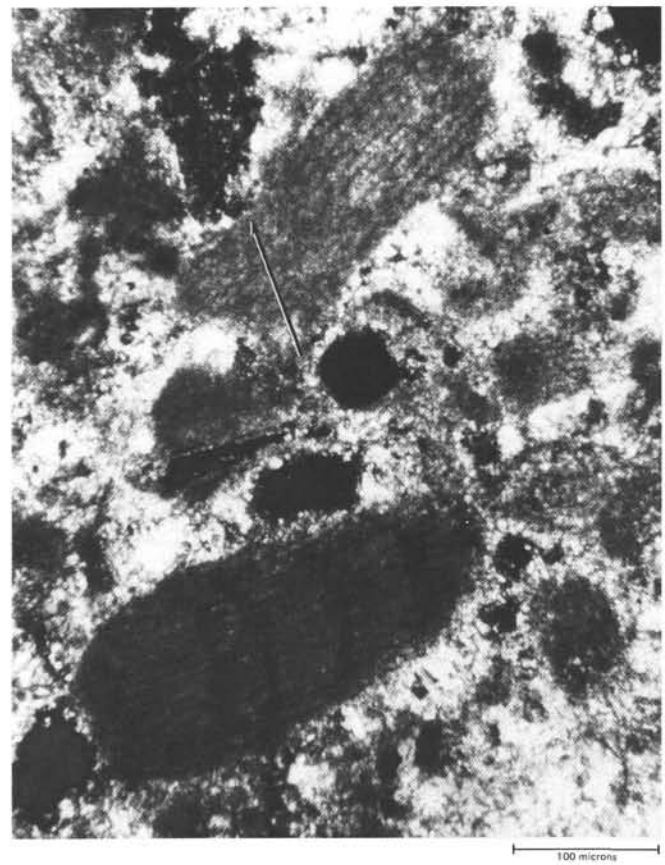

Figure 9. Thin-section photomicrograph of lithified skeletal grainstone (crossed nicols). Grains are principally of shallow-water origin and consist of fragments of red algae, echinoid spines, micritized skeletal fragments, and foraminifers. Cement is finely crystalline spar. Note pressure-solution contact between echinoid spine and red algal fragment at right. Bar is 100 microns. Section 626D-28R, CC, 437.3–446.8 m sub-bottom, Unit III.

The dominant lithology in Hole 626D (recovered in 9 of 11 cores) is an unlithified clast–skeletal–foraminiferal packstone. Clasts generally consist of lithified skeletal packstone and grainstone. Again, these packstones represent sediments that have been partly winnowed by the Florida Current. Core 626D-3R contains unlithified clast rudstone and grainstone, and Core 626D-4R contains an unlithified, glauconitic foraminiferal grainstone. These grainstones and rudstones represent sediments that have been thoroughly winnowed by the Florida Current. Their juxtaposition with only partly winnowed packstones indicates fluctuations in velocity of the Florida Current during deposition of Unit III.

Core cuttings in Cores 626D-6R, 626D-15R, 626D-16R, 626D-17R, 626D-25R, and 62D-28R are essentially all lithified skeletal grainstones (Fig. 9). They presumably represent lithified layers interbedded with unlithified layers represented by the sediments recovered in other cores in this section. Chert fragments (dark olive gray, 5Y 3/2) also were recovered in Cores 626D-16R, 626D-17R, 626D-19R, 626D-20R, and 626D-27R. The upper four occurrences coincide with a decrease in drilling rate and suggest that the interval from 322.2 to 370.4 m sub-bottom is cherty. Based on this drastic change in drilling rates and the concomitant appearance of chert in the interval 322.2–370.4 m sub-bottom, we have subdivided Unit III into three subunits:

Subunit IIIA (169.6–322.2 m sub-bottom), representing unlithified clast–skeletal–foraminiferal packstones and grainstones.

Subunit IIIB (322.2–370.4 m sub-bottom), assumed to consist of similar unlithified packstones and grainstones as Subunit IIIA with numerous interbeds of chert and limestone.

Subunit IIIC (370.4–446.8 m sub-bottom), similar to Subunit IIIA and containing only minor amounts of limestone.

It is likely that Subunit IIIA contains lithified layers in the interval from 236.9 to 274.4 m sub-bottom, based on a decrease in drilling rate. However, this interval has not been designated as a separate unit because Cores 626D-7R to 626D-10R recovered no sediment or rock; thus no lithologic control exists for this interval.

In Hole 626B, Unit III is represented by an interval of unlithified foraminiferal–skeletal grainstone, recovered in Core 626D-5R (147.3–185.5 m sub-bottom), overlying several centimeters of unlithified, homogeneous foraminiferal–skeletal packstone, which in turn overlies three large (>5 cm) clasts of lithified skeletal grainstone and laminated calcareous mudstone. These sediments and rocks were recovered from a washed interval, and so their exact stratigraphic relationships are uncertain. However, the juxtaposition of foraminiferal–skeletal grainstones and packstones in Core 626D-5R implies some variation in the intensity of winnowing by the Florida Current during deposition of Unit III and hence minor fluctuations in its velocity.

Discussion

A number of cores contain graded intervals; however, except for Cores 626B-5W and 626C-13H, where graded intervals overlie a finer grained section, the grading extends throughout the total sediment recovered in a single core. Thus all grading is believed to be an artifact produced by drilling and *not* a product of turbidite deposition.

The mass-gravity-flow deposits sampled in Holes 626B and 626C are middle Miocene in age. They are therefore coeval, in part, with the early to middle Miocene Great Abaco Member of the Blake Ridge Formation (Bliefnick et al., 1983). However, Site 626 mass gravity flows and mass gravity flows in the Great Abaco Member are lithologically distinct. For example, Site 626 mass gravity flows contain no radiolarian-diatom mudstone intraclasts. In addition, the thickness of Site 626 mass gravity flows is only 57.5 m, whereas the Great Abaco Member attains thicknesses of nearly 500 m. Furthermore, Site 626 mass gravity flows remain unlithified, whereas the Great Abaco Member is fully lithified. Nevertheless, the close temporal association of these two mass gravity flows and their occurrence in the vicinity of the Bahama Platform suggest a related origin.

The sandy and gravelly nature of the section at Site 626 is clearly the result of winnowing by the Florida Current since at least the late Oligocene. Apart from the mass gravity flows, the deposits are essentially contourites. They presented a difficult problem in sampling because, under the influence of drilling fluids (seawater and mud), they turned into quicksand and flowed away from the core barrel. Only when the HPC was used were full cores obtained. The interbedding of grainstones and rudstones with packstones clearly indicates fluctuations in the intensity of winnowing by the Florida Current and hence of its current velocity.

Lithified layers cored at Site 626 apparently were cemented in the subsurface. These layers show no evidence of boring or corrosion expected for surficial hardgrounds. Such layers are not plentiful in Unit I. They are, however, abundant (about 50%) in Unit III, as indicated by decreased drilling rates and relatively low porosity on the porosity log. The cement lithifying these layers may be derived from dissolution of shallow-water skeletal fragments composed of aragonite and magnesian calcite. The dominance of skeletal fragments of shallow-water origin in lithified layers, and their subordinance in unlithified sands, support such an interpretation. It is not clear whether or not the lithified cuttings recovered in Hole 626D are pieces of such lithified layers or clasts washed from debris flows.

In summary, the section drilled at Site 626 consists of three major units: (1) Unit I, 0–121.7 m sub-bottom, foraminiferal-skeletal packstone and grainstone; (2) Unit II, 121.7–169.6 m sub-bottom, clast-foraminiferal-skeletal floatstone; (3) Unit III, 169.6–446.8 m sub-bottom, clast-foraminiferal-skeletal packstone and grainstone.

BIOSTRATIGRAPHY

Introduction

Site 626 was chosen to examine the nature of prominent seismic horizons in the eastern Straits of Florida in order to facilitate their correlation with better documented areas in the North Atlantic Ocean and the Gulf of Mexico. In addition, drilling at the site would help to clarify and document the history of the Gulf Stream.

Three groups of microfossils were examined in the shipboard labs. Planktonic foraminifers and calcareous nannofossils were used to establish a biostratigraphic framework for the core material and to monitor the degree of pelagic reworking through time. Larger foraminifers were examined to monitor the input of redeposited shallow-water-platform microfossils to the site as well as to identify sediments containing shallow-water material reworked from older strata.

All depths referred to are sub-bottom depths, and samples are from the core catcher unless otherwise specified.

Calcareous Nannofossils

Hole 626A

Drilling at Hole 626A was abbreviated owing to the unstable nature of the sediment. Core 626A-1R, taken at or near the mud line, consists of less than one full section of coarse bioclastic limestone with abundant ahermatypic corals and few bryozoan fragments. Nannofossils were isolated by gravitational settling from this coarse debris. The settled samples contain few nannofossils with moderate to good preservation. The dominant nannofossils include a late Quaternary assemblage including *Emiliania huxleyi, Gephyrocapsa caribbeanica*, and small *Gephyrocapsa* spp., indicating nannofossil Zone NN21. Reworked forms include *Sphenolithus abies* (late Miocene–early Pliocene) and *Watznaueria barnesae* (Cretaceous). Core 626A-2R (12.8 m sub-bottom) contains finer grained calcareous sands with more abundant nannofossils of Zone NN21. Reworked forms are more common, with taxa such as *Pseudoemiliana lacunosa* (late Pliocene–early Quaternary), *S. abies, Reticulofenestra pseudoumbilica* (late Miocene–early Pliocene), *Markalius astroporous* (Cretaceous–Oligocene), and *Watznaueria barnesae* (Cretaceous). This suggests that at least three, and possibly more, stratigraphic zones have been reworked by local bottom-current activity.

Hole 626B

Drilling at Hole 626B recovered three washed cores and two rotary cores. Nannofossil preservation is generally poor in these sections. Most samples contain only traces of nannofossil material, with mixed assemblages consisting of Quaternary and older material. Only one core (626B-1W) contains an assemblage rich enough to yield a reliable biostratigraphic age, although nannofossils from the late Pleistocene, early Pliocene, and late Miocene were recovered. The predominant assemblage in this sample is Miocene, including such forms as *Discoaster quinqueramus, D. challengeri, D. berggreni*, and *D. variabilis*. This assemblage indicates a late Miocene age (NN11), an age that is corroborated by planktonic foraminifers.

Hole 626C

Hole 626C was drilled with the XCB (Cores 626C-1X through 626C-12X) and with the advanced HPC (Cores 626C-13H through 626C-19H). Core 626C-1X recovered only coral remains and pebbles that contained no nannofossils. Cores 626C-2X through 626C-5X can be confidently assigned to the late Pleistocene–Holocene nannofossil Zone NN21, based on *Emiliana huxleyi, Gephyrocapsa oceanica*, small *Gephyrocapsa* spp., and *Umbellosphaera irregularis*. The core catcher from Core 626C-6X lacks *E. huxleyi* but contains *Pseudoemiliana lacunosa*, indicating Zone NN19 of early Pleistocene age. This Pleistocene assemblage contains significant amounts of reworked material from older Neogene assemblages. The predominant source of the reworked material appears to be strata of early Pliocene age similar to that which underlies the Pleistocene section at this hole. Specimens of Cretaceous forms, such as *Watznaueria barnesae* and *Cretarhabdus crenulatus*, are a rare but consistent component of the reworked assemblage. The Pleistocene assemblages are generally well preserved, with only slight evidence of dissolution and overgrowth. The reworked Neogene material is noticeably more altered by diagenesis. The Cretaceous reworked component varies in preservational state within a sample from poor to good.

Core 626C-7X contains a late Miocene (NN12) assemblage including forms such as *Discoaster berggreni, D. surculus, D. brouweri* (early forms), *D. tamalis*, and *Reticulofenestra pseudoumbilica*. Preservation is moderate to good with some overgrowth evident in many specimens. Trace amounts of reworked Cretaceous taxa (especially *W. barnesae*) are present. The base of the Pliocene could not be recognized, as Core 626C-8X failed to recover any sediment.

Core 626C-9X contains assemblages that include *Discoaster quinqueramus, D. berggreni, D. brouweri* (early forms), and *D. variabilis*. This assemblage indicates a late Miocene (NN11) age for the material. The preservation of this assemblage is moderate to poor. Trace amounts of Cretaceous reworked nannofossils (*W. barnesae*) occur in these sediments. Core 626C-10X did not contain any sediment. Core 626C-11X contained only strongly overgrown and dissolved nannofossils of Oligocene age. These are interpreted to be reworked forms based on the results of planktonic-foraminiferal examinations. Core 626C-13H largely consists of similar, reworked Oligocene forms. A few taxa, such as *Discoaster variabilis* and *D. exilis*, are present, however, which suggest a Miocene (NN5–9) age. All of the specimens in this sample exhibit strong diagenetic alteration. Core catchers from Cores 626C-14H and 626C-15H did not include any age-diagnostic nannofossils. Foraminiferal evidence indicates that these cores are middle Miocene. Cores 626C-16H through 626C-19H contain *Sphenolithus heteromorphus* without *Helicopontosphaera ampliaperta*, indicating nannofossil Zone NN5. The assemblages are sparse. Coring was discontinued following Core 626C-19H in order to rotary-drill toward the deep objectives at this site.

Hole 626D

Coring at Hole 626D commenced at 179.4 m, following washing through the overlying sediment. Recovery was poor throughout the cored interval in this hole. Sufficient sediment was recovered from some cores, however, to allow recognition of nannofossil zones for part of the hole. Cores 626D-1R, 626D-3R, and 626D-4R contain *Sphenolithus heteromorphus* and *S. moriformis* without *Helicopontosphaera ampliaperta*. This assemblage is indicative of middle Miocene nannofossil Zone NN5. Assemblages from Core 626D-1R are sparse and contain common reworked Oligocene forms (such as *Sphenolithus ciperoenis* and *Reticulofenestra abisecta*) as well as some Pleistocene downhole contaminants. Cores 626D-3R and 626D-4R have much richer, better preserved assemblages with only a trace of Oligocene reworking and no appreciable Pleistocene downhole contamination. Cores 626D-5R through 626D-9R recovered no nannofossil-bearing sediment. Cores 626D-10R through 626D-13R contained sediment of early Miocene nannofossil Zone NN3, as indicated by the presence of *Sphenolithus belemnos* without *Triquetrorhabdulus carinatus*. In Core 626D-14R, both species were found, and therefore this sparse flora can be assigned to Zone NN2 of early Miocene age. No nannofossils were recovered from Cores 626D-15R through 626D-17R. In Cores 626D-18R and 626D-19R, *S. belemnos* and *T. carinatus* occur together in significant abundance, indicating the early Miocene nannofossil Zone NN2. Nannofossils are few to rare in this interval, with only moderate preservation. Only trace amounts of Cretaceous reworking (*Watznaueria barnesae*) are evident. No age-diagnostic nannofossils were observed in Core 626D-20R. Cores 626D-21R and (probably) 626D-22R contained an earliest Miocene assemblage (NN1) with moderately preserved, common nannofossils. Assignment of Core 626D-22R is difficult owing to the transitional nature of the assemblage. It may belong to the latest Oligocene NP25 Zone, although further study will be necessary to confirm this. Cores 626D-23R through 626D-27R are of the late Oligocene NP25 Zone based on the occurrence of *Sphenolithus ciperoensis* and *Reticulofenestra abisectus*. Some specimens of *R. abisectus* seem to be reworked from older Oligocene strata. In addition, a shallow-water form of *Zygrhablithus bijugatus* is present. No age-diagnostic forms were recovered from Core 626D-28R.

Planktonic Foraminifers

Hole 626A

Two rotary cores (1.4 m and 12.8 m sub-bottom) recovered Pleistocene sediments (*Globorotalia truncatulinoides* Zone, N22/N23) at Hole 626A. A mixture of carbonate-platform and deeper water benthic species is present in both cores, with the proportion of platform species lessening in Core 626A-2R (12.8 m). Reworked Pliocene and Miocene planktonic species are present in small numbers in both cores.

Hole 626B

Hole 626B was washed to 80.3 m sub-bottom. The planktonic-foraminiferal assemblage from this level contains downhole contamination of Pleistocene species. The co-occurrence of *Globoquadrina dehiscens* and *Globorotalia margaritae* is anomalous and indicates reworking of the former or downhole contamination of the latter. As this question could not be resolved, an early Pliocene to late Miocene age (*Globorotalia margaritae* Zone to *Neogloboquadrina acostaensis* Zone, N18/N19 part) is assigned to this level.

A second washed interval to 128.1 m sub-bottom contains an upper Miocene *Globorotalia mayeri* (N13 part/N14) Zone fauna. Species present include *Globorotalia mayeri, G. menardii*, and *Globigerina nepenthes*. Core 626B-3R (137.7 m) was retrieved empty. Core 626B-4R (147.3 m) contains middle Miocene sediments of the *Globorotalia fohsi lobata/robusta* Zone (N11 part/N12/N13 part). Species present include *Globorotalia fohsi robusta, G. fohsi lobata, G. fohsi peripheroacuta*, and *G. mayeri*. The hole was then washed to a depth of 185.5 m. Core 626B-5W contains a mixed early middle Miocene fauna. Diagnostic taxa include *Globorotalia fohsi peripheroronda, G. fohsi peripheroacuta, G. fohsi fohsi, G. fohsi* cf. *lobata, G. praemenardii, Globigerinoides sicanus*, and *Praeorbulina glomerosa* (s.l.).

Hole 626C

Hole 626C was drilled using an XCB to a depth of 112.1 m (Cores 626C-1X through 626C-12X). Drilling then continued using an HPC to a depth of 179.3 m (Cores 626C-13H through 626C-19H). Cores 626C-1X through 626C-6X (0–54.3 m) are Pleistocene (*Globorotalia truncatulinoides* Zone, N22/N23). The co-occurrence of *G. truncatulinoides* and *G. tosaensis* at 54.3 m (base of Core 626C-6X) indicates an early Pleistocene age for this level. Only a small amount of volcanic ash was recovered from the core catcher of Core 626C-7X (63.9 m). Rare planktonic foraminifers include *Globorotalia plesiotumida, Globigerina nepenthes, Globoquadrina altispira altispira, G. venezuelana*, and *Globigerina nepenthes*, which indicate an early Pliocene to late Miocene age. All planktonic specimens are small, perhaps owing to size sorting, and benthics are absent. Core 626C-8X (63.9 m) was empty. A late Miocene age (*Neogloboquadrina acostaensis* Zone, N16/N17) is indicated for Core 626C-9X (83.0 m), based on *Neogloboquadrina acostaensis, Globoquadrina dehiscens*, and *Globorotalia plesiotumida*. Core 626C-10X (92.7 m) was retrieved empty.

Core 626C-11X (102.4 m) contains sediments of late middle Miocene age (*Globorotalia mayeri* Zone, N13 part/N14). This is indicated by the presence of *Globorotalia mayeri, G. menardii*, and *G. lenguaensis*. Core 626C-12X was empty. Cores 626C-13H and 626C-14H (121.7 m, 131.3 m) contain foraminifers di-

agnostic of the middle Miocene *Globorotalia fohsi lobata/robusta* Zone (N11 part/N12/N13 part). Species present include *Globorotalia fohsi lobata, G. fohsi fohsi, G. fohsi praefohsi*, and *G. praemenardii*. Cores 626C-15H through 626C-18H (140.8 m-169.6 m) are contained within the middle Miocene *Globorotalia fohsi fohsi* Zone (N10/N11 part). Diagnostic taxa include *Globorotalia fohsi fohsi, G. fohsi peripheroacuta*, and *G. praemenardii*. Earliest middle Miocene sediments are present in Core 626C-19H (179.3 m). Species indicative of the *Globorotalia peripheroronda/Praeorbulina glomerosa* Zones (N8 part/N9) include *Globigerinoides sicanus, Praeorbulina*? *glomerosa* s.l., and *Globorotalia fohsi peripheroronda*. *Orbulina* is absent, as are the younger members of the *Globorotalia fohsi* lineage.

Hole 626D

Hole 626D was washed to 179.4 m sub-bottom and then rotary-cored to 446.8 m. Core 626D-1R (189.0 m) contains *Globorotalia fohsi peripheroronda, G. fohsi peripheroacuta*, and *Globorotalia fohsi fohsi*, indicating a middle Miocene age (*Globorotalia fohsi fohsi* Zone, N10/11 part). However, the occurrence of rare *Praeorbulina glomerosa* s.l. suggests that this level may actually be somewhat older (earliest middle Miocene; *Globorotalia peripheroronda/Praeorbulina glomerosa* Zones, N8 part/N9). This latter view would agree with the age of Core 626C-19H, in which case significant downhole mixing must be invoked to explain the abundance of *G. fohsi fohsi* Zone fauna in Core 626D-1R. Core 626D-2R (198.6 m) was empty. Core 626D-3R (208.1 m) contains an early middle Miocene fauna that includes *Orbulina suturalis, Globorotalia fohsi peripheroronda, G. fohsi peripheroacuta, G. fohsi* cf. *praefohsi*, and *Praeorbulina glomerosa* s.l., indicative of the *Globorotalia fohsi peripheroronda* Zone (N9). This assemblage, too, may be enriched in slightly younger middle Miocene faunas owing to caving of unconsolidated foraminiferal sands from above. Core 626D-4R (217.7 m) is of earliest middle Miocene age (*Praeorbulina glomerosa* Zone, N8 part/N9) as indicated by *Praeorbulina glomerosa* s.l., *Globigerinatella insueta*, and *Globorotalia fohsi peripheroronda*. Species of *Orbulina* and the younger members of the *Globorotalia fohsi* lineage are absent. Core 626D-5R (227.3 m) was empty. A fragment of lithified foraminiferal grainstone recovered from Core 626D-6R (236.9 m) contains *Globorotalia mayeri* and *Globigerinoides* spp. and is assigned an early to middle Miocene age. Cores 626D-7R, 626D-8R, 626D-9R, and 626D-12R (245.6 m, 255.2 m, 264.8 m, 293.2 m) were empty.

Planktonic foraminifers are common in Cores 626D-10R, 626D-11R, and 626D-13R (274.4 m, 283.7 m, 302.9 m), but no zonal-marker species are present. The absence of *Praeorbulina* and *Catapsydrax* suggests that these sediments are of late early Miocene age (probably *Globigerinatella insueta* Zone, N7/8 part). The top of the undifferentiated *Catapsydrax stainforthi* Zone and the *Catapsydrax dissimilis* Zone (N5/N6) is present in Core 626D-14R (312.6 m) where *C. dissimilis* first appears. The paucity of *Globigerinatella insueta* at Site 626 did not allow differentiation of these zones. Sediments of this age are present through Core 626D-19R (360.7 m). Cores 626D-15R, 626D-16R, and 626D-18R (322.2 m, 331.8 m, 351.0 m) were empty. Core 626D-17R (341.3 m) consists of fragments of lithified foraminiferal grainstone containing *Globigerinoides* spp., indicating a Neogene age.

The early Miocene *Globorotalia kugleri* Zone (N4) is present in Core 626D-20R (370.4 m). The co-occurrence of *Globorotalia kugleri* and *G. pseudokugleri* suggests that the top of the zone lies above this level. Core 626D-21R (380.1 m) is also contained within this zone.

Core 626D-22R (389.6 m) is of earliest Miocene to latest Oligocene age. Species present include *Globorotalia pseudokugleri, G.* cf. *opima nana*, and *Globigerina* cf. *ciperoensis*. Upper Oligocene sediments belonging to the *Globigerina ciperoensis* Zone (P22) were recovered from Cores 626D-23R, 626D-24R, and 626D-27R (399.3 m, 408.9 m, 446.8 m). Diagnostic taxa include *Globigerina ciperoensis* and *Globorotalia opima nana*. Cores 626D-25R, 626D-26R, and 626D-28R (418.5 m, 427.7 m, 446.8 m) were empty.

Larger Benthic Foraminifers

Hole 626A

Redeposited benthic foraminifers occur in the core catchers of Cores 626A-1R and 626A-2R. Taxa present include *Amphistegina* sp. gr. *lessonii* and *Archaias angulatus*. *A. angulatus* is known from the Oligocene to the Holocene, where it lives in very shallow platform waters.

Hole 626B

Samples from Core 626B-2W, CC and Core 626B-4R, CC contain redeposited larger foraminifers including *Amphistegina* sp. gr. *lessonii, Nummulites cojimarensis, Sphaerogypsina vericularis*, and *Miogypsina antillea*. This assemblage is indicative of a middle Miocene age, which agrees with the planktonic-foraminiferal biostratigraphy. *Miogypsina antillea* and *Lepidocylina* sp. were found from 50 to 54 cm in Core 626B-5W, indicating an early to middle Miocene age, which also agrees with the planktonic-foraminiferal age.

Hole 626C

Larger benthic foraminifers were also found in samples from this hole. Most of them can be interpreted as penecontemporaneously redeposited, although some of them are reworked from older stratigraphic zones (Butterlin and Moullade, 1983). Samples 626C3X-3, 50–52 cm, 626C-4X-2, 50–52 cm, and 626C-5X, CC (dated as Pleistocene, N22/N23, based on planktonic foraminifers) contain *Amphistegina* sp. gr. *lessonii, Sphaereogypsina* sp., *Gypsina vesicularis*, and *Archaias angulatus*. The first two taxa are also present in Core 626C-13H, CC. Samples 626C-14H-5, 50–52 cm, 626C-15H-7, 50–52 cm, and 626C-16H-2, 50–52 cm, contain *Lepidocylina* (*L*) *miraflorensis* and *Miogypsina antillea*, indicating a middle Miocene age. Sample 626C-17H-5, 51–53 cm, yields only *Nummulites cojimarensis, Amphistegina* sp., *Sphaereogypsina* sp., and *Miogypsina antillea*. In Core 626C-18H, CC, *Miogypsina antillea, Lepidocyclina* (*L*) *canellei, Nummulites cojimarensis, Gypsina vesicularis*, and *Sphaerogypsina* sp. are present, indicating the middle Miocene.

All these larger benthic foraminifers occur in the middle Miocene, but the genus *Lepidocyclina* disappears in sediments of early Miocene age, suggesting that it is reworked here. Most of the samples studied from Sections 626C-14H-1 to 626C-18H, CC contain larger foraminifers.

Hole 626D

Many of the cores from Hole 626D contain a small number of moderately preserved, redeposited benthic foraminifers. Core 626D-1R, CC (assigned to planktonic-foraminiferal Zones N10/N11) contains *Amphistegina* sp. gr. *lessonii, Sphaereogypsina* sp., *Lenticulina* sp., and *Miogypsina antillea*. The latter species occurs in the early and middle Miocene. This agrees with the planktonic-foraminiferal assignment of this interval to Zones N10/N11. Sections 626D-11R-2 and 626D-11R, CC yielded assemblages that include *Miogypsina mexicana, Lepidocyclina canellei, L.* (*L*) *miraflorensis, Lepidocyclina* (*L*) *giraudi, Lepidocyclina* (*L*) *yuragunensis*, and *Nummulites cojimarensis*. In the Caribbean province, *Lepidocyclina* (*L*) *canellei* disappears within planktonic-foraminiferal Zones N7/N8. This indicates that this assemblage is of early Miocene age. Cores 626D-13R, CC and 626D-14R, CC contain *Miogypsina* sp. and *Lepidocyclina*

sp. Core 626D-19R, CC yields *Miogypsina* cf. *antillea* and *Heterostegina antillea*. This assemblage indicates the early Miocene. Core 626D-20R, CC contains *Miogypsina mexicana, Miogypsina gunteri, Heterostegina antillea, Gypsina* sp., *Amphistegina* sp., *Lepidocyclina (L) giraudi, Lepidocyclina (L) miraflorensis, Lepidocyclina (L) canellei, Nummulites* cf. *dia*, and *Peneroplis discoideus*. These forms indicate an early Micoene age, which agrees with the planktonic-foraminiferal age (N4). Some specimens of *Lepidocyclina* sp. and *Heterostegina* sp. are present in Cores 626D-21R, CC and 626D-23R, CC, but Core 626D-27R, CC contains only one fragment of *Lepidocyclina* sp.

It appears that the larger foraminifers of the shallow platform present in Cores 626D-11R to 626D-20R have been redeposited penecontemporaneously in deep basins.

Conclusions

Despite hole problems, sufficient material was recovered to allow the construction of a reliable composite section for the upper Oligocene through Pleistocene.

Calcareous nannofossils are generally rare in the recovered core material. Much of this material was severely washed during coring operations. Downhole contamination was a frequent occurrence, with the problem being especially acute in upper parts of the cored sections. Nannofossil reworking from older sections was also a common phenomenon. This was especially troublesome in view of the generally sparse assemblages that were recovered. As a result, nannofossils provided much poorer biostratigraphic control at this site than the planktonic foraminifers.

Planktonic-foraminiferal tests constitute the bulk of the sediments recovered at Site 626. Preservation ranges from moderately poor to good. Many of the indigenous assemblages have been modified by mixing, either by recycling of older faunas and/or by downhole contamination. Downhole mixing of foraminiferal assemblages is an obvious problem in the washed intervals of Hole 626B (Cores 1W, 2W, and 5W), making age determinations tenuous. Mixing at Holes 626C and 626D was compounded by caving and poor sediment recovery in many cored intervals. Pleistocene assemblages of Holes 626A and 626C contain reworked middle Miocene–early Pliocene taxa. Late Oligocene planktonics are recorded in the middle Miocene of Hole 626C. Several core-catcher samples appear to be size sorted. It is questionable whether this size sorting is the product of deposition and subsequent modification by bottom currents or merely an artifact of coring unconsolidated sands.

The combination of calcareous-nannofossil and planktonic-foraminiferal biostratigraphies indicates that a nearly complete Neogene section is preserved in the sediments of this site. Both late and early Pleistocene pelagic and/or hemipelagic sedimentation is recorded near the top of the sequence. A significant unconformity appears to separate the Pleistocene from the lower Pliocene (between Cores 626C-6X and 626C-7X, for example). Another unconformity may separate the upper Miocene–lower Pliocene section from the underlying middle Miocene, although the younger interval may be a condensed or reduced sequence. Sedimentation appears to have been relatively continuous from the late Oligocene through the early Miocene. It is possible that a minor break in the sedimentary record occurs within the lower Miocene (N4/N5). With the poor recovery, however, this cannot be adequately documented.

The larger benthic foraminifers found in the Site 626 material are neritic species derived from a shallow-water, platform environment. Specimens generally occur as isolated individuals as opposed to being incorporated within a limestone matrix. The larger foraminifers found in upper Oligocene to Pleistocene sediments in the four holes at Site 626 have biostratigraphic ranges that correlate with the results of other microfossil studies. This fact, and the disaggregated nature of the specimens, indicate that these specimens have been penecontemporaneously redeposited from the platform into the deep basin. An exception to this trend occurs in Core 626C-18, CC, where *Lepidocyclina canellei* was obviously reworked from older Miocene strata. However, no reworked macroforaminifers from the Eocene or Cretaceous have been recognized at Site 626.

SEDIMENT-ACCUMULATION RATES

High sediment-accumulation rates (Fig. 10) characterize much of the upper Oligocene–Pleistocene section drilled at Site 626. Pleistocene sediments recovered at Hole 626C accumulated at a rate greater than 30 m/m.y., perhaps as high as 50 m/m.y. A hiatus of about 2–2.5 m.y. separates Pleistocene from lower Pliocene sediments. A relatively thin upper Miocene–lower Pliocene section was drilled at Hole 626C, but owing to poor recovery, biostratigraphic age assignments are tentative through this interval; accumulation-rate estimates vary between 4 and 14 m/m.y. Punctuated sedimentation, erosion, and/or reduced accumulation rates have characterized late Miocene–early Pliocene time at this site. Another stratigraphic break of perhaps one to several million years separates the middle Miocene from the upper Miocene.

A relatively complete upper Oligocene through middle Miocene sequence was deposited in the Site 626 area. Average sediment-accumulation rates were high through this interval but waned with time. The upper Oligocene–lowermost Miocene (Hole 626D) accumulated at an average rate in the range of 13–35 m/m.y., the lower Miocene to lowermost middle Miocene (Hole 626D) at an average rate of 39–50 m/m.y., and the middle Miocene (Hole 626C) at a reduced rate of about 18 m/m.y.

INORGANIC GEOCHEMISTRY

Interstitial Waters

Four interstitial-water samples were taken from Hole 626C and analyzed for (Ca + Sr), total alkaline earths, alkalinity, chlorinity, salinity, and pH according to the methods described by Gieskes (1974). In addition, SO_4^{2-} was determined using ion chromatographic techniques. All samples were normalized to the IAPSO standard, and for purposes of the initial reports it will be assumed that the Sr/Ca ratio of the squeezed waters remains similar to seawater. Results of this study are presented in Table 2 and Figure 11 (surface seawater is plotted at a depth of 0 m sub-bottom).

The sampling program for this site in general, particularly for Hole 626C, was dictated by the recovery of undisturbed sediments suitable for squeezing. Therefore, considering the generally poor recovery, the distribution of samples is not particularly well suited to reflect changes in pore-water chemistry. Nevertheless, all geochemical parameters were observed to change with increasing burial (see Figs. 11 and 12). Salinity, chlorinity, alkalinity, and calcium values all increase with depth; Mg maintains a relatively constant composition, whereas pH shows a small decline.

The increase in Ca with depth is typical of that observed in other calcareous oceanic sediments (see Gieskes, 1981) and has been ascribed to the influence of the weathering of underlying basaltic material (Perry et al., 1976). Such reactions release both Ca and Mg to the pore waters, but subsequent formation of clay minerals depletes the waters in Mg. If the increase in Ca at Hole 626C is a result of alteration of igneous materials, the source for such minerals must be local or detrital, as previously published studies indicate that between 3000 and 4000 m of carbonate sediment covers the underlying igneous basement materials (Tator and Hatfield, 1975). The further possibility exists that part of

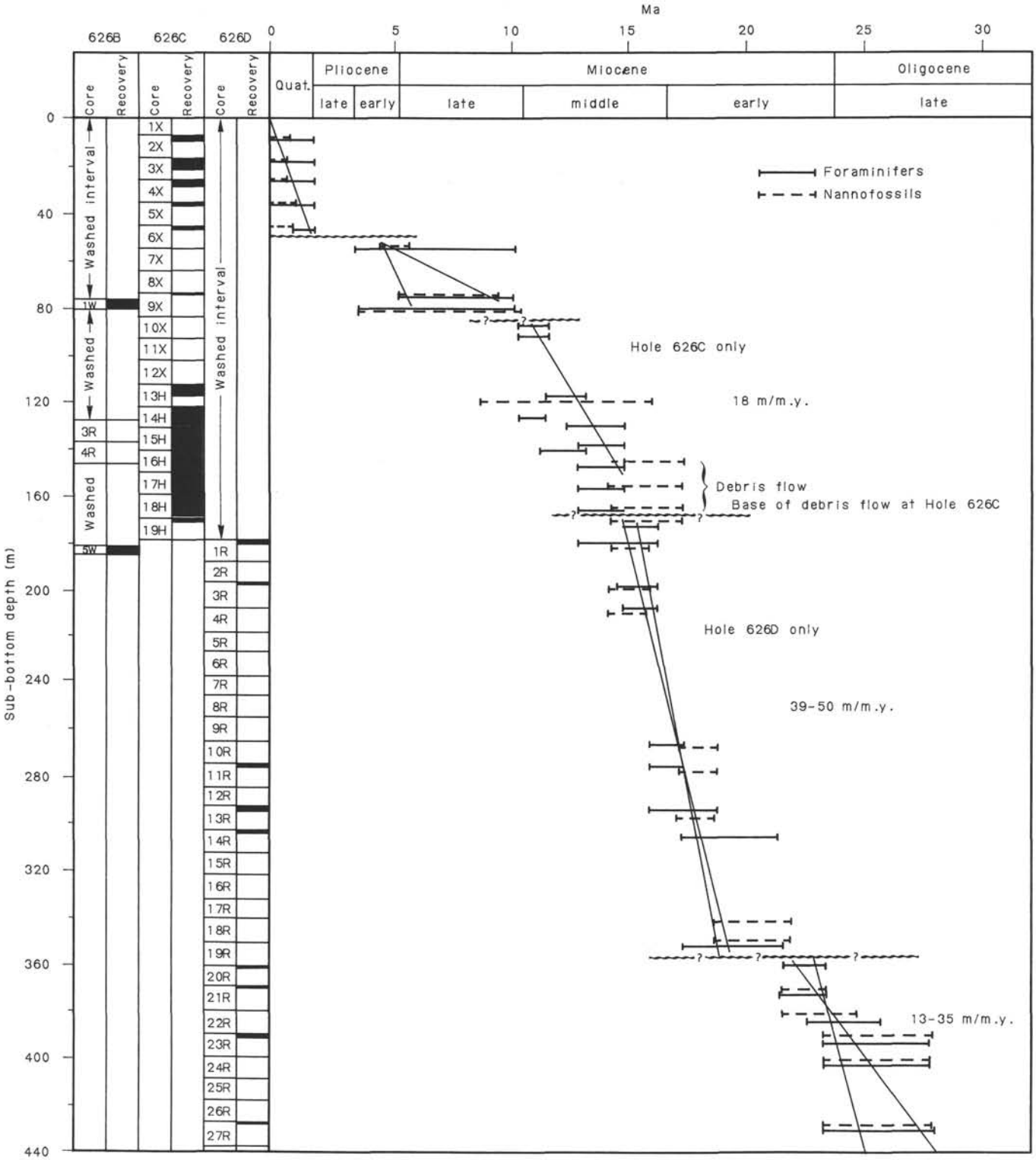

Figure 10. Sediment-accumulation rates for Site 626 (see "Biostratigraphy" section, this chapter).

the increase may be a result of changes in the concentration of Sr, as the titration method used is unable to distinguish between these two elements. Such an increase may be a result of the dissolution of aragonite, which could also raise the observed Ca concentrations, as originally proposed by Sayles and Manheim (1975). Such a theory may be confirmed by the absence of any inverse correlation between Ca and Mg, which might be expected if the model of Perry et al. (1976) is appropriate.

The precipitation of dolomite may further act to alter the Mg composition of interstitial pore waters, although it must be stressed that both concentrations of dolomite and the observed changes in Mg were extremely small.

Table 2. Analyses of interstitial waters from Hole 626C.

Sample	pH	Alkalinity (meq/kg)	Salinity (‰)	Chlorinity (‰)	Ca (mmol/L)	Mg (mmol/L)	SO_4 (mmol/L)
Surface seawater	8.20	2.25	35.5	19.11	10.27	52.53	28.21
626D-3X-3	7.83	1.81	36.4	19.41	10.13	50.99	27.78
626D-14H	7.44	3.36	37.0	19.84	14.40	52.10	26.16
626D-15H	7.38	3.28	37.5	20.13	16.22	45.46	26.17
626D-18H	7.33	3.62	38.0	20.66	14.25	52.19	28.34
IAPSO standard	8.02	2.32	35.5	19.37	10.55	53.99	28.9

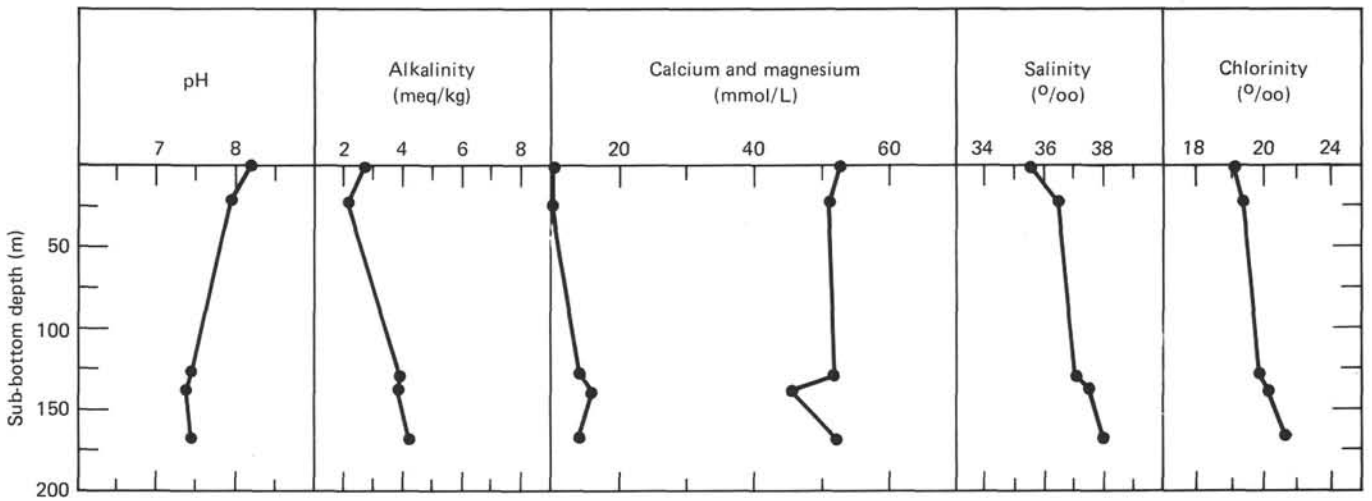

Figure 11. Interstitial-water summary, Hole 626C.

No significant gradient was observed in the SO_4^{2-} content, in spite of the obvious presence of H_2S.

X-Ray Data from Bulk Samples

Samples were taken from (1) the squeezed samples used for interstitial-water analysis from Hole 626C and (2) materials from the core catchers from Hole 626D. The results of these analyses (see Tables 3 and 4; Fig. 13) reveal that most of the sediments are now composed of low-Mg calcite, although small amounts of aragonite and high-Mg calcite were detected. In both Holes 626C and 626D, concentrations of dolomite were measured, with compositions of mol% $MgCO_3$ varying between 47% and 42%.

Carbonate-Bomb Analyses

Carbonate-bomb data from Holes 626C and 626D appear in Table 5 and Figure 14. Values range from 90% to 100% $CaCO_3$, with no trends evident.

ORGANIC GEOCHEMISTRY

Seven rock samples were taken from Site 626 for analysis, using the Rock-Eval method. Preliminary data were also obtained on some asphaltic residues found in Cores 626C-1R, CC (lower-middle Miocene) and 626C-19H, CC (lower Miocene). The Rock-Eval data are given in Table 6.

The lithology at Site 626 appears to be fairly homogeneous. The sediments consist of a series of unlithified foraminiferal-skeletal packstones and grainstones containing clasts of more lithified material. These lithologies consist almost entirely of calcium carbonate.

Rock-Eval data revealed that kerogen contained within these sands was usually immature ($T_{max} < 420°C$, reworked organic matter of type IV kerogen). These sediments were of poor source-rock character ($S_2/S_3 > 2.0$). From the production index, $S_1/(S_1 + S_2)$ of all samples (except 626D-1R, CC), there is no clear indication of generated or migrated hydrocarbons.

Sample 626D-1R, CC was anomalous in its high T_{max}, high S_2/S_3 peak ratio, and relatively high S_1 peak (see Table 5). These values, and the asymmetry of the S_2 peak, are typical of tarry, highly degraded oils that mainly contain high-molecular-weight, high-boiling-point components. The distortion of the S_2 peak is a result of components still being volatilized when pyrolysis heating is terminated.

Section 626C-19H-1 appeared to be similar visually but was retained unanalyzed for shore-based studies.

Both Sections 626C-19H-1 and 626D-1R, CC contain obvious specimens of asphalt as fine flecks, "strings," discrete grains, and as coatings on carbonate grains.

The asphalt was sparingly soluble in a trichloroethane and methanol (2/1) mixture. It did not fluoresce under ultraviolet light and consequently appeared to be heavily biodegraded.

The origin of this asphaltic material is controversial. A close examination of the textural relations of the asphalt blebs within the rock matrix shows a virtual absence of staining. Staining would be a fairly reliable guide that the asphaltic residues were formed from the migration of crude oil. An x-ray-diffraction study of the mineral matrix surrounding the asphalt grains showed that the dominant lithology was high-magnesium calcite and aragonite. These two unstable minerals, particularly the high-magnesium calcite, are highly susceptible to diagenetic alteration. Their combined presence indicates that the brines accompanying migrating oil were unlikely to have percolated through this rock. The asphalt grains are thus seen to be part of the primary depositional fabric. The implications are that the "dead oil" or asphalt found in the two zones originated from paleoseepage(s) or oil seepages into the water column during the early Miocene. This oil, after evaporation, biodegradation, and

Table 3. X-ray analyses of samples from Hole 626D.

Sample	Minerals			Composition		Comments
	Aragonite (%)	Calcite (%)	Dolomite (%)	$CaCO_3$ (%)	$MgCO_3$ (%)	
626D-1R, CC	13	87.0	0	90.25	9.73	High-Mg calcite; low-Mg calcite
626D-11R, CC	0	100.0	0	96.0	4.0	
626D-14R, CC	0	99.5	0.5	[a]53.0	[a]47.0	Low-Mg calcite
626D-17R, CC	0	98.0	2.0	[a]58.0	[a]42.0	Low-Mg calcite
626D-20R, CC	2.6	95.2	2.2	[a]58.0	[a]42.0	Low-Mg calcite
626D-23R, CC	0	96.6	3.4	[a]58.0	[a]42.0	Low-Mg calcite
626D-25R, CC	0	100.0	0	~99.0	0	Hard clast
626D-26R, CC	0	84.4	15.6	[a]55.0	[a]45.0	Low-Mg calcite
626D-28R, CC	0	100.0	0	~99.0	0	Hard clast

[a] Dolomite only.

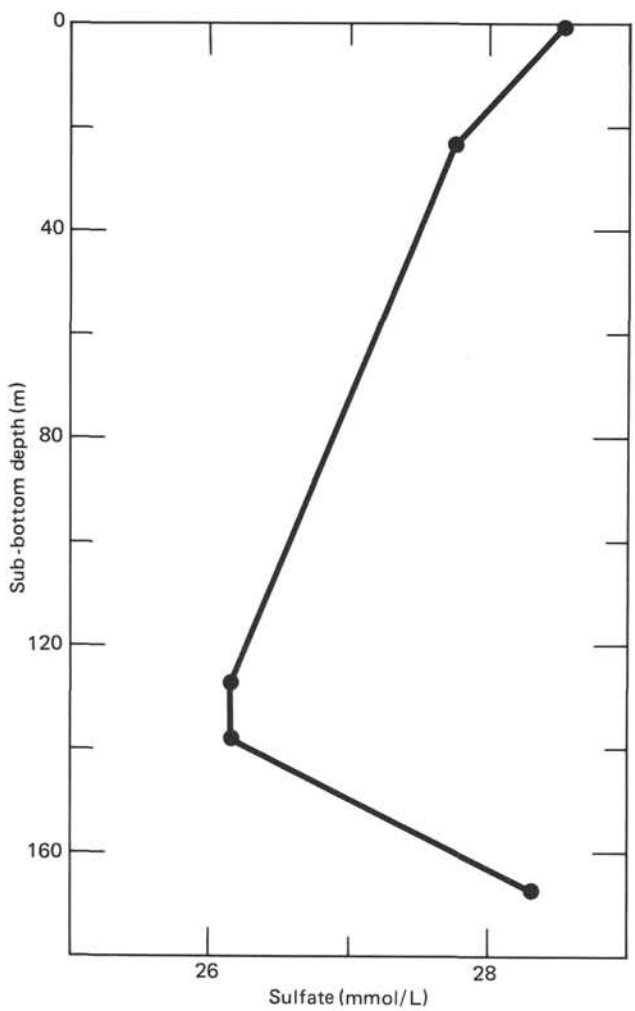

Figure 12. Sulfate vs. depth plot, Hole 626D.

mixing with inorganic material, would have become heavy enough to sink in the water column and join the depositional cycle.

Provenance of the Asphalt

Without gas-chromatography–mass-spectrometry studies of the asphalt's cycloalkane fraction, a comparative study of possible oil precursors could not be made. However, Site 626 is near the South Florida Basin, which contains the Sunniland oil fields.

Table 4. X-ray analyses of samples from Hole 626C.

Sample	Minerals			Composition	
	Aragonite (%)	Calcite (%)	Dolomite (%)	$CaCO_3$ (%)	$MgCO_3$ (%)
626C-6X	Tr	100	0	~99	0
626C-13H, CC	0	100	0	~99	0
626C-14H	0	100	Tr	[a]60	[a]40
626C-15H	0	99	1	[a]55	[a]45
626C-18H	25	75	0	~99	0

[a] Dolomite only.

If these asphalt clasts are of Sunniland oil provenance, then a tentative date for the start of oil generation in the South Florida Basin would be early Miocene at the latest.

PALEOMAGNETISM

Natural Remanent Magnetization

Thirty-four oriented paleomagnetic samples were obtained from cores recovered from Site 626. Two of these samples, consisting of carbonate sand, were taken from Core 5W of Hole 626B. The remainder were taken from calcareous sand, silt, and mud from Hole 626C. Most of the samples have magnetic moments less than 8×10^{-7} emu and thus cannot be accurately measured on the Molspin spinner magnetometer in the shipboard paleomagnetic laboratory. Whether or not useful paleomagnetic data can be gleaned from the samples is a question that must await their measurement in a more sensitive cryogenic magnetometer.

The two samples from Core 626B-5W and five samples from Core 626C-4X are a notable exception. They have much higher magnetizations, ranging from 9.6×10^{-5} to 5.1×10^{-4} emu. Their common trait is that they are samples of foraminiferal sand in which there is a significant amount of authigenic glauconite and pyrite, both iron-bearing minerals. Interestingly, four of the five samples from Core 626C-4X are reversely magnetized. Although it is believed that the sand contained in Core 626C-4X was reworked by the drilling process (see "Sedimentology," this chapter), the reversed magnetizations are most easily explained by assuming that the material was instead recovered with little disturbance. If this sand had been suspended in water and then allowed to settle out in the present geomagnetic field, a normal magnetization should have occurred.

Magnetic Susceptibility

Volume magnetic-susceptibility measurements were made on cores from Site 626 using a Bartington Instruments Model MS-1

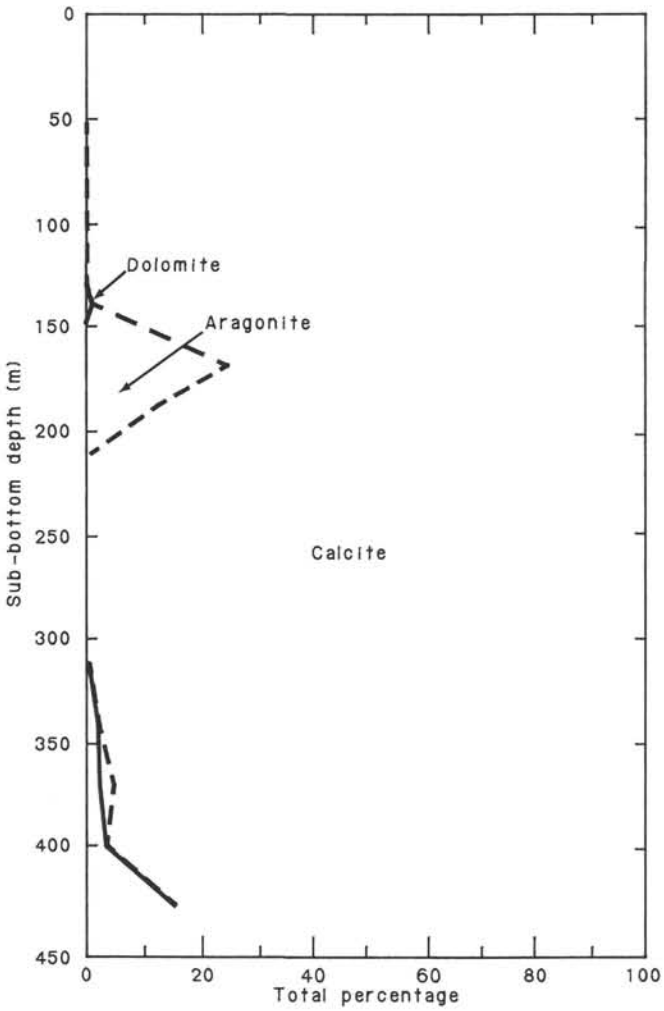

Figure 13. X-ray data, Site 626.

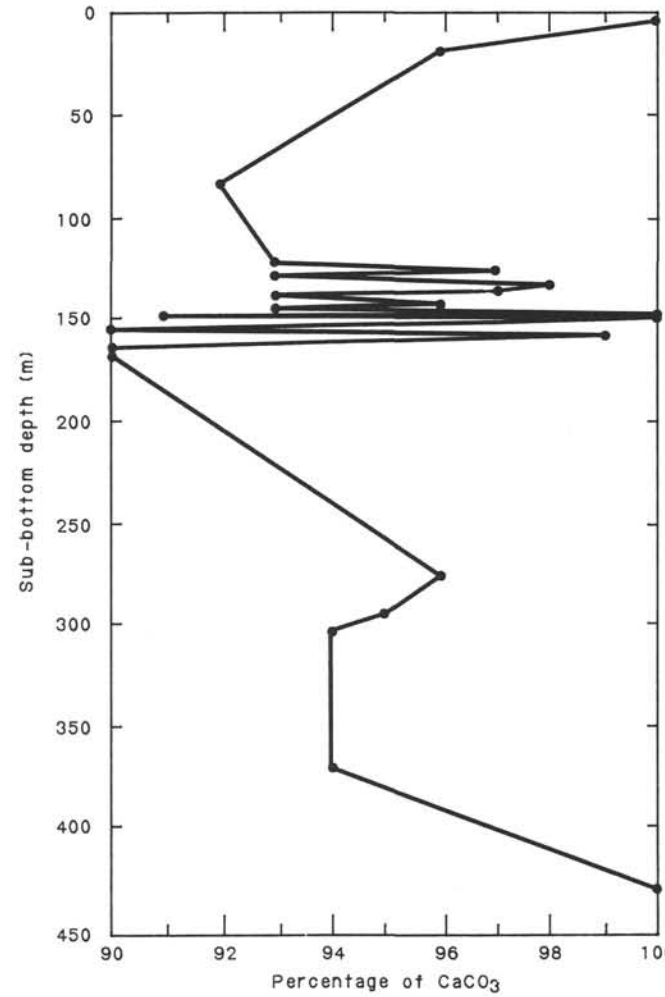

Figure 14. Carbonate-bomb data, Site 626.

Table 5. Carbonate-bomb data, Site 626.

Sub-bottom depth (m)	$CaCO_3$ content (%)
3.6	100
18.7	96
85.2	92
123.9	93
126.9	97
129.9	93
133.5	98
136.5	97
139.5	93
143.0	96
146.0	93
148.1	100
149.4	91
149.5	100
152.6	97
155.6	90
158.6	99
165.2	90
168.2	90
276.6	96
293.9	95
303.6	94
370.4	94
429.9	100

susceptibility meter with a 100-mm sensor coil through which whole cores could be passed. Measurements were taken at 10-cm intervals, from top to bottom, of each 1.5-m core section before it was split. Susceptibility readings were taken from 1 core from Hole 626A, 3 from 626B, and 10 from 626C. No measurements were made on cores from Hole 626D, as these consisted mainly of samples of long, washed intervals that were unlikely to give any reliable stratigraphic information. The susceptibility values and core mean values are plotted versus depth in Figure 15.

For reference, an empty core liner and one full of seawater were measured. As expected, the susceptibility of the empty liner was undetectable, but the seawater displayed a weak diamagnetism (i.e., negative susceptibility), registering a value of -0.4×10^{-6} gauss/oersted (G/Oe). As calcium carbonate has a diamagnetic susceptibility similar to that of water (Collinson, 1983), negative susceptibility values are taken as an indication that the cored material contains very little other than water and carbonate. Conversely, cores giving positive susceptibility readings are assumed here, as elsewhere (e.g., Radhakrishnamurty et al., 1972; Ellwood, 1980), to indicate the presence of minute amounts of iron-bearing minerals.

The few cores measured from Holes 626A and 626B all showed either diamagnetism or weak paramagnetism generally ranging from -0.4×10^{-6} to 9.3×10^{-6} G/Oe. One reading of 186.2×10^{-6} G/Oe was obtained (Core 626B-4R) owing to the inclusion in the sediment of a fragment from the drill pipe.

Table 6. Organic-geochemical (Rock-Eval) values, Site 626.

Sample (levels in cm)	S_1	S_2	S_3	T_{max} (°C)	Production index $S_1/(S_1 + S_2)$	S_2/S_3
626C-4X-1, 32–41	0.20	0.34	1.01	378	0.37	0.34
626C-6X-1, 101–110	0.14	0.12	1.20	395	0.54	0.10
[a]626C-6X-1, 101–110	0.77	1.65	2.91	390	0.32	0.57
626C-9X-1, 27–38	0.01	0.02	1.36	420	0.33	0.01
626C-13H-1, 41–50	0.36	0.21	0.78	413	0.63	0.27
626C-15H-1, 10–19	0.20	0.36	2.07	390	0.36	0.17
626D-1R, CC	0.09	0.57	0.75	480	0.14	0.76

[a] Acidified sample.
$S_1 < 0.5$ = poor oil source; 0.5–1.0 = fair; > 1.0 = oil show.
$S_2 > 2.0$ = poor oil source.
$T_{max} < 435°C$ = immature source rock.
Production index: $S_1(S_1 + S_2) < 0.1$ = immature; 0.1–0.4 = oil zone; > 0.4 = post-mature.
S_2/S_3 kerogen type < 2.5 = gas prone; 2.5–5.0 = mixed; > 5.0 = oil prone.

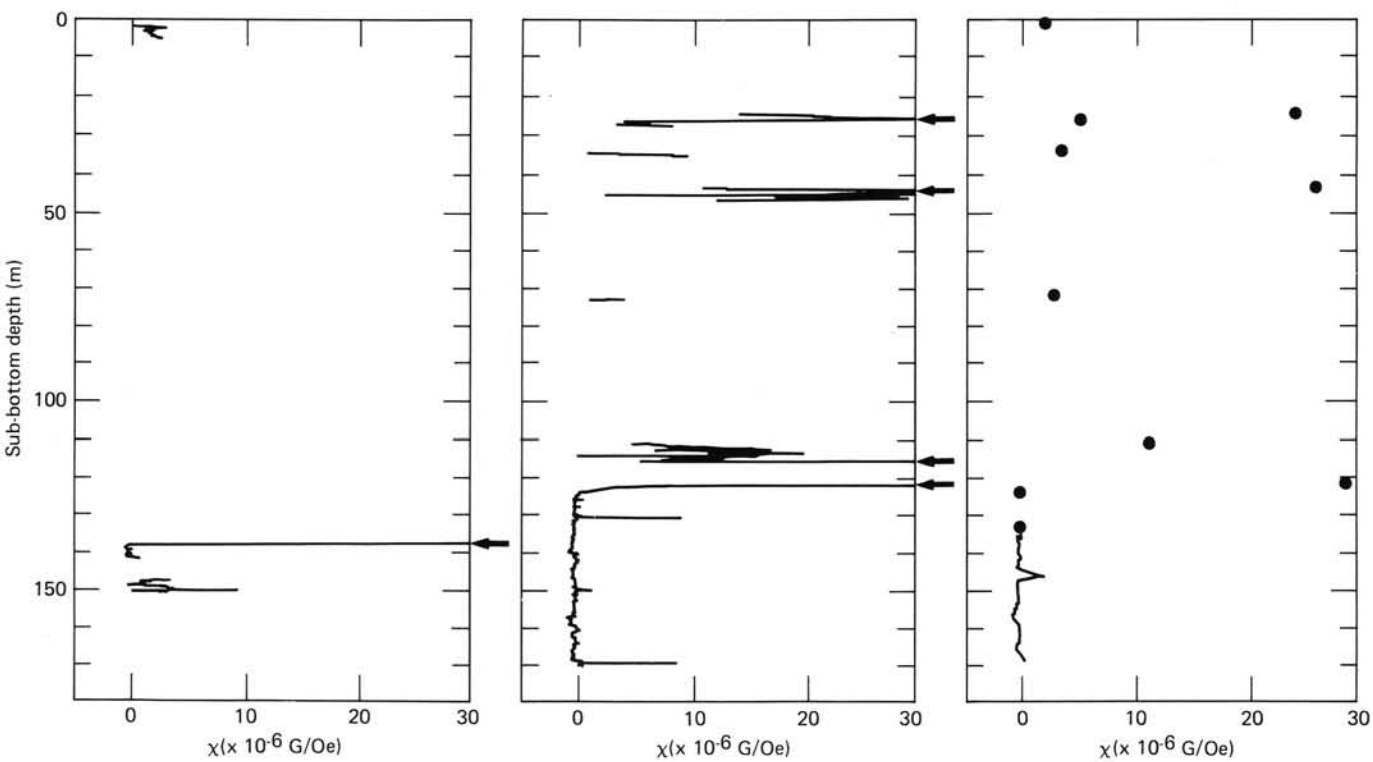

Figure 15. Susceptibility values ($\times 10^{-6}$ G/Oe) plotted vs. depth in meters. At far left are the individual measurements made at 10-cm intervals in the recovered sections of Holes 626A and 626B. The middle plot shows the individual readings from Hole 626C. A few large values do not fit on the graph and are sacrificed so that the smaller variations of suceptibility can be shown. At right the mean susceptibility value of each core is plotted against depth. Arrows indicate off-scale values.

A sharp dichotomy of magnetic behavior was noted in cores from Hole 626C. Above 122 m sub-bottom (Core 626C-13H and shallower), susceptibility values tend to be positive, large, and wildly scattered (Fig. 15). Conversely, deeper cores display a weak but consistent diamagnetism. The diamagnetic results suggest that these cores contain water and calcareous material and lack magnetic minerals. The paramagnetic readings appear to correlate with two types of sediments in particular, glauconite-rich sands and coarse-grained sands appearing as downhole contamination. As noted above, the glauconite-rich sands have strong magnetic properties. The downhole contaminants, on the other hand, probably pick up a trace of metal fragments as they are ground around the upper part of the hole by the drill string.

At the top of Section 626C-14H-1, susceptibility measurements as high as 598.8×10^{-6} G/Oe were obtained. Similarly high values of susceptibility were measured in Core 626C-13H. On examination of the split cores, both were found to contain small flakes of rusted metal. The susceptibility decreases with depth in Core 626C-14H, but it is not until Section 3 that values typical of the succeeding cores are reached. It appears that some metal contaminates both Sections 1 and 2. Although the dark metal fragments are visible to the naked eye in Section 1, they are not obvious in Section 2. Core 626C-13H and the top of Core 626C-14H have been interpreted as consisting partly or entirely of material that has fallen down the hole from above. It appears that such material is dislodged from the sides of the

hole as the drill string is raised slightly during core retrieval. When coring resumes, the contaminated material is incorporated in the upper part of the core. Higher than average susceptibility values were measured in the top few centimeters of Cores 626C-15H, 626C-17H, and 626C-19H. Even though none of these readings approached the extremely high values measured in Core 626C-14H, they suggest that the upper few tens of centimeters of most HPC cores may be slightly contaminated with metal as a result of the coring process.

PHYSICAL PROPERTIES

Physical-property measurements were made as described in the "Introduction and Explanatory Notes."

Hole 626A

Two rotary cores were recovered from Hole 626A. Since sediment disturbance was pervasive, only Gamma Ray Attenuation Porosity Evaluator (GRAPE) measurements were made. GRAPE-measured density averaged 1.9 to 2.0 g/cm^3.

Hole 626B

Three wash cores and two rotary cores were recovered from Hole 626B. Recovery was poor, and considerable sediment disturbance was evident. Although water and air pockets were present, GRAPE data were collected from all five cores. Average GRAPE density ranged from 1.85 to 2 g/cm^3. Porosity calculated from GRAPE data, assuming calcareous sediment, is 45%.

Thermal-conductivity measurements made of Cores 626B-4R and 626B-5W averaged 29.69 cal $\times$ °C^{-1} $\times$ cm^{-1} $\times$ s^{-1}.

Index-property measurements of Core 626B-5W give an average porosity of 59%, an average bulk density of 1.75 g/cm^3, an average dry water content of 51%, and an average grain density of 2.70 g/cm^3 (see Table 7).

Hole 626C

Nineteen cores were recovered from Hole 626C. Recovery was poor within the first 12 cores (XCB cores), and sediment disturbance was a problem. Thus, most of the physical-property data were measured from Cores 626C-13 through 626C-18 and are illustrated in Figure 16.

These cores contain several debris flows capped by a graded bed of rubble and sand, which is interpreted as downhole contamination (see "Sedimentology," this chapter). In the matrix-rich upper part of the debris flow (120.0–150.0 m), the expected increase and decrease of the index-property values as a result of burial compaction seem to be reflected. The tendency can be seen in Figure 16 and is also shown by the data at the base and at the top of this interval (Table 7).

Below 150 m in the sub-bottom, the debris flow comprises larger and more abundant well-lithified clasts in a soft carbonate matrix. This heterogeneous composition is recorded by the wide variation of all the physical properties. The continuous GRAPE measurements document the changes of density between the lithified clasts and the soft matrix (Fig. 17).

Compressional wave velocities were measured at 450 kHz. Measurements were made normal to the bedding plane, because samples were too soft to permit rotation for measurement in the plane parallel to bedding. Measured values are very low, indicating a high water content and low density. The lithified clast in Core 626C-17H is the only exception, with a measured velocity of 2361 m/s.

Hole 626D

The high velocity (5469 m/s) recorded from Core 626D-28R, CC was measured on a rock fragment of spar-cemented foraminiferal grainstone (Table 7).

Table 7. Physical properties of sediments, Site 626.

Sample (level in cm)	Sub-bottom depth (m)	Sonic velocity (vertical) (m/s)	Density (g/cm^3)	Dry water content (%)	Porosity (%)	Thermal conductivity (10^{-3} $\times$ cal $\times$ °C^{-1} $\times$ cm^{-1} $\times$ s^{-1})	Shear strength (kPa)	$CaCO_3$ (%)	Lithology
Hole 626B									
4R-2, 45						2.81			
5W-1, 73–76	183.4		1.70	57.1	62.0	2.73		100	Foraminiferal-skeletal grainstone
5W-2, 73–76	184.9		1.81	44.7	56.0	2.77		100	
Hole 626C									
3X-2, 70–73	22.6		1.55	78.4	68.8			96	
13X-4, 47–50	117.0		1.91	36.8	51.1				
14H-3, 70–73	125.4	1556	1.89	35.9	49.7	3.04	2.61	93	Foraminiferal-skeletal grainstone
14H-4, 70–73	126.8	3554	1.95	35.1	50.3	3.14	3.63	97	
14H-6, 70–73	129.9	1578	1.94	34.9	49.9	3.24	2.61	93	
15H-2, 70–73	133.5	1519	1.88	37.0	50.6	3.15	1.81	98	
15H-4, 70–73	136.5	1516	1.92	35.6	50.3	3.15	3.06	93	
15H-6, 70–73	139.5	1566	1.91	35.0	49.5	3.13	4.53	97	
16H-2, 70–73	143.0	1410	1.94	34.1	49.1	3.08	2.38	96	Debris flow
16H-4, 70–73	146.0	1679	1.99	31.1	46.8	3.17	9.74	93	
16H-6, 112–115	149.0	2053	1.99	30.7	46.8	3.34	9.40	91	
17H-2, 70–73	152.6		2.02	26.5	42.0	3.19	9.29	97	
17H-4, 70–73	155.6	1580	1.98	34.0	50.0	2.85	4.77	90	
17H-6, 70–73	158.6	2361	2.25	19.4	36.0	3.02		99	Lithoclast
18H-2, 70–73	162.5		1.84	41.5	53.7	2.69	3.26	90	Debris flow
18H-4, 70–73	165.5	1757	1.87	38.2	51.4	2.70	2.51	90	
18H-6, 67–70	178.5	1585	1.87	39.3	52.5	2.96	7.28		Foraminiferal packstone
Hole 626D									
11R-1, 70–73	283.1	2437	1.92	36.4	50.8				Intraclastic-skeletal-foraminiferal packstone
13R-1, 70–73	302.1		1.80	44.1	55.0				
14R-1, 70–73	312.2		1.88	38.1	51.6				
28, CC	446.0	5469							Cemented foraminiferal grainstone

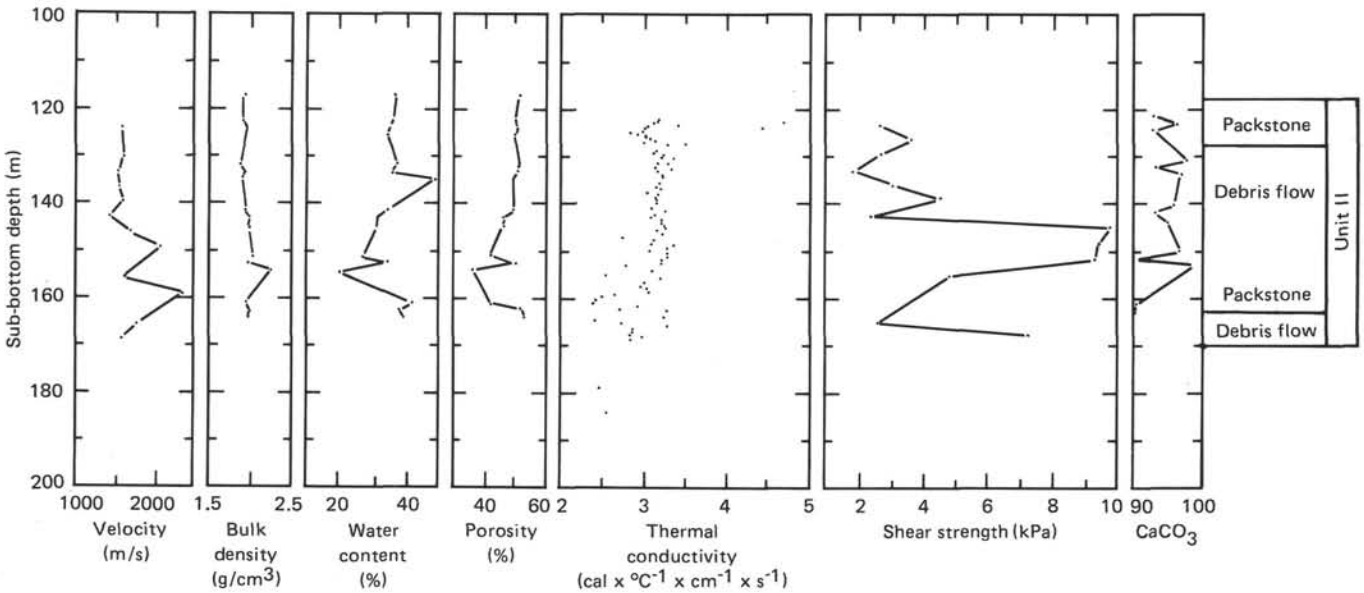

Figure 16. Graphic summary of the physical properties of lithologic Unit II from Hole 626C. Density, water content, and porosity values were determined by gravimetric and volumetric techniques.

Conclusions

For physical-property measurements such as undrained shear strength and velocity to be valid, sediment must be as close to *in-situ* conditions as possible. Thus, most values reported from Hole 626B and Hole 626D are best estimates, as many of the cores received were highly disturbed. The data reported from Hole 626C represent the best quality physical-property data from this site. These data seem to be controlled mainly by the lithologic composition of the sediment and not by burial compaction.

DOWNHOLE MEASUREMENTS

Originally, an extensive set of logging runs was planned for Hole 626D, but the hole conditions that ensnared the drill string and forced premature abandonment of the drilling program also precluded any open-hole logging, thus eliminating almost all of the planned runs. The single logging run performed was undertaken by running a Standard Gamma Ray and Compensated Neutron Tool (CNTG) combination through the drill string while the string was still in place. The CNTG yields two measurements of formation porosity through the use of a dual detector system for both thermal (ϕth) and epithermal (ϕepi) neutron counts. In a dual detector system, two pairs of detectors are placed on either side of the neutron source, and the ratio of the near detector count rate to the far detector count rate is used as a measurement of the porosity of the formation. The gamma-ray tool produces a measurement of the total formation background gamma radiation.

The logs were run at depths from 0 to 345 m sub-bottom. The presence of iron drill pipe and surrounding seawater effectively blocked much of the formation radiation, rendering the gamma-ray curve relatively useless except for its ability to indicate the location of pipe collars. The neutron log also suffered from these adverse environmental conditions, but judicious comparison with both recorded drilling rates and physical-property measurements made possible a qualitative correlation with the lithologic data.

Log Characterization

The neutron curves displayed in Figure 18 show three types of response to formation conditions. First, in zones extending from 130 to 183 m sub-bottom and 220 to 290 m sub-bottom, the thermal and epithermal porosities agree closely and yield values that average between 40% and 50%. Second, in zones extending from 20 to 50 m sub-bottom, 77 to 130 m sub-bottom, and 183 to 220 m sub-bottom, the curves separate, with the epithermal porosity averaging about 70% and the thermal porosity averaging about 55% to 60%. Third, in zones extending from 50 to 77 m sub-bottom and 290 to 345 m sub-bottom, the epithermal porosity decreases dramatically in value to a near-zero average punctuated by numerous peaks reading over 25%.

Interpretation

According to the lithologic data available from Holes 626C and 626D, the top of a large debris flow appears between 120 and 125 m sub-bottom, developing into a flow of lithified clasts in a soft packstone matrix by 130 m sub-bottom. This flow is clearly reflected in the neutron log by the appearance of one of the low-porosity zones (130 to 183 m sub-bottom). The section of graded gravel may be reflected in the log by the appearance of a continuous decrease in porosity from 119 to 122 m sub-bottom, as GRAPE measurements of the gravel section reveal a small but noticeable increase in density (decrease in porosity) with depth (see "Physical Properties" section, this chapter).

The second low-porosity zone (220 to 290 m sub-bottom) develops in a section of poor core recovery, but records of drilling speed indicate that a hard layer exists in the same interval. It naturally follows that harder carbonate material would exhibit lower porosity. The curves in this zone also exhibit a number of abrupt peaks and dips; these small-scale variations may be either a reflection of alternating hard and soft layers or an indication of variable borehole diameter.

In general, the three zones of higher porosity (20 to 50 m, 77 to 130 m, and 183 to 220 m sub-bottom) correspond to layers of soft skeletal grainstone–packstone, which can be characterized in general terms as muddy sand. In addition to exhibiting higher

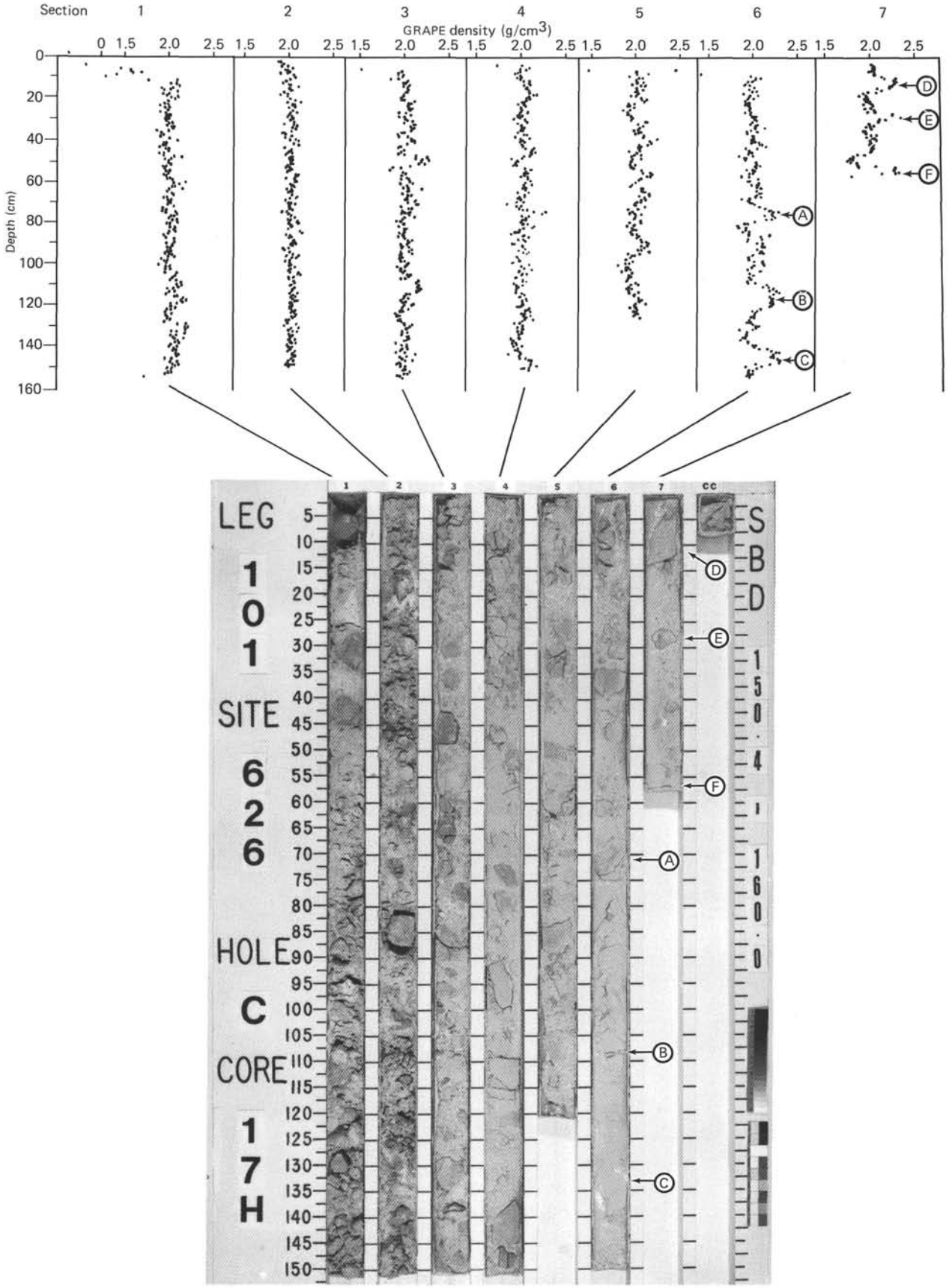

Figure 17. The continuous density log made by GRAPE on Core 626C-17 documents the changes of density between the lithified clasts (indicated by the letters *A* through *F*) and the soft matrix at the base of the debris flow.

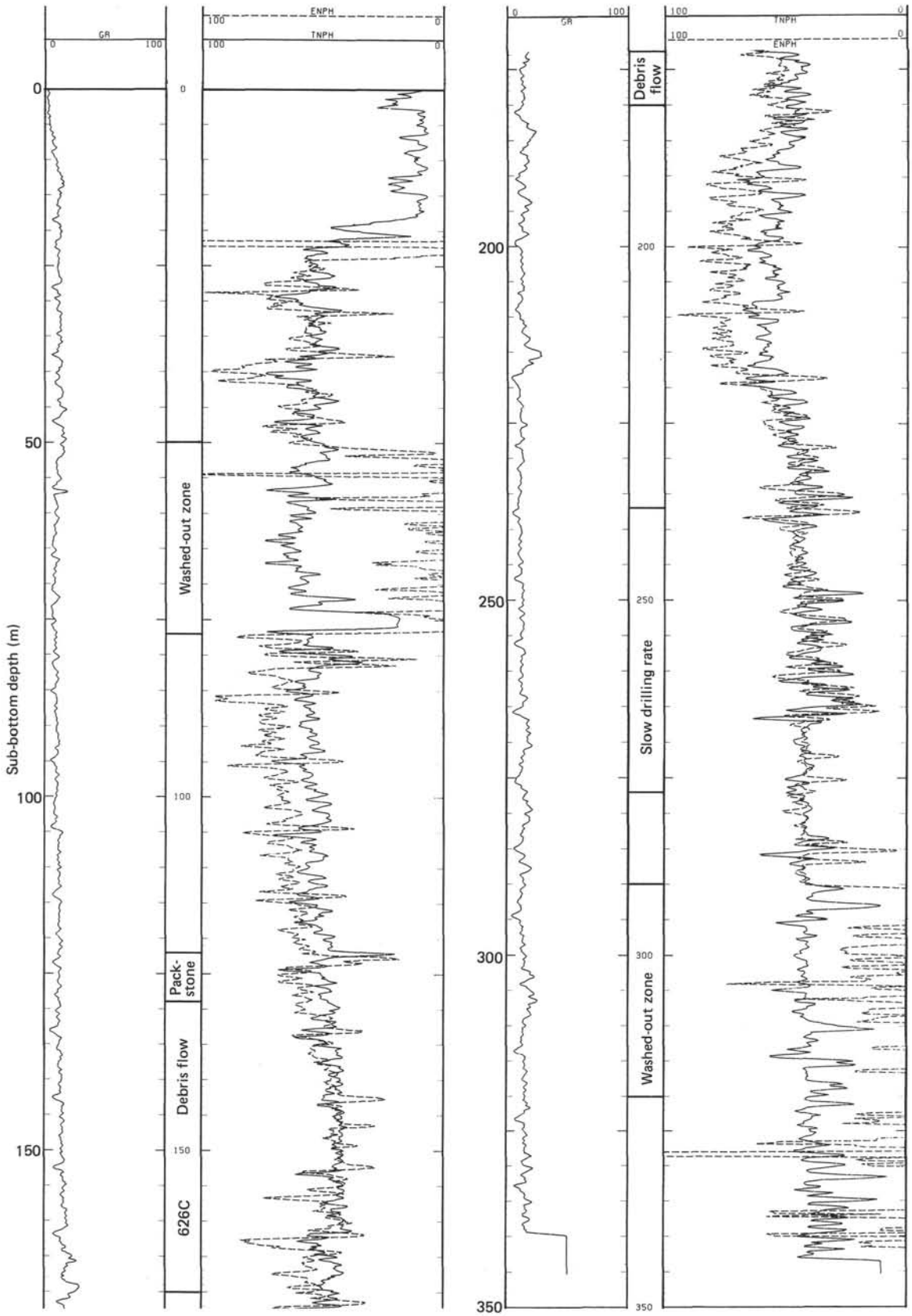

Figure 18. Neutron porosity and gamma-ray logs from Hole 626D, with prominent lithologies from Hole 626C indicated. *ENPH* stands for epithermal porosity, and *TNPH* for thermal porosity. Natural gamma radiation is given in standard API units.

porosities, these soft layers may correspond to larger hole diameters, as they are more easily disturbed by drilling. This possibility is reflected by the higher porosity given by the epithermal curve, as the epithermal detectors are more sensitive to variable borehole size than are the thermal detectors (Davis et al., 1981). For example, a tool stand-off of 2.3 in. in an 8-in.-diameter limestone borehole leads to a positive error in the epithermal porosity curve of greater than 6 porosity units (6%).

The zones with very low epithermal porosities developed as difficult problems in interpretion until an examination of the raw count-rate data was made. As the Schlumberger tool calculates porosity by taking the ratio of near detector to far detector count rates, a large ratio implies high porosity (short neutron slowing-down length), and a ratio near 1 implies low porosity (long slowing-down length). In these zones the epithermal counts were so low for both detectors that the ratios mistakenly indicated low porosity. The low count rates actually reflect a large amount of hydrogen, so these drops in the epithermal curve should correspond to zones that have experienced significant washout. Consequently, the porosity curves are of little value in the depth ranges from 50 to 77 m sub-bottom and from 290 to 345 m sub-bottom. As the beginning of the proposed chert layer is at 322.2 m sub-bottom (see "Sedimentology" section, this chapter), the logs are unable to provide any information about its existence.

SEISMIC STRATIGRAPHY

Introduction

Site 626 was the culmination of an effort that began in April 1984, when the University of Texas Institute for Geophysics (UTIG) vessel *Fred H. Moore* collected approximately 250 n. mi of 24-trace, 12-fold seismic-reflection profiles as a site-specific survey for drilling in the Straits of Florida (Fig. 4). Sonobuoys were also collected for additional velocity control.

The next step in preparing for Leg 101 took place at Lamont-Doherty Geological Observatory (LDGO), where semblance velocity analyses were carried out every 10 common depth points (CDP) (approximately every 180 m) on all seismic lines on which a prospective Straits of Florida site had been designated: FS-02, FS-04, FS-08, FS-14, FS-17, FS-19, and FS-21 (Fig. 4). These velocities were then available for time-to-depth conversions of sequence boundaries identified within the grid.

Through the fall of 1984, all Straits of Florida lines were interpreted according to the principles set forth by Vail et al. (1977). Eleven seismic sequences above the basal velocity discontinuity were identified and mapped (see Fig. 3). Using the detailed velocity calculations, isopach and structure maps for each sequence and bounding acoustic horizon were prepared at UTIG.

Site 626

As a result of 4 drilling attempts near BAH-1-C (Holes 626A through 626D), 6 of 11 mapped seismic sequences (10, 9, 8, 7, 6, and 5) and 5 (perhaps 6) of 11 sequence boundaries (11/10?, 10/9, 9/8, 8/7, 7/6, and 6/5) were encountered (Fig. 3). The following is an interpretation of the physical basis for these seismic features. At the outset, it should be noted that, as a result of early dynamic-positioning problems (see "Operations Summary," this chapter), all four of the penetrations at Site 626 were approximately 1.0 n. mi north-northeast of the originally designated site position (Fig. 4, inset). Fortunately, Holes 626B, 626C, and 626D were located within 0.25 n. mi of FS-08, CDP 700, which also happened to be the crossing of that seismic line with LDGO multichannel seismic profile 92 (Fig. 4; Sheridan et al., 1981). A comparison of the Site 626 correlations with line 92 is made at the end of this discussion.

Hole 626A

Hole 626A penetrated only 12.8 m of lime rubble and sand, which translates to less than 0.02 s of travel time below water bottom at the water velocity characteristic of sequence 10 (Fig. 3 and Table 8). No sequence boundaries could be resolved at this depth with the site-survey profiles. The fact that spud in could not be completed at Hole 626A was ultimately fortunate from the standpoint of seismic correlation, because Holes 626B, 626C, and 626D were all close to each other and closer to seismic control than was Hole 626A (Fig. 4, inset).

Holes 626B Through 626D

Introduction

Holes 626B through 626D lie approximately 0.25 n. mi east of line FS-08, CDP 700 (Fig. 19). In order to make an indirect assessment of the local depth variation of pertinent sequence boundaries across that gap, their depths were calculated at points 0.25 n. mi *along* FS-08 in both directions from point 700 (CDP 675 and CDP 725, Fig. 19). Those results are tabulated below (depths are sub-bottom):

Sequence boundary	CDP 700 depth	CDP 675-725 depth range
10/9	88 m	86–90 m
9/8	187 m	164–187 m
8/7	213 m	206–213 m
7/6	334 m	327–342 m
6/5	360 m	359–374 m

Hole 626B

Hole 626B penetrated 185.5 m sub-bottom. Recovery was only 8% because most of the section was washed. Core 626B-4R did recover 73% of the interval between 137.7 and 147.3 m sub-bottom, and this section was tied to Samples 626C-16H-1 through 5, 0–40 cm, but both the 10/9 and 9/8 sequence boundaries are contained within washed intervals. However, based on the nannofossil and foraminifer dates obtained for Core 626B-1W (80.27 m sub-bottom), all of the sequence boundaries listed above must be older than late Miocene–early Pliocene.

Holes 626C and 626D

By means of XCB and HPC techniques, Hole 626C sampled to 179.3 m sub-bottom with an overall recovery of 37%. The XCB (Cores 626C-1X through 626C-12X) recovered 11% to 112.1 m sub-bottom, whereas the HPC recovered 80% of the interval from 112.1 to 179.3 m sub-bottom. As a complement to Hole 626C, Hole 626D was washed to 179.4 m sub-bottom, where continuous rotary coring began and continued to 446.8 m sub-bottom. Unfortunately, recovery in this cored interval was only 3%, but the two holes together provide the best stratigraphic record available from Site 626 for comparison with the regional seismic data.

Three lithologic units were recognized ("Sedimentology" section, this chapter). Within Unit I, an alternating sequence of skeletal grainstones and packstones, only two depositional breaks can be documented. The first separates lower Pliocene (Core 626C-7X) from lower Pleistocene (Core 626C-6X) sediments between 54.3 and 63.9 m sub-bottom. The 11/10 sequence boundary could not be recognized in the vicinity of BAH-1-C because of poor near-bottom resolution and/or erosion, but we tentatively correlate 11/10 with the early Pliocene–early Pleistocene hiatus.

The second break within Unit I occurs between 83.0 m sub-bottom (Core 626C-9X) and 102.4 m sub-bottom (Core 626C-

Table 8. Seismic stratigraphy and velocity structure of site-survey profile FS-08 at its closest point of approach to Holes 626B, 626C, and 626D.

Sequence	Sequence boundary	Depth below sea level (m)	Sequence thickness (m)	Cumulative thickness: sub-bottom depth (m)	Sequence velocity (km/s)
10			88		1.5
	10/9	939		88	
9			99		1.98 ± 0.05
	9/8	1038		187	
8			26		2.11 ± 0.02
	8/7	1064		213	
7			121		2.11 ± 0.02
	7/6	1185		334	
6			26		2.11 ± 0.02
	6/5	1211		360	
5			102		2.11 ± 0.02
	5/4	1313		462	

Water depth = 851 m (multichannel seismics), 839 (3.5 kHz); total depth = 447 m sub-bottom; total sediment thickness to original target = 1213 m; total depth below sea level to original target = 2064 m.

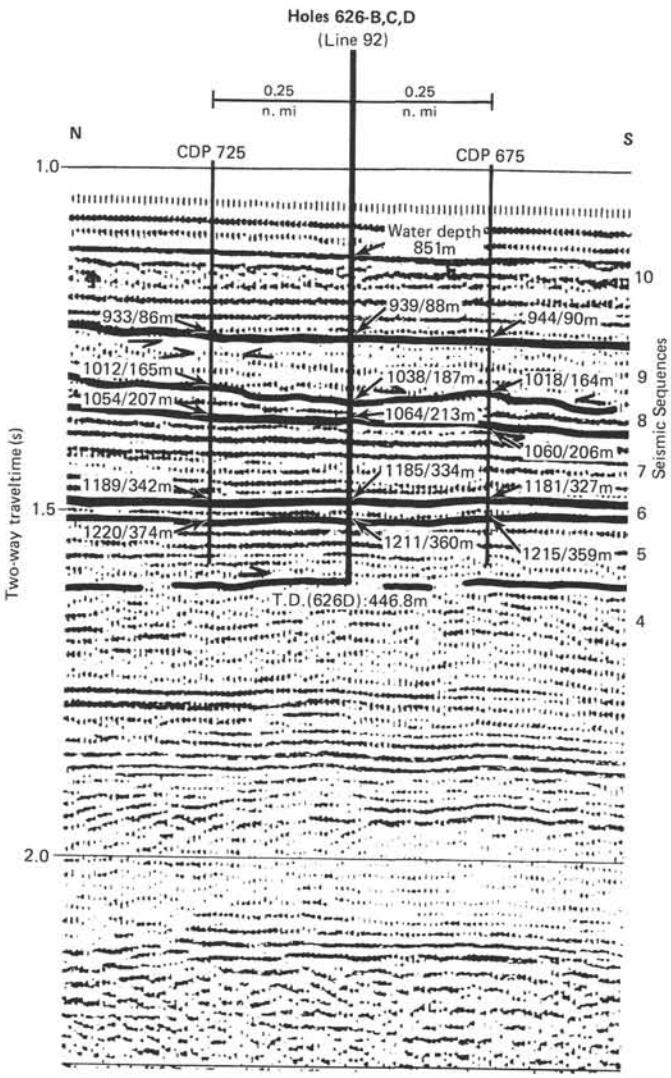

Figure 19. Portion of multichannel seismic line FS-08 (see Fig. 3) closest to Holes 626B, 626C, and 626D. CDP 700 is the calculated point of closest approach, ~0.25 n. mi.

11X). It coincides both with a shift in faunal assemblages (from middle Miocene to upper Miocene) and a change in depositional rates ("Sediment-Accumulation Rates," this chapter). This hiatus was tied to the 10/9 sequence boundary.

Unit II (121.7 to 169.6 m sub-bottom) is composed of gravity-flow deposits, implying rapid, episodic deposition. Biostratigraphic evidence suggests a constant age throughout Unit II. The only break in this pattern is noted when the earliest middle Miocene age obtained from Core 626C-19H, CC (179.3 m sub-bottom) is compared with the middle Miocene or slightly older age from Core 626D-1R (189.0 m sub-bottom), suggesting either significant downhole contamination in Core 626D-1R or at least 9.7 m of depositional relief. If the section immediately underlying the debris flows had been disturbed by their emplacement, some mixing of faunas could be explained, perhaps partially resolving the biostratigraphic complexity. By correlating the 9/8 sequence boundary (Table 8) with the base of the oldest debris flow at 169.6 m sub-bottom, erosion of the underlying sequence is suggested. First, its calculated depth range correlates with the base of the flow sequence. Second, 9/8 displays 23 m of relief over 0.25 n. mi, more than any other sequence boundary encountered at Site 626 (Table 8), thereby indicating its erosional nature. Furthermore, the map of the depth to this surface (Fig. 20) indicates relief of more than 200 m over the 400 mi^2 covered by the site-survey grid. Finally, by making 9/8 the base of the flows, the acoustic sequence between 9/8 and 10/9 must correlate with the flows themselves, and these sediments would indeed be expected to produce the observed seismic facies: hummocky, with little internal reflector continuity.

Correlating sequence boundaries within Unit III (169.6 to 446.8 m sub-bottom) becomes more problematic because of the poor recovery in this interval in Hole 626D. The entire unit is composed of unlithified intraclastic–skeletal–foraminiferal packstone alternating with lithified foraminiferal/foraminiferal–skeletal packstone and grainstone, including some cemented shallow-water-platform debris. The interval velocity for Unit III is 2.11 km/s at FS-08, CDP 700 (Table 8), but we recovered numerous limestone fragments with compressional wave velocities of 2.0 to 2.4 km/s (Hamilton Frame measurements). One sample of lithified, spar-cemented limestone at the base of Core 626D-28R yielded a velocity greater than 5 km/s, so an alternation of hard and soft layers seems likely for this part of the section. This would also explain the acoustic response of Unit III: high-amplitude, parallel, continuous reflectors (seismic sequences 5 through 8; Table 8).

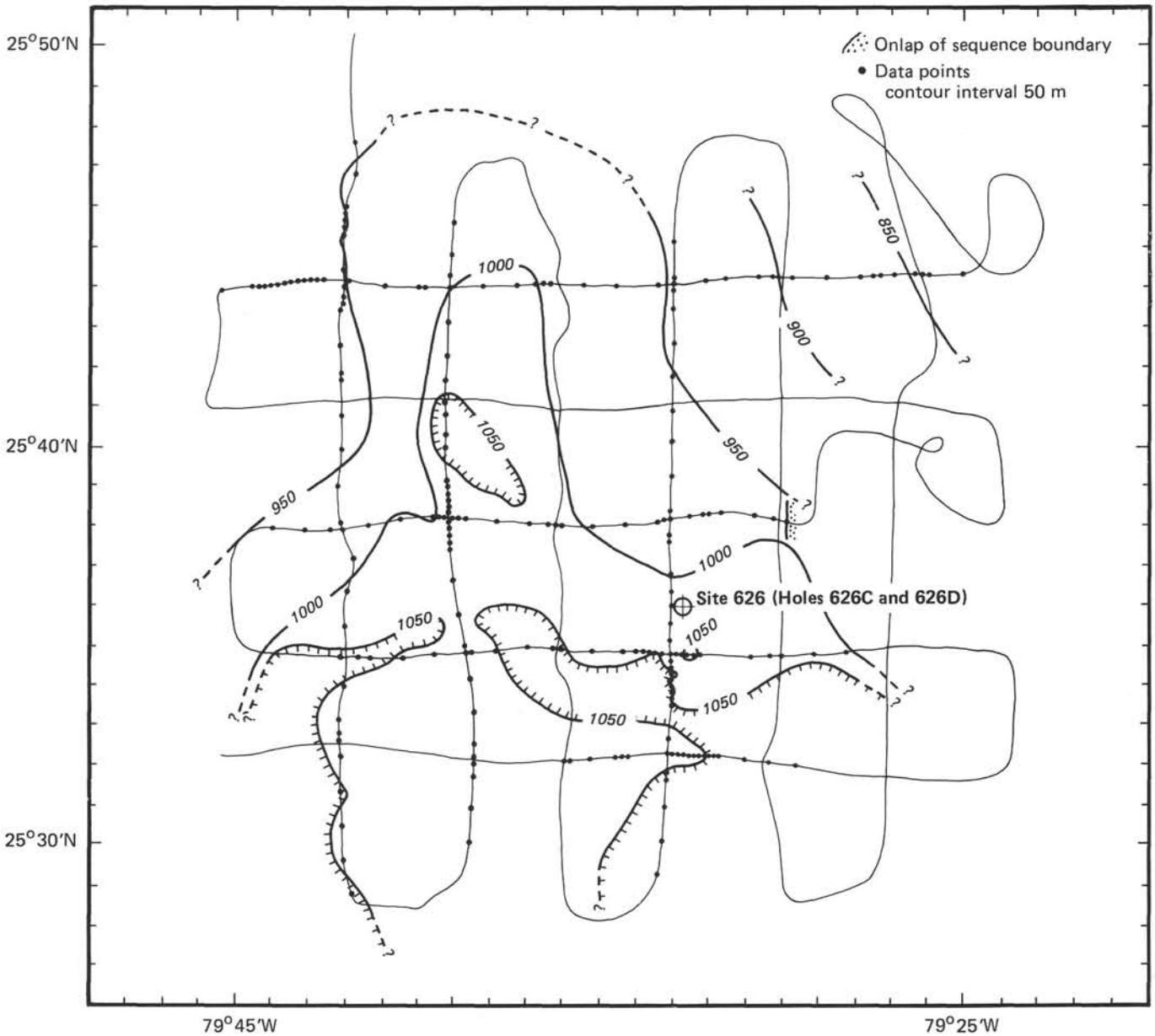

Figure 20. Structure map of seismic-sequence boundary 9/8, interpreted as the base of the middle Miocene debris flows sampled at Site 626.

Neither lithology nor biostratigraphy allows any correlation with the 8/7 sequence boundary. Based on its calculated depth on FS-08, this acoustic horizon should have been encountered in Core 626D-4R, but only a core-catcher sample was recovered and no biostratigraphic gap is evident. However, the neutron log shows a pronounced decrease in formation porosity (from 75%–80% to 55%) in the interval 210–230 m sub-bottom ("Downhole Measurements," this chapter), and this suggests a concomitant density increase and perhaps the impedance contrast that produces 8/7. If that is the case, 8/7 must be early to middle Miocene in age.

Both the recovery of limestone and chert fragments in Cores 626D-16R, 626D-17R, 626D-19R, 626D-20R, and 626D-27R and a decrease in drilling rates ("Summary and Conclusions," this chapter) suggest that the interval from 327.4 to 370.4 m sub-bottom in Hole 626D is partly lithified. Both the 7/6 (327–342 m sub-bottom) and 6/5 (356–382 m sub-bottom) sequence boundaries fall in this range, suggesting that both acoustic horizons correlate with the presence of lithified limestones–packstones–grainstones in an otherwise soft sequence of contourite sediments. However, the fact that both 7/6 and 6/5 are correlative as sequence boundaries over 400 n. mi^2 of the subsurface of the Straits of Florida argues for their primary character, i.e., as unconformities, perhaps as surficial hardgrounds, and against a purely diagenetic origin through subsurface cementation.

In summary, 5 (and perhaps 6, if 11/10 is included) sequence boundaries and 6 sequences were sampled at Site 626. The available evidence suggests the following conclusions (refer to Fig. 21):

1. Sequence boundaries 11/10 and 10/9 correspond to a latest early Pliocene–early Pleistocene and a middle Miocene–late Miocene hiatus, respectively. This raises the question of correlation of these hiatuses with the global cycles of relative changes of sea level originally proposed by Vail et al. (1977). One of the original goals of Leg 101 was to test the applicability of Vail's cycles in carbonate environments. In the Straits of Florida, fluc-

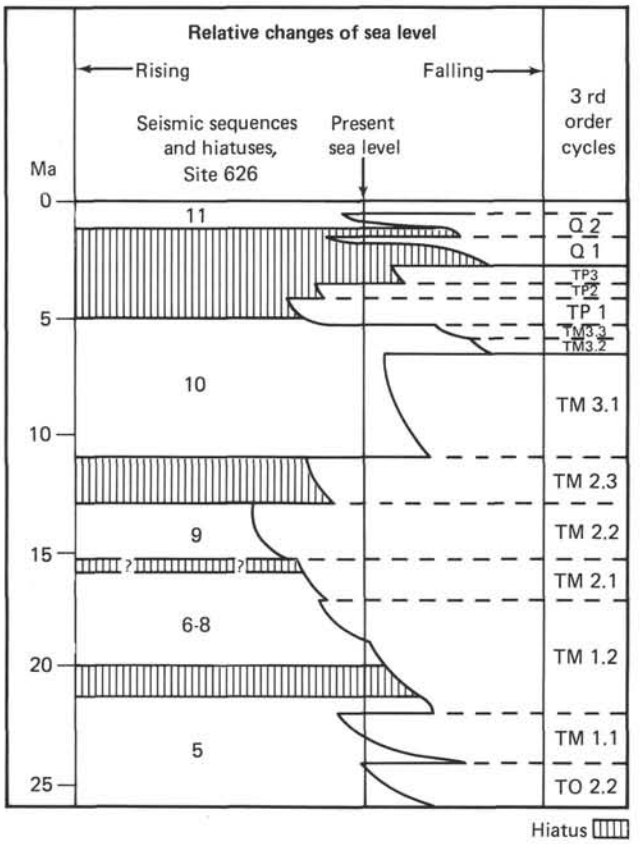

Figure 21. Hiatuses and boundaries of seismic stratigraphic sequences at Site 626, correlated with the third-order cycles of the Vail et al. (1977) sea-level curve.

tuations in sea level should have had a direct effect on the intensity of Gulf Stream circulation, with lowstands presumably intensifying current erosion by decreasing the effective cross-sectional area of the Straits, thereby creating unconformities that should subsequently show up as seismic-sequence boundaries. This appears to be at least partly corroborated by results at Site 626. The latest early Pliocene–early Pleistocene hiatus, which is here tied to 11/10, represents the interval from 5 to 15 Ma. This time interval effectively spans the TP3/Q1 cycle transition (lowstand) at 2.8 Ma (Vail et al., 1977; Fig. 21) and marks an extended period of low sea level (Vail and Hardenbol, 1979).

2. The middle Miocene–late Miocene hiatus at Site 626 encompasses the time interval 12.1–10.2 Ma, although it could be longer. Therefore, erosion at sequence boundary 10/9 can be attributed to the TM2.3/TM3.1 lowstand at 9.8 Ma within Vail et al.'s (1977) supercycle Tc and Vail and Hardenbol's (1979) supercycle Te.

3. Sequence boundary 9/8 ties to the base of a series of middle Miocene debris flows. These flows are a prevalent feature of the middle Miocene section in the western North Atlantic region ("Sedimentology" section, this chapter), but their cause is a mystery. At Site 626, dated material within the flows spans the time interval 15.5–13 Ma. A pronounced lowstand occurring at Vail's TM2.2/TM2.3 cycle transition at 13 Ma, perhaps acting in concert with some kind of tectonic event, could have been the generating mechanism for these extensive deposits, which incorporated older material as they traveled into the Straits. Erosion created by the passage and deposition of the flows presumably produced 9/8 but left the depositional record largely intact.

4. Sequence boundary 8/7 corresponds to a pronounced decrease in formation porosity in the lower to middle Miocene. We cannot ascertain anything else about this surface with the information available.

5. Boundaries 7/6 and 6/5 probably represent lower Miocene cherty zones–hardgrounds intercalated with an unlithified series of contourite deposits. Both horizons coincide with the extended lowstand in cycle TM1.2 of Vail et al. (1977; Fig. 21).

Site 626 and LDGO Line 92

Correlations between line 92, a large-volume air-gun profile, and the higher resolution site-survey results are not straightforward, but one preliminary conclusion is clear. The Straits of Florida sequence drilled at Site 626 is considerably younger than believed by Sheridan et al. (1981). The youngest unconformity interpreted on line 92 in the Straits is interpreted to separate the upper Eocene from the upper Oligocene section, but approximately corresponds in traveltime to the 8/7 boundary, an early to middle Miocene horizon at Site 626. Site 626 bottoms at 1.6 s in the upper Oligocene, while line 92 suggests that this part of the section is middle to late Eocene in age, a discrepancy of some 20 m.y.

SUMMARY AND CONCLUSIONS

Four holes were drilled at Site 626. Two of them (626C and 626D) were scientifically important. Together they penetrated 447 m of deep-water carbonate sediments of Pleistocene to Oligocene age ("Sedimentology" and "Biostratigraphy," this chapter). From top to bottom, the sequence consists of three major units of formation rank (Fig. 22): (1) Unit I, skeletal carbonate sands, muddy or clean, composed of planktonic foraminifers and neritic skeletal grains from the platforms, middle Miocene to Pleistocene, 122 m; (2) Unit II, muddy lime rubble, graded rubble and sand, and muddy sand, interpreted as debris flows and turbidites with intercalations of pelagic sediment, middle Miocene, 48 m; and (3) Unit III, skeletal carbonate sands as in Unit I with numerous intercalations of lithified layers (skeletal grainstones and packstones), late Oligocene to middle Miocene, 277 m.

We interpret Units I and III as contourite deposits of the Gulf Stream. This current presently sweeps the drill site with bottom velocities of 20-40 cm/s (Brooks, 1979). It has evidently existed in similar strength since the Oligocene, winnowing most of the planktonic and platform-derived carbonate mud and mixing the remaining globigerinid sands with the coarse residue of neritic turbidite material. Poor recovery makes a decision impossible both as to whether all of Units I and III are contourite deposits and what the exact proportions of planktonic and neritic material are.

Unit II interrupts the contourite record in a rather dramatic way. During an interval of 4 m.y. in the middle Miocene, debris flows and turbidites were emplaced too rapidly to be reworked by the bottom current. Unit II has the highest mud content and contains debris flows in pristine condition. Timing and inferred depositional processes of this unit closely resemble those of the coeval Abaco Member of the Bermuda Rise Formation in the western North Atlantic Ocean (Benson, Sheridan, et al., 1978; Sheridan, Gradstein, et al., 1983). Material in sediment gravity flows of Unit II points to sources on the adjacent platform, on its flanks, and on the floor of the Straits of Florida. The synchroneity with the "Abaco episode" in the western North Atlantic suggests a common trigger. The relatively long duration of the event makes tectonism a likely candidate, even though environmental factors such as fluctuating sea level cannot be ruled out.

The effects of diagenesis are demonstrated in various ways. The number and thickness of hard layers in Units I and III increase with depth. Interstitial-water analyses suggest some dissolution of calcium carbonate with depth, and x-ray-diffraction

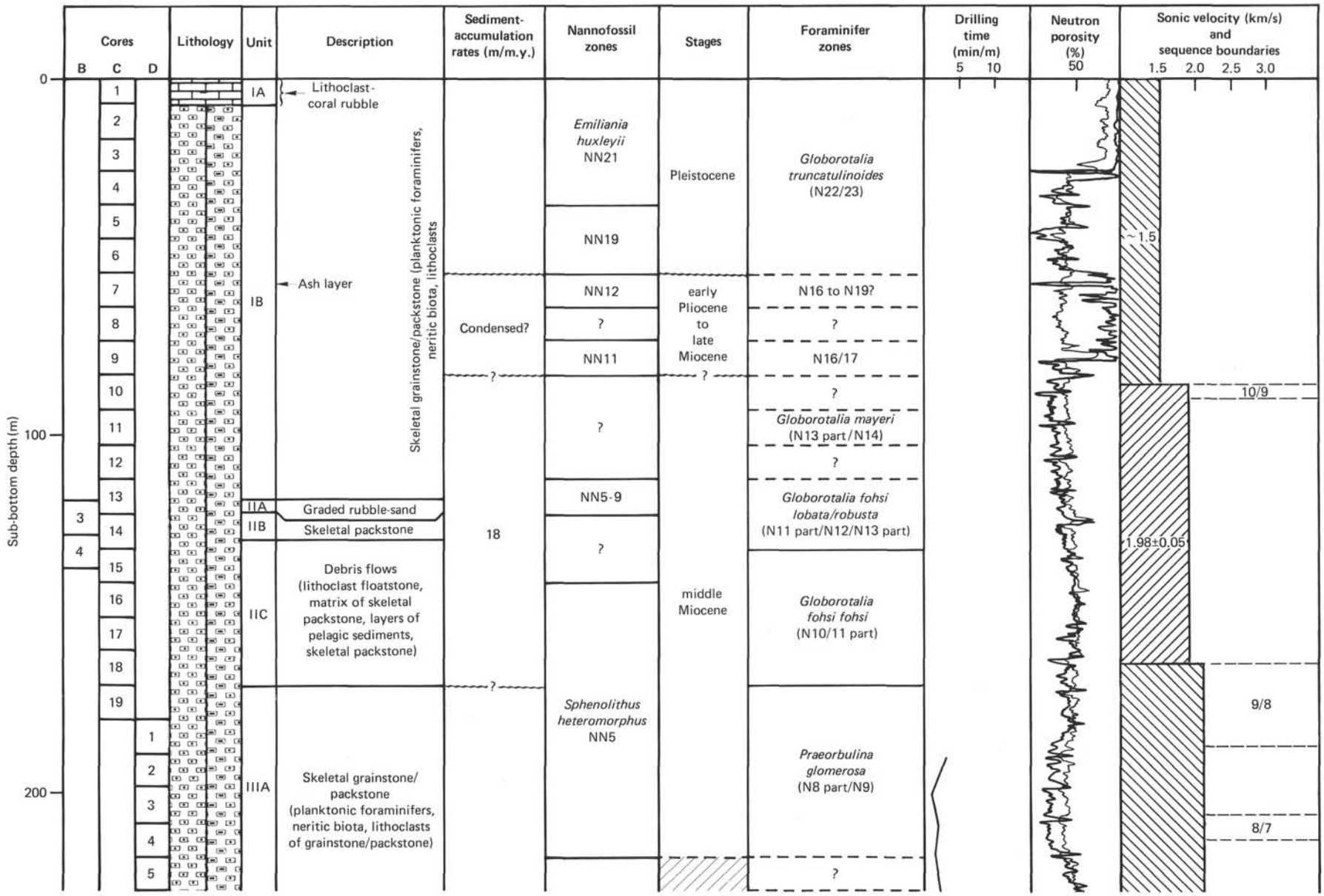
Cores
B
C
D
Lithology
Unit
Description
Sediment-accumulation rates (m/m.y.)
Nannofossil zones
Stages
Foraminifer zones
Drilling time (min/m)
5 10
Neutron porosity (%)
50
Sonic velocity (km/s) and sequence boundaries
1.5 2.0 2.5 3.0
Sub-bottom depth (m)
0
100
200
IA
Lithoclast-coral rubble
IB
Ash layer
Skeletal grainstone/packstone (planktonic foraminifers, neritic biota, lithoclasts
IIA
Graded rubble-sand
IIB
Skeletal packstone
IIC
Debris flows (lithoclast floatstone, matrix of skeletal packstone, layers of pelagic sediments, skeletal packstone)
IIIA
Skeletal grainstone/packstone (planktonic foraminifers, neritic biota, lithoclasts of grainstone/packstone)
Condensed?
18
Emiliania huxleyii NN21
NN19
NN12
?
NN11
?
NN5-9
?
Sphenolithus heteromorphus NN5
Pleistocene
early Pliocene to late Miocene
middle Miocene
Globorotalia truncatulinoides (N22/23)
N16 to N19?
?
N16/17
?
Globorotalia mayeri (N13 part/N14)
?
Globorotalia fohsi lobata/robusta (N11 part/N12/N13 part)
Globorotalia fohsi fohsi (N10/11 part)
Praeorbulina glomerosa (N8 part/N9)
?
~1.5
10/9
1.98±0.05
9/8
8/7

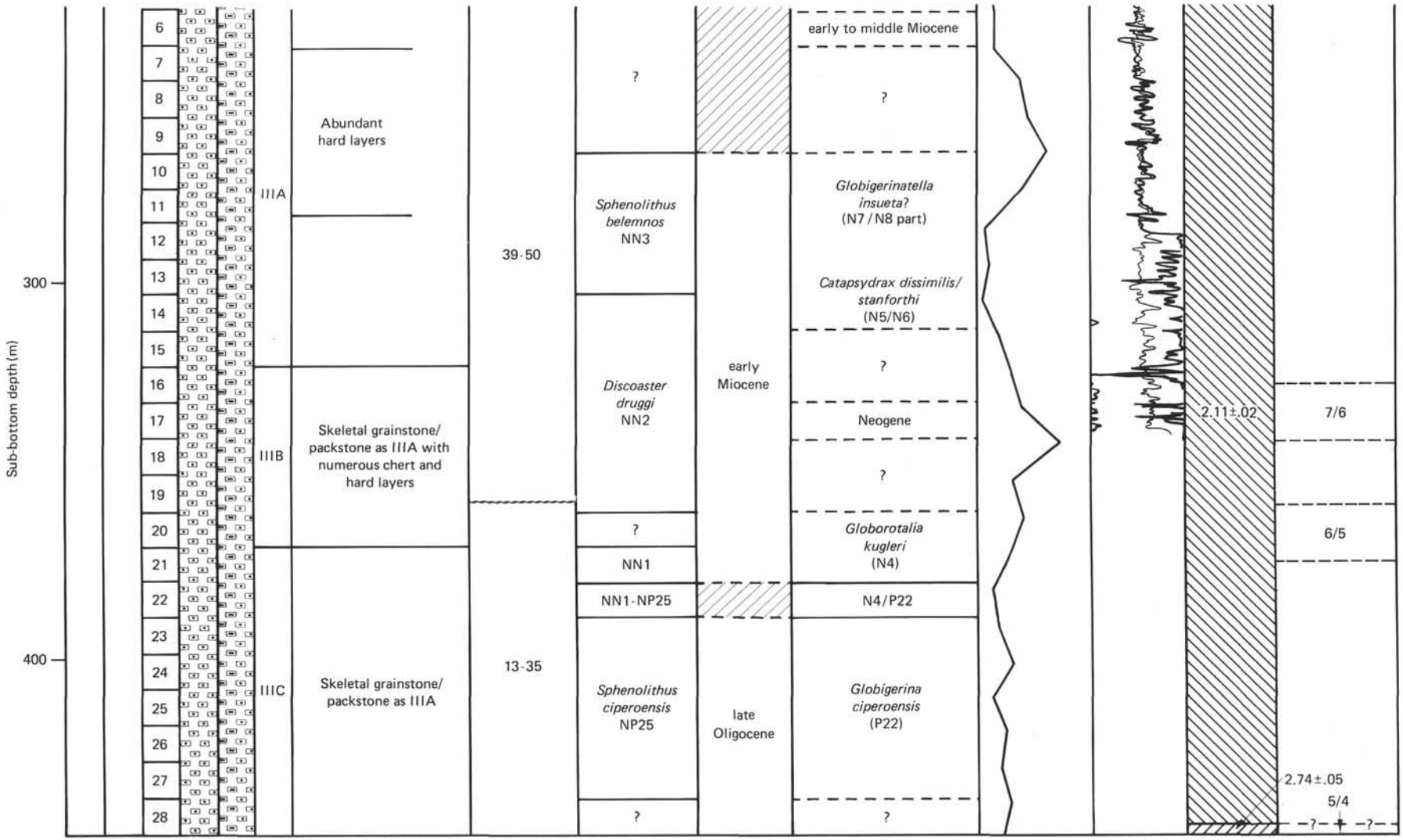

Figure 22. Summary of data from Site 626.

analysis indicates downhole disappearance of aragonite and magnesian calcite, along with precipitation of calcite cement and some dolomite. However, most of these processes are unexpectedly slow. Magnesian calcite is still present in lower Miocene sediments at 275 m, and aragonite occurs even deeper in the hole. The muddy sediments of Unit II are essentially unlithified, whereas the coeval Abaco Member in the western North Atlantic consists of chalk and limestone. Downhole measurements of physical properties indicate only an insignificant decrease in porosity and sonic velocity of the loose material. The neutron log confirms this observation with regard to porosity. The causes for the retardation of diagenesis remain obscure.

Organic matter in the sequence was scarce and immature, with the exception of flecks and strings of asphalt in middle Miocene skeletal grainstone (Core 626C-19H, CC). This "dead oil" must have originated deeper in the section. It may represent the reworked material of a seepage or the degraded residue of a former accumulation.

Borehole stratigraphy, in conjunction with physical-property measurements and wireline logs, provides some good ties with the seismic stratigraphy developed during the site survey. The alternation of soft and hard layers in the contourite units is consistent with the high-amplitude reflectors observed in these intervals. The interpretation of some seismic patterns as sediment waves, although these were not sampled, has been strengthened by the recovery of extensive contour-current deposits. Finally, the hypothesis that a global lowstand of relative sea level would have caused erosion within the consequently narrower, shallower Straits of Florida received some corroboration.

Even though Site 626 did not reach the mid-Cretaceous target, a comparison of Site 626 and the Great Isaac well (I. Bourgeois, G. Mackenzie, W. Schlager, unpubl. data) provides arguments in favor of the "megabank" hypothesis, which holds that Florida and the Bahama Banks formed a single, unsegmented platform until mid-Cretaceous time. Mid-Miocene and older rocks at Sites 626 and Great Isaac seem to be connected by layer-cake stratigraphy without offset. Oligocene and Miocene sediment facies in the two wells are also similar (Fig. 23). The 850-m relief currently existing between the two wells apparently developed during the late Miocene–Pliocene, when the margin of Greater Bahama Bank prograded westward to its current position. This strongly suggests that the unsampled "target" reflector at Site 626 corresponds to the boundary of Albian platform carbonates and Cenomanian pelagic chalks at Great Isaac. These mid-Cretaceous platform carbonates appear to represent the drowned top of the Florida–northwestern Bahamas megabank.

However, the mid-Cretaceous drowning of the megabank was not complete, which is borne out by continuous shallow-water sequences in the Andros 1 and Cay-Sal IV-1 wells (Paulus, 1972)

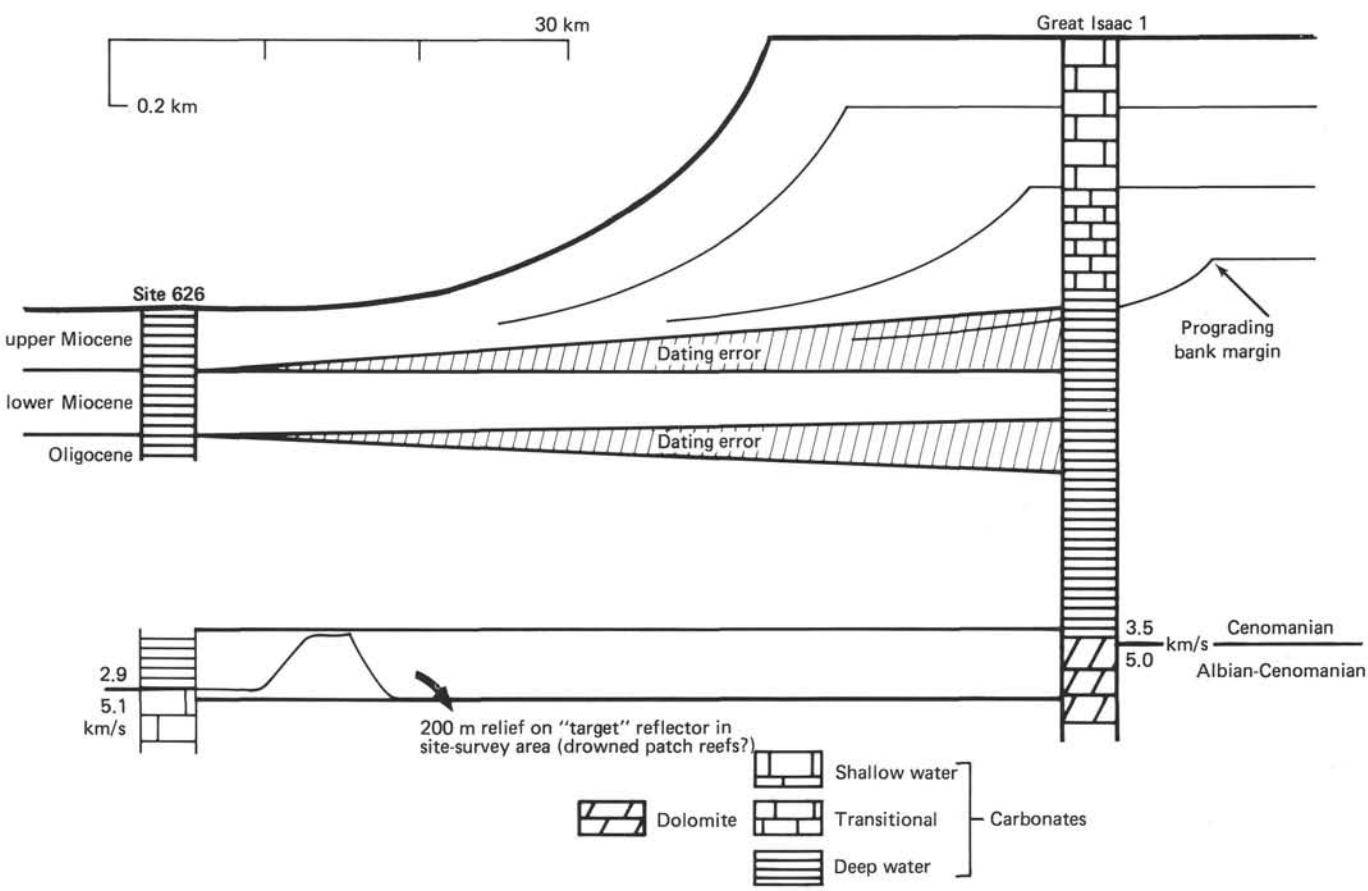

Figure 23. Correlation of stratigraphy at Site 626 with seismic stratigraphy in the Straits of Florida and with the Great Isaac 1 well on Great Bahama Bank. Heavy lines represent factual information; thin lines are interpretations. The Great Isaac well complements results of seismic surveys and drilling at Site 626. Horizontal time lines between Great Isaac and ODP Site 626 argue against fault control of the present bank margin. A similar elevation of drowned bank top in the Great Isaac well and a prominent seismic reflector in the Straits support the interpretation of this reflector as the top of a Cretaceous platform (the "megabank"). The succession of facies encountered in the Great Isaac well indicates mid-Cretaceous drowning, followed by Tertiary progradation of the bank margin.

as well as sections on the Bahama Escarpment (Freeman-Lynde et al., 1981). By the late Oligocene, these surviving platforms had risen more than 500 m above the seafloor in the Straits of Florida. This is indicated by a comparison of the elevation of late Oligocene–early Miocene deposits in the Straits and in the Andros and Cay-Sal wells. Furthermore, seismic reflector 5/4 (Oligocene) can be traced from the bottom of Hole 626D to the top of the Oligocene platform on the Miami Terrace, 800 m higher (Freeman-Lynde et al., 1981).

REFERENCES

Benson, W. E., Sheridan, R. E., et al., 1978. *Init. Repts. DSDP*, 44: Washington (U.S. Govt. Printing Office).

Bliefnick, D. M., Robertson, A. H. F., and Sheridan, R. E., 1983. Deposition and provenance of Miocene intraclastic chalks, Blake-Bahama Basin, western North Atlantic. *In* Sheridan, R. E., Gradstein, F. M., et al., *Init. Repts. DSDP*, 76: Washington (U.S. Govt. Printing Office), 727–748.

Brooks, I. H., 1979. Fluctuations in the transport of the Florida Current at periods between tidal and two weeks. *J. Phys. Oceanogr.*, 9: 1048–1053.

Buffler, R. T., 1984. Early history and structure of the deep Gulf of Mexico basin [paper presented at the Gulf Coast SEPM Research Symposium, Austin, TX].

Buffler, R. T., et al., 1981. A model for the early evolution of the Gulf of Mexico basin. *In Geology of Continental Margins Symposium*: Proc. 26th Int. Congr., *Oceanol. Acta*, C3:120–136.

Butterlin, J., and Moullade, M., 1983. Redeposited and/or reworked larger benthic Foraminifera from Miocene debris flows, Blake-Bahama Basin (western North Atlantic), Deep Sea Drilling Project Legs 44 (Site 391) and 76 (Site 345). *In* Sheridan, R. E., and Gradstein, F. M., et al., *Init. Repts. DSDP*, 76: Washington (U.S. Govt. Printing Office), 645–650.

Collinson, D. W., 1983. *Methods in Rock Magnetism and Palaeomagnetism*: London (Chapman and Hall).

Davis, R. R., Hall, J. E., Boutemy, Y. L., and Flaum, C., 1981. A dual porosity CNL* logging system. *Soc. Pet. Eng. Reprint* 10296.

Ellwood, B. B., 1980. Induced and remanent magnetic properties of marine sediments as indicators of depositional processes. *Mar. Geol.*, 38:233–244.

Freeman-Lynde, R., Cita, M. B., Jadoul, F., Miller, E. L., and Ryan, W. B. F., 1981. Marine geology of the Bahama Escarpment: *Mar. Geol.*, 44:119–156.

Gieskes, J. M., 1974. Interstitial water studies, Leg 25. *In* Simpson, E. S. W., Schlich, R., et al., *Init. Repts. DSDP*, 25: Washington (U.S. Govt. Printing Office), 361–394.

———, 1981. Deep-sea drilling interstitial water studies: Implications for chemical alteration of the oceanic crust, Layers 1 and 2. *SEPM Spec. Publ.*, 32:149–167.

Hollister, C. D., Ewing, J. I., et al., 1972. *Init. Repts. DSDP*, 11: Washington (U.S. Govt. Printing Office).

Meyerhoff, A. A., and Hatten, C. W., 1974. Bahamas salient of North America. *In* Burk, C. A., and Drake, C. L. (Eds.), *The Geology of Continental Margins*: New York (Springer-Verlag), 429–446.

Mullins, H. T., and Lynts, G. W., 1977. Origin of the northwestern Bahama platform: review and reinterpretation. *Geol. Soc. Am. Bull.*, 88:1447–1461.

Paulus, F. J., 1972. The geology of Site 98 and the Bahama Platform. *In* Hollister, C. D., Ewing, J. I., et al., *Init. Repts. DSDP*, 11: Washington (U.S. Govt. Printing Office), 877–897.

Perry, E. A., Jr., Gieskes, J. M., and Lawrence, J. R., 1976. Mg, Ca and O^{18}/O^{16} exchange in the sediment-pore water system, Hole 149, DSDP. *Geochim. Cosmochim. Acta*, 40:413–423.

Radhakrishnamurty, C., Likhite, S. D., Amin, B. S., and Somayajulu, B. L. K., 1972. Magnetic susceptibility stratigraphy in ocean sediment cores. *Earth Planet. Sci. Lett.*, 4:464–468.

Sayles, F. L., and Manheim, F. T., 1975. Interstitial solutions and diagenesis in deeply buried marine sediments: results from the Deep Sea Drilling Project. *Geochim. Cosmochim. Acta*, 39:103–127.

Schlager, W., Austin, J. A., Jr., et al., 1984. Early Cretaceous platform re-entrant and escarpment erosion in the Bahamas. *Geology*, 12: 147–150.

Schlager, W., Buffler, R. T., Angstadt, D., and Phair, R., 1984. Geologic history of the southeastern Gulf of Mexico. *In* Buffler, R. T., Schlager, W., et al., *Init. Repts. DSDP*, 77: Washington (U.S. Govt. Printing Office), 715–738.

Schlager, W., and Ginsburg, R. N., 1981. Bahama carbonate platforms—the deep and the past. *Mar. Geol.*, 44:1–24.

Sheridan, R. E., 1974. Atlantic continental margin of North America. *In* Burk, C. A., and Drake, C. L. (Eds.), *Geology of Continental Margins*: New York (Springer-Verlag), 391–407.

Sheridan, R. E., Crosby, J. T., Bryan, G. M., and Stoffa, P. L., 1981. Stratigraphy and structure of southern Blake Plateau, northern Florida Straits, and northern Bahama Platform from multichannel seismic reflection data. *AAPG Bull.*, 65:2571–2593.

Sheridan, R. E., Gradstein, F. M., et al., 1983. *Init. Repts. DSDP*, 76: Washington (U.S. Govt. Printing Office).

Talwani, M., Worzel, J. L., and Ewing, M., 1960. Gravity anomalies and structure of the Bahamas. *2nd Caribbean Geol. Conf. Trans.*, Univ. Puerto Rico, 156.

Tator, B. A., and Hatfield, L. E., 1975. Bahamas represent complex geology. *Oil Gas J.*, 73(43):172–176; 73(44):120–122.

Vail, P. R. and Hardenbol, J., 1979. Sea level changes during the Tertiary: *Oceanus*, 22:71–80.

Vail, P. R., Mitchum, R. M., Jr., and Thompson, S., III, 1977. Seismic stratigraphy and global changes of sea level, Part 4: Global cycles of relative changes of sea level. *In* Payton, C. E. (Ed.), *Seismic Stratigraphy—Applications to Hydrocarbon Exploration*: AAPG Mem., 26: 83–97.

SITE 626 HOLE A CORE 1R CORED INTERVAL 848.0-849.4 mbsl; 0.0-1.4 mbsf

TIME-ROCK UNIT	BIOSTRAT. ZONE / FOSSIL CHARACTER: FORAMINIFERS	NANNOFOSSILS	RADIOLARIANS	DIATOMS	PALEOMAGNETICS	PHYSICAL PROPERTIES	CHEMISTRY	SECTION	METERS	GRAPHIC LITHOLOGY	DRILLING DISTURB.	SED. STRUCTURES	SAMPLES	LITHOLOGIC DESCRIPTION
PLEISTOCENE	C/M *Globorotalia truncatulinoides* Zone (N22/N23) C/P	C/M NN21				ρ = 1.8 - 1.9		1 CC	0.5 1.0	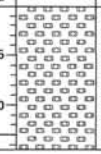	X X X X X X X X X			UNLITHIFIED RUDSTONE, normally graded (is probably an artifact of drilling disturbance) UNLITHIFIED RUDSTONE throughout the core, white (10YR 8/1), major components are ahermatypic coral fragments, bivalve fragments, echinoid spines, *Halimeda*, serpulids, bryozoans, *Homotrema*, planktonic foraminifers, and clasts.

Information on Core Description Forms, for ALL sites, represents field notes taken aboard ship. Some of this information has been refined in accord with post-cruise findings, but production schedules prohibit definitive correlation of these forms with subsequent findings. Thus the reader should be alerted to the occasional ambiguity or discrepancy.

SITE 626 HOLE A CORE 2R CORED INTERVAL 849.4-860.8 mbsl; 1.4-12.8 mbsf

TIME-ROCK UNIT	BIOSTRAT. ZONE / FOSSIL CHARACTER: FORAMINIFERS	NANNOFOSSILS	RADIOLARIANS	DIATOMS	PALEOMAGNETICS	PHYSICAL PROPERTIES	CHEMISTRY	SECTION	METERS	GRAPHIC LITHOLOGY	DRILLING DISTURB.	SED. STRUCTURES	SAMPLES	LITHOLOGIC DESCRIPTION
PLEISTOCENE	A/G *Globorotalia truncatulinoides* Zone (N22/23)	C/M NN21				ρ = 1.7 - 1.9	● 100%	1 2 CC	0.5 1.0	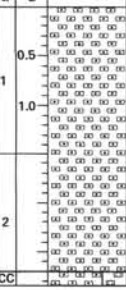			*	UNLITHIFIED GRAINSTONE and minor UNLITHIFIED RUDSTONE, high water content; graded, possibly an artifact of drilling disturbance UNLITHIFIED GRAINSTONE in Section 1, 68-150 cm, white (2.5Y 8/2), fine grained, 70% foraminifers, 30% other skeletal grains, some glauconitic foraminiferal test molds, in Sections 2, 3, and the CC, 0-6 cm, white (2.5Y 8/2), coarser grained than above. UNLITHIFIED RUDSTONE with CHALK clasts (2 cm diameter) in lower 6 cm of the CC. SMEAR SLIDE SUMMARY (%): 2,75 D TEXTURE: Sand 100 COMPOSITION: Glauconite Tr Skeletal Fragments 50 Foraminifers 50

SITE 626 HOLE B CORE 1W CORED INTERVAL 918.6-928.3 mbsl; 70.6-80.2 mbsf

TIME-ROCK UNIT	BIOSTRAT. ZONE / FOSSIL CHARACTER: FORAMINIFERS	NANNOFOSSILS	RADIOLARIANS	DIATOMS	PALEOMAGNETICS	PHYSICAL PROPERTIES	CHEMISTRY	SECTION	METERS	GRAPHIC LITHOLOGY	DRILLING DISTURB.	SED. STRUCTURES	SAMPLES
EARLY PLIOCENE	A/G *Globorotalia margaritae/Neogloboquadrina acostaensis* Zone (N16/N19 part)	NN11 F/M						1, 2, 3, CC	0.5, 1.0				*

LITHOLOGIC DESCRIPTION

UNLITHIFIED GRAINSTONE. Core was water-saturated upon recovery, and grading may be an artifact.

UNLITHIFIED GRAINSTONE throughout the core, light gray (5Y 7/1), medium to coarse sand with foraminifers (some glauconite-filled) and skeletal debris, fining upwards.

SMEAR SLIDE SUMMARY (%):

	1,80 D	2,80 D
TEXTURE:		
Sand	100	100
COMPOSITION:		
Glauconite	5	5
Foraminifers	80	75
Skeletal Fragments	20	25

SITE 626 HOLE B CORE 2W CORED INTERVAL 966.5-976.1 mbsl; 118.5-128.1 mbsf

TIME-ROCK UNIT	BIOSTRAT. ZONE / FOSSIL CHARACTER: FORAMINIFERS	NANNOFOSSILS	RADIOLARIANS	DIATOMS	PALEOMAGNETICS	PHYSICAL PROPERTIES	CHEMISTRY	SECTION	METERS	GRAPHIC LITHOLOGY	DRILLING DISTURB.	SED. STRUCTURES	SAMPLES
LATE MIDDLE MIOCENE	A/P *Globorotalia mayeri(=siakensis)* Zone (N13 part/N14)							CC					

LITHOLOGIC DESCRIPTION

Empty core liner

LITHIFIED GRAINSTONE fragments, light gray (5Y 7/1), up to 5 cm in size recovered from the CC. Planktonic foraminifers constitute predominant grain type.

CORE 3 NO RECOVERY

SITE 626 HOLE B CORE 4R CORED INTERVAL 985.7-995.3 mbsl; 137.7-147.3 mbsf

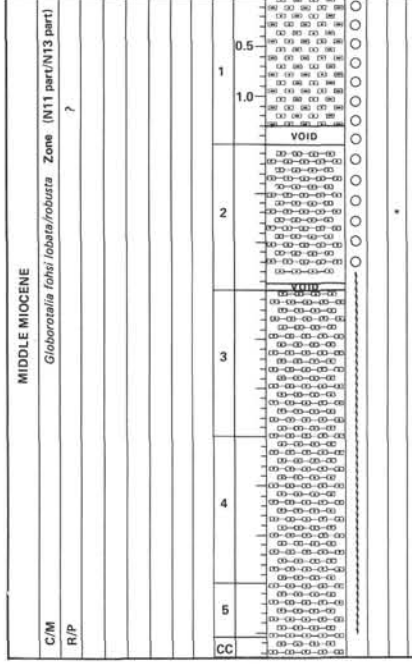

LITHOLOGIC DESCRIPTION

PARTIALLY LITHIFIED GRAINSTONE and UNLITHIFIED PACKSTONE, high water content throughout, hydrogen sulfide odor

PARTIALLY LITHIFIED GRAINSTONE, light gray (10YR 7/2), occurs from Section 2, 0 cm, to the base of the core. Coarsest grains are clasts and skeletal fragments, sand grains are predominantly planktonic foraminifers. Sediment is partially indurated, approaching chalk.

UNLITHIFIED PACKSTONE, pinkish gray (7.5YR 6/2), occurs in Section 1, 0-130 cm, possibly a drilling artifact.

SMEAR SLIDE SUMMARY (%):

	2,70
	D
TEXTURE:	
Sand	80
Silt	20
COMPOSITION:	
Micrite	20
Clasts	10
Foraminifers	70

SITE 626 HOLE B CORE 5W CORED INTERVAL 1023.9-1033.5 mbsl; 175.9-185.5 mbsf

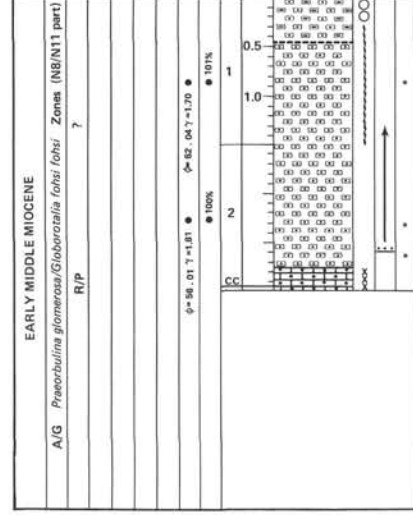

LITHOLOGIC DESCRIPTION

UNLITHIFIED GRAINSTONE, UNLITHIFIED PACKSTONE, and LITHIFIED GRAINSTONE, graded (possibly an artifact of drilling).

UNLITHIFIED GRAINSTONE, light gray (2.5Y 7/2), occurs from Section 1, 45 cm, to Section 2, 125 cm. Grain size is medium to fine, with foraminifers and bioclastic grains predominant.

UNLITHIFIED PACKSTONE, light gray (2.5Y 7/2), is present in Section 1, 0-45 cm.

LITHIFIED GRAINSTONE, light gray (2.5Y 7/2), is present in Section 2, 125-145 cm, and the CC; grains are skeletal fragments.

SMEAR SLIDE SUMMARY (%):

	1,80	2,80	2,115
	D	D	D
TEXTURE:			
Sand	100	100	40
Silt	–	–	60
COMPOSITION:			
Micrite	–	–	55
Foraminifers	60	20	5
Nannofossils	–	–	5
Skeletal Fragments	40	60	5
Clasts	–	–	30

SITE 626 HOLE C CORE 1X CORED INTERVAL 844.5-851.4 mbsl; 0-6.9 mbsf

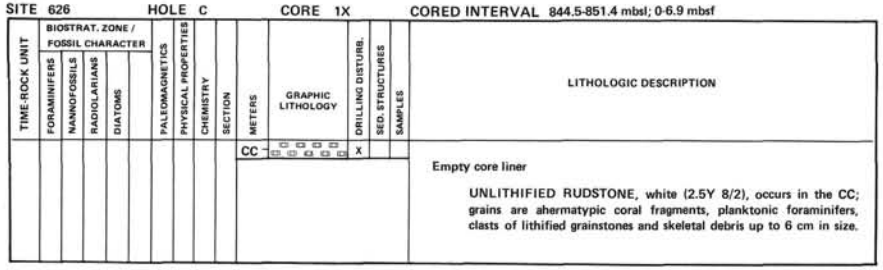

Empty core liner

UNLITHIFIED RUDSTONE, white (2.5Y 8/2), occurs in the CC; grains are ahermatypic coral fragments, planktonic foraminifers, clasts of lithified grainstones and skeletal debris up to 6 cm in size.

SITE 626 HOLE C CORE 2X CORED INTERVAL 851.4-861.0 mbsl; 6.9-16.5 mbsf

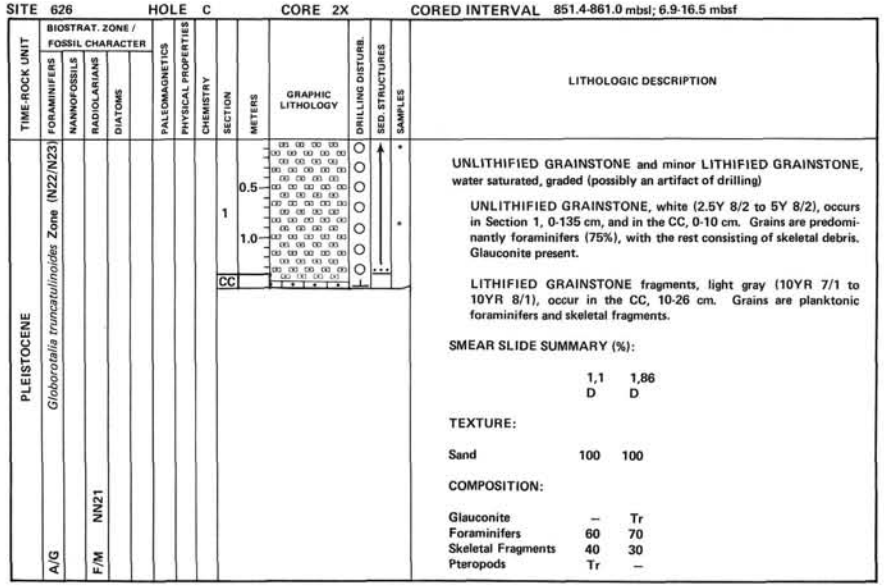

UNLITHIFIED GRAINSTONE and minor LITHIFIED GRAINSTONE, water saturated, graded (possibly an artifact of drilling)

UNLITHIFIED GRAINSTONE, white (2.5Y 8/2 to 5Y 8/2), occurs in Section 1, 0-135 cm, and in the CC, 0-10 cm. Grains are predominantly foraminifers (75%), with the rest consisting of skeletal debris. Glauconite present.

LITHIFIED GRAINSTONE fragments, light gray (10YR 7/1 to 10YR 8/1), occur in the CC, 10-26 cm. Grains are planktonic foraminifers and skeletal fragments.

SMEAR SLIDE SUMMARY (%):

	1,1	1,86
	D	D
TEXTURE:		
Sand	100	100
COMPOSITION:		
Glauconite	–	Tr
Foraminifers	60	70
Skeletal Fragments	40	30
Pteropods	Tr	–

SITE 626 HOLE C CORE 3X CORED INTERVAL 861.0-870.0 mbsl; 16.5-25.5 mbsf

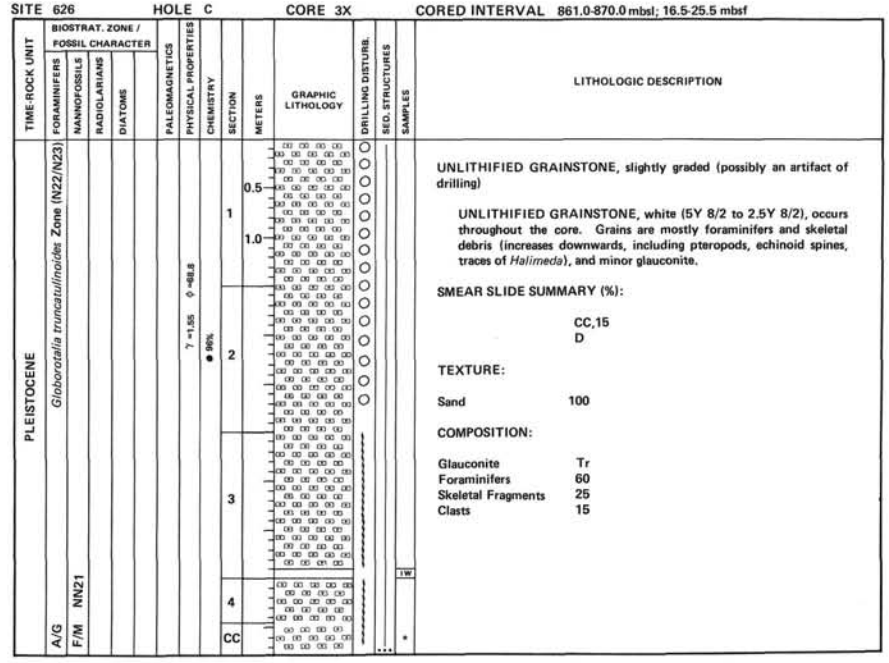

UNLITHIFIED GRAINSTONE, slightly graded (possibly an artifact of drilling)

UNLITHIFIED GRAINSTONE, white (5Y 8/2 to 2.5Y 8/2), occurs throughout the core. Grains are mostly foraminifers and skeletal debris (increases downwards, including pteropods, echinoid spines, traces of *Halimeda*), and minor glauconite.

SMEAR SLIDE SUMMARY (%):

	CC,15
	D
TEXTURE:	
Sand	100
COMPOSITION:	
Glauconite	Tr
Foraminifers	60
Skeletal Fragments	25
Clasts	15

SITE 626 HOLE C CORE 4X CORED INTERVAL 870.0-879.6 mbsl; 25.5-35.1 mbsf

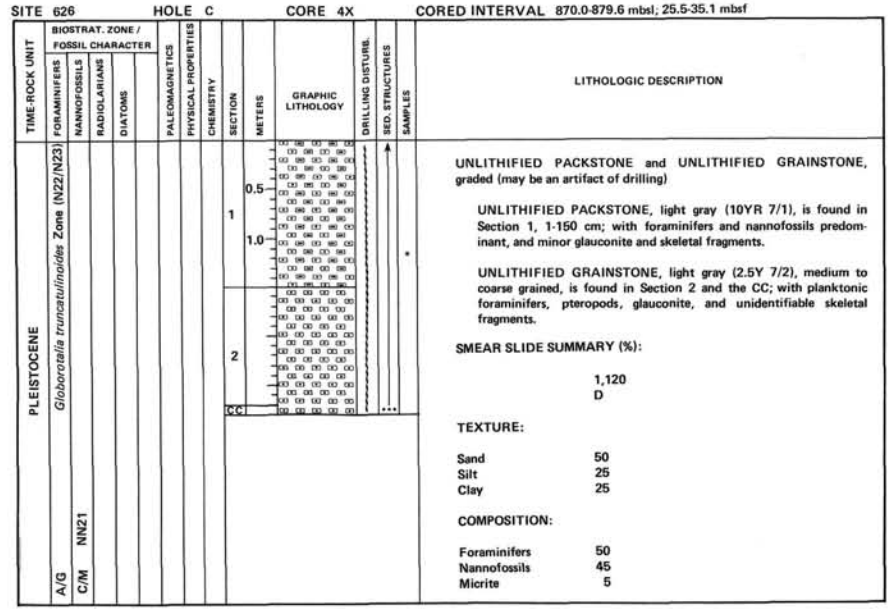

UNLITHIFIED PACKSTONE and UNLITHIFIED GRAINSTONE, graded (may be an artifact of drilling)

UNLITHIFIED PACKSTONE, light gray (10YR 7/1), is found in Section 1, 1-150 cm; with foraminifers and nannofossils predominant, and minor glauconite and skeletal fragments.

UNLITHIFIED GRAINSTONE, light gray (2.5Y 7/2), medium to coarse grained, is found in Section 2 and the CC; with planktonic foraminifers, pteropods, glauconite, and unidentifiable skeletal fragments.

SMEAR SLIDE SUMMARY (%):

	1,120
	D
TEXTURE:	
Sand	50
Silt	25
Clay	25
COMPOSITION:	
Foraminifers	50
Nannofossils	45
Micrite	5

SITE 626 HOLE C CORE 5X CORED INTERVAL 879.6-889.2 mbsl; 35.1-44.7 mbsf

TIME-ROCK UNIT	BIOSTRAT. ZONE / FOSSIL CHARACTER: FORAMINIFERS	NANNOFOSSILS	RADIOLARIANS	DIATOMS	PALEOMAGNETICS	PHYSICAL PROPERTIES	CHEMISTRY	SECTION	METERS	GRAPHIC LITHOLOGY	DRILLING DISTURB.	SED. STRUCTURES	SAMPLES	LITHOLOGIC DESCRIPTION
PLEISTOCENE	A/G *Globorotalia truncatulinoides* Zone (N22/N23)	C/M NN21						CC	0.5					

UNLITHIFIED PACKSTONE and UNLITHIFIED GRAINSTONE, slightly graded (probably an artifact of drilling)

UNLITHIFIED PACKSTONE, light gray (10YR 7/1), in Section 1, 0-73 cm, consisting of nannofossils and foraminifers.

UNLITHIFIED GRAINSTONE, light gray (2.5Y 7/2), in the CC, contains planktonic foraminifers, pteropods, *Halimeda*, and glauconite.

SITE 626 HOLE C CORE 6X CORED INTERVAL 889.2-898.2 mbsl, 44.7-54.3 mbsf

TIME-ROCK UNIT	BIOSTRAT. ZONE / FOSSIL CHARACTER: FORAMINIFERS	NANNOFOSSILS	RADIOLARIANS	DIATOMS	PALEOMAGNETICS	PHYSICAL PROPERTIES	CHEMISTRY	SECTION	METERS	GRAPHIC LITHOLOGY	DRILLING DISTURB.	SED. STRUCTURES	SAMPLES	LITHOLOGIC DESCRIPTION
EARLY PLEISTOCENE	A/G *Globorotalia truncatulinoides* Zone (N22)	C/M NN19						1	0.5				*	
								CC						

UNLITHIFIED GRAINSTONE and UNLITHIFIED PACKSTONE, with minor UNLITHIFIED RUDSTONE, graded (probably an artifact of drilling)

UNLITHIFIED GRAINSTONE, light gray (2.5Y 7/2 grading to 10YR 7/1 and 10Y 6/1) in Section 1, 40-90 cm and 100-106 cm, and the CC, 0-20 cm. Medium grained except for very coarse grains at Section 1, 94 cm (grains are predominantly planktonic foraminifers and skeletal debris, including ahermatypic coral fragments).

UNLITHIFIED PACKSTONE, light gray (10Y 7/1), in Section 1, 0-40 cm and 90-100 cm. Foraminifers, nannofossils, and skeletal fragments are predominant grain types.

UNLITHIFIED RUDSTONE and UNLITHIFIED GRAINSTONE in the CC, light gray (2.5Y 7/2), contains planktonic foraminifers, skeletal debris, CHALK clasts, pteropods, *Halimeda*, and glauconite (1%). Skeletal fragments are up to 0.5 cm.

SMEAR SLIDE SUMMARY (%):

	1,95
	D
TEXTURE:	
Sand	75
Silt & Clay	25
COMPOSITION:	
Quartz	Tr
Feldspar	Tr
Glauconite	Tr
Foraminifers	70
Nannofossils	20
Fragments	5
Micrite	5

SITE 626 HOLE C CORE 7X CORED INTERVAL 898.2-908.4 mbsl; 54.3-63.9 mbsf

TIME-ROCK UNIT	BIOSTRAT. ZONE / FOSSIL CHARACTER: FORAMINIFERS	NANNOFOSSILS	RADIOLARIANS	DIATOMS	PALEOMAGNETICS	PHYSICAL PROPERTIES	CHEMISTRY	SECTION	METERS	GRAPHIC LITHOLOGY	DRILLING DISTURB.	SED. STRUCTURES	SAMPLES	LITHOLOGIC DESCRIPTION
EARLY PLIOCENE	R/G *Neogloboquadrina acostaensis/Globorotalia margaritae* Zones N16 to N19	NN12	R/M					CC						

Empty core liner

VOLCANIC ASH, light gray (5Y 6/1), in the CC, highly disturbed.

SMEAR SLIDE SUMMARY (%):

	CC,3
	D
TEXTURE:	
Sand	Tr
Silt	100
COMPOSITION:	
Volcanic Glass	90
Accessory Min.	Tr
Foraminifers	Tr
Nannofossils	10

CORE 8 NO RECOVERY

SITE 626 HOLE C CORE 9X CORED INTERVAL 917.9-927.5 mbsl; 73.4-83.0 mbsf

TIME-ROCK UNIT	BIOSTRAT. ZONE / FOSSIL CHARACTER: FORAMINIFERS	NANNOFOSSILS	RADIOLARIANS	DIATOMS	PALEOMAGNETICS	PHYSICAL PROPERTIES	CHEMISTRY	SECTION	METERS	GRAPHIC LITHOLOGY	DRILLING DISTURB.	SED. STRUCTURES	SAMPLES	LITHOLOGIC DESCRIPTION
LATE MIOCENE	A/G *Neogloboquadrina acostaensis* Zone (N16/N17)	R/M NN11						1						
								CC						

UNLITHIFIED PACKSTONE and UNLITHIFIED GRAINSTONE, graded (possibly an artifact of drilling)

UNLITHIFIED PACKSTONE, light gray (5Y 7/2), medium to coarse grained, in Section 1, 0-32 cm, and CC, 0-12 cm. Grains consist predominantly of foraminifers (70% filled with glauconite or pyrite) and bioclasts.

UNLITHIFIED GRAINSTONE, light gray (5Y 7/2), in CC, 12-31 cm. Grains consist of foraminifers and bioclasts.

SMEAR SLIDE SUMMARY (%):

	1,3
	M
TEXTURE:	
Sand	65
Silt	5
Clay	25
COMPOSITION:	
Quartz	Tr
Foraminifers	70
Nannofossils	25
Skeletal Fragments (Echinoid Spines)	5

CORE 10 NO RECOVERY

SITE 626 HOLE C CORE 11X CORED INTERVAL 937.2-946.9 mbsl; 92.7-102.4 mbsf

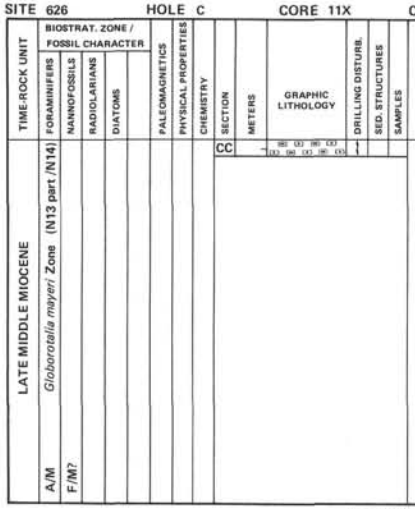

LITHOLOGIC DESCRIPTION

Empty core liner

UNLITHIFIED PACKSTONE, light gray (2.5Y 7/2), in CC, highly disturbed. ? Medium to coarse sand, grains consist of planktonic foraminifers (1-5% filled with glauconite or pyrite), unidentifiable skeletal grains, *Halimeda* and pteropods, nannofossils in matrix.

CORE 12 NO RECOVERY

SITE 626 HOLE C CORE 13H CORED INTERVAL 956.6-966.2 mbsl; 112.1-121.7 mbsf

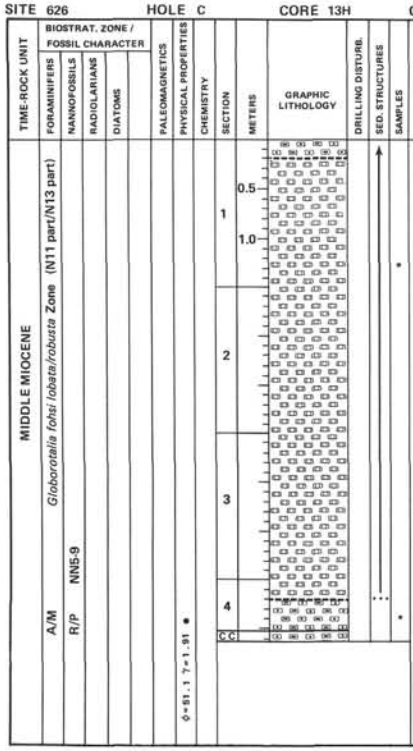

LITHOLOGIC DESCRIPTION

UNLITHIFIED RUDSTONE and UNLITHIFIED PACKSTONE, normally graded (may be real; magnitude and extent of drilling disturbance is unknown; possible downhole contamination)

UNLITHIFIED RUDSTONE, white (10YR 8/1 to 2.5Y 8/2 and 5Y 8/2), in Section 1, 20 cm, to Section 4, 19 cm. Larger grains consist of ahermatypic coral fragments, subrounded to angular; other components include *Halimeda*, bivalve fragments, clasts, echinoids, red algae, pteropods, and unidentifiable skeletal fragments. This is possibly downhole contamination.

UNLITHIFIED PACKSTONE, light gray (5Y 7/1), in Section 1, 0-20 cm, Section 4, 19-51 cm, and in the CC; grains are predominantly planktonic foraminifers, with minor glauconite. PACKSTONE in Section 1 is a graded portion of downhole contamination.

SMEAR SLIDE SUMMARY (%):

	1,130 D	4,34 D
TEXTURE:		
Gravel	80	—
Sand	20	20
Silt	—	80
COMPOSITION:		
Micrite	—	80
Foraminifers (Plank.)	—	20
Halimeda	15	—
Bivalves	20	—
Clasts	35	—
Echinoids	5	—
Red Algae	7	—
Unidentified	18	—

SITE 626 HOLE C CORE 14H CORED INTERVAL 966.2-975.8 mbsl; 121.7-131.3 mbsf

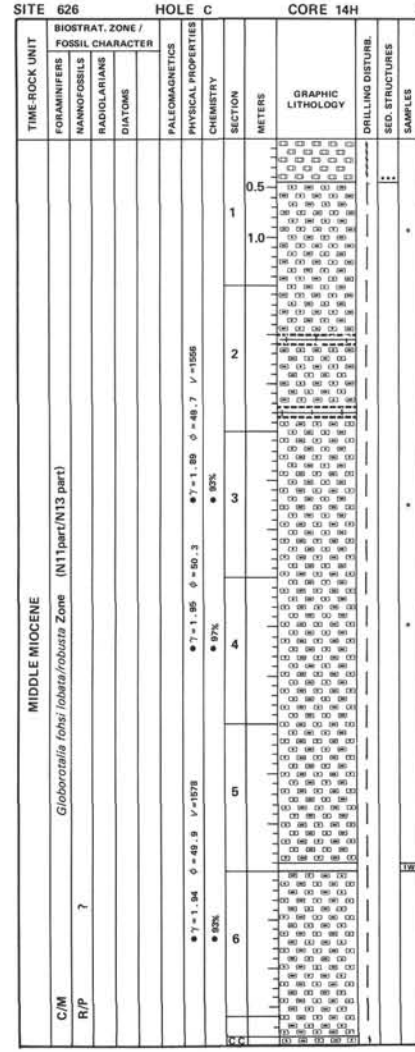

LITHOLOGIC DESCRIPTION

UNLITHIFIED PACKSTONE with minor interbedded UNLITHIFIED RUDSTONE and NANNO-FORAM OOZE

UNLITHIFIED PACKSTONE, white (2.5Y 8/2), occurs in Section 1, 48 cm, to Section 2, 50 cm; Section 2, 55-124 cm; Section 2, 136 cm, to Section 5, 140 cm, and Section 6. Grain types include planktonic foraminifers, skeletal debris and clasts. Some foraminifers have glauconite fill.

PACKSTONE, and the RUDSTONE is probably downhole contamination as in Core 13H.

FORAM-NANNOFOSSIL CHALK, light gray (5Y 7/2), in Section 2, 50-55 cm and 124-136 cm, approximately 30% foraminifers and 45% nannofossils.

SMEAR SLIDE SUMMARY (%):

	1,90 D	3,130 D	4,50 D
TEXTURE:			
Sand	60	10	40
Silt	40	50	30
Clay	40	40	30
COMPOSITION:			
Foraminifers	45	10	30
Nannofossils	10	70	50
Sponge Spicules	—	—	Tr
Skeletal Fragments	15	—	20
Micrite	20	20	—

SITE 626 HOLE C CORE 15 H CORED INTERVAL 975.8-985.3 mbsl; 131.3-140.8 mbsf

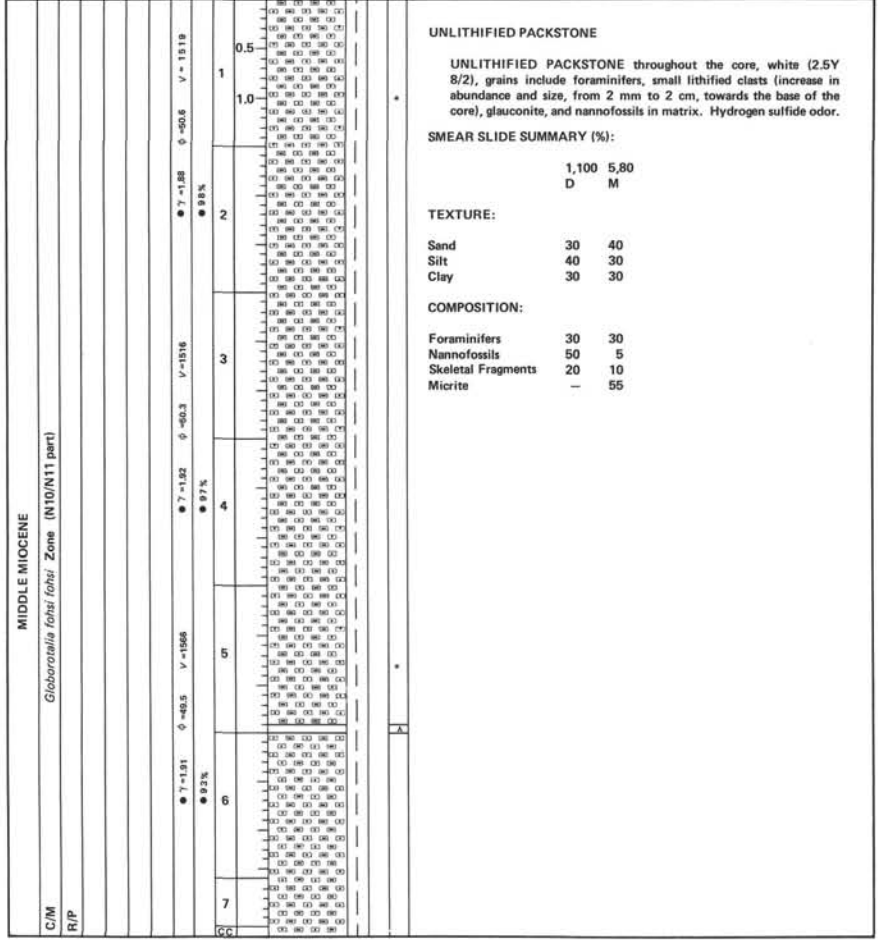

LITHOLOGIC DESCRIPTION

UNLITHIFIED PACKSTONE

UNLITHIFIED PACKSTONE throughout the core, white (2.5Y 8/2), grains include foraminifers, small lithified clasts (increase in abundance and size, from 2 mm to 2 cm, towards the base of the core), glauconite, and nannofossils in matrix. Hydrogen sulfide odor.

SMEAR SLIDE SUMMARY (%):

	1,100 D	5,80 M
TEXTURE:		
Sand	30	40
Silt	40	30
Clay	30	30
COMPOSITION:		
Foraminifers	30	30
Nannofossils	50	5
Skeletal Fragments	20	10
Micrite	—	55

SITE 626 HOLE C CORE 16H CORED INTERVAL 985.3-994.9 mbsl; 140.8-150.4 mbsf

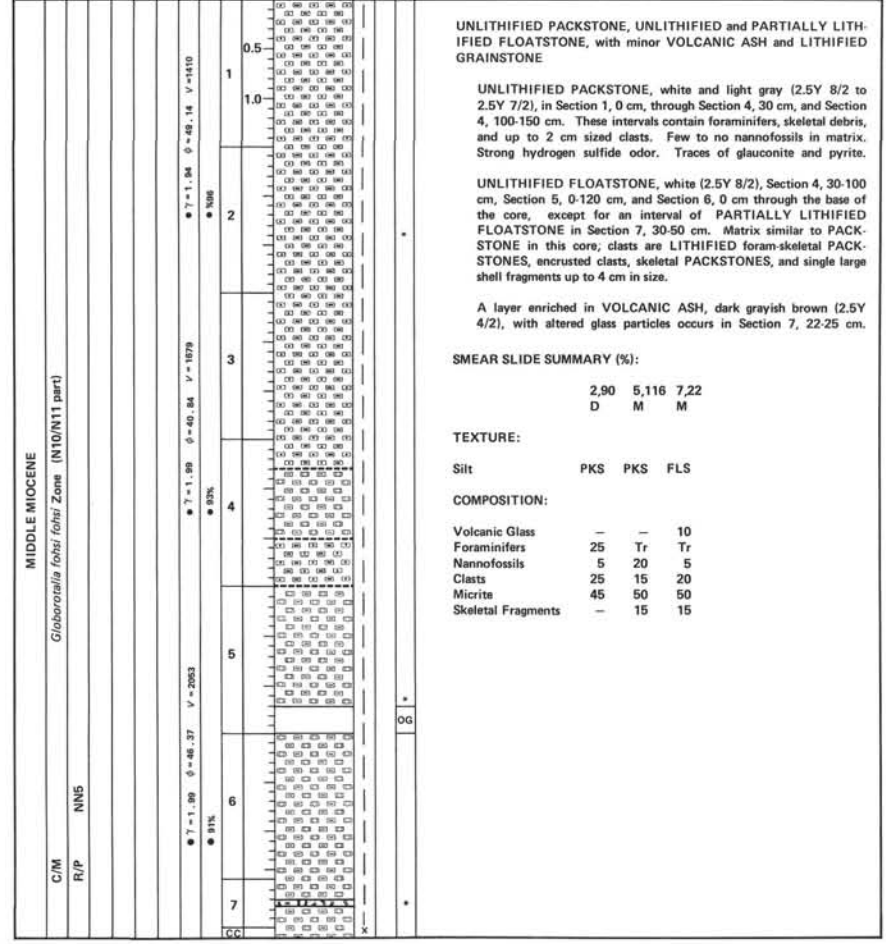

LITHOLOGIC DESCRIPTION

UNLITHIFIED PACKSTONE, UNLITHIFIED and PARTIALLY LITHIFIED FLOATSTONE, with minor VOLCANIC ASH and LITHIFIED GRAINSTONE

UNLITHIFIED PACKSTONE, white and light gray (2.5Y 8/2 to 2.5Y 7/2), in Section 1, 0 cm, through Section 4, 30 cm, and Section 4, 100-150 cm. These intervals contain foraminifers, skeletal debris, and up to 2 cm sized clasts. Few to no nannofossils in matrix. Strong hydrogen sulfide odor. Traces of glauconite and pyrite.

UNLITHIFIED FLOATSTONE, white (2.5Y 8/2), Section 4, 30-100 cm, Section 5, 0-120 cm, and Section 6, 0 cm through the base of the core, except for an interval of PARTIALLY LITHIFIED FLOATSTONE in Section 7, 30-50 cm. Matrix similar to PACKSTONE in this core; clasts are LITHIFIED foram-skeletal PACKSTONES, encrusted clasts, skeletal PACKSTONES, and single large shell fragments up to 4 cm in size.

A layer enriched in VOLCANIC ASH, dark grayish brown (2.5Y 4/2), with altered glass particles occurs in Section 7, 22-25 cm.

SMEAR SLIDE SUMMARY (%):

	2,90 D	5,116 M	7,22 M
TEXTURE:			
Silt	PKS	PKS	FLS
COMPOSITION:			
Volcanic Glass	—	—	10
Foraminifers	25	Tr	Tr
Nannofossils	5	20	5
Clasts	25	15	20
Micrite	45	50	50
Skeletal Fragments	—	15	15

SITE 626 HOLE C CORE 17H CORED INTERVAL 994.9-1004.5 mbsl; 150.4-160.0 mbsf

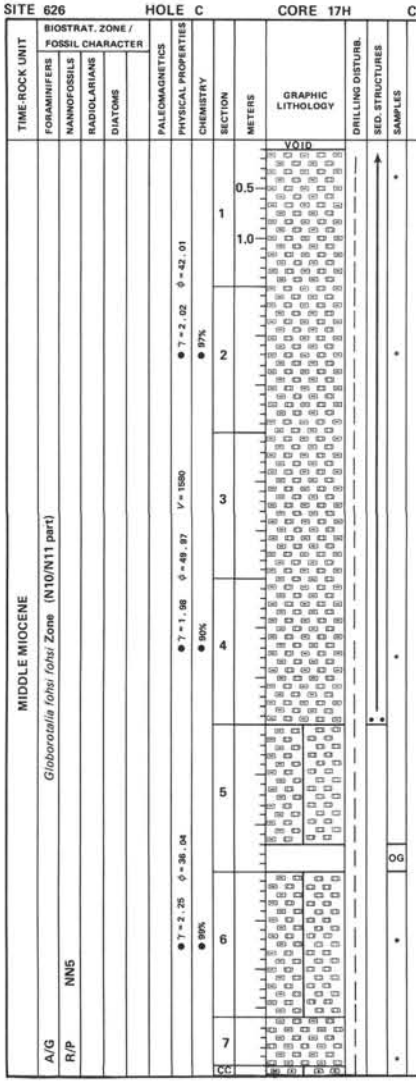

LITHOLOGIC DESCRIPTION

UNLITHIFIED FLOATSTONE and UNLITHIFIED RUDSTONE, with minor UNLITHIFIED PACKSTONE and UNLITHIFIED GRAINSTONE; slight drilling disturbance. Slight odor of hydrogen sulfide.

UNLITHIFIED FLOATSTONE, white (2.5Y 8/2), in Section 1, 10 cm, to Section 4, 150 cm, and Section 7, 0-45 cm. The sediment in these intervals consists of clasts in a matrix of unlithified planktonic foraminifers, skeletal fragments and micrite; nannofossils are rare. Some less well-indurated clasts of coarse-grained skeletal fragments (white, 10YR 8/2) occur in Section 1, along with a clast (or layer?) of unlithified micritic MUDSTONE (pale olive, 5Y 6/3). Large shell fragments occur in Section 3. Maximum clast size increases from 5 cm in Section 1 to 10 cm in Section 4. Traces of glauconite.

UNLITHIFIED FLOATSTONE/RUDSTONE, white (2.5Y 8/2), occurs in Section 5, 0 cm, through Section 6, 150 cm. Clast size ranges to 10 cm diameter with most clasts being angular, porous, fine-grained foram-skeletal PACKSTONE to GRAINSTONE, pale olive in color (5Y 6/3) in both FLOATSTONE/RUDSTONE and FLOATSTONE.

A minor interval of UNLITHIFIED PACKSTONE to UNLITHIFIED GRAINSTONE, light gray (5Y 7/2), occurs from Section 7, 45 cm, to the base of the core. Grains are predominantly planktonic foraminifers, the fine fraction in this interval is micritic with subordinate nannofossils, and contains 1% glauconite.

SMEAR SLIDE SUMMARY (%):

	1,43 M	2,75 D	4,75 D	6,75 D	7,50 M
TEXTURE:					
Sand	5	10	5	5	40
Silt	40	10	10	10	30
Clay	55	80	85	85	30
COMPOSITION:					
Foraminifers	—	10	5	5	40
Nannofossils	5	5	5	5	10
Clasts	5	—	—	—	—
Micrite	90	75	80	80	50
Skeletal Fragments	—	10	10	10	—

SITE 626 HOLE C CORE 18H CORED INTERVAL 1004.5-1014.1 mbsl; 160.0-169.6 mbsf

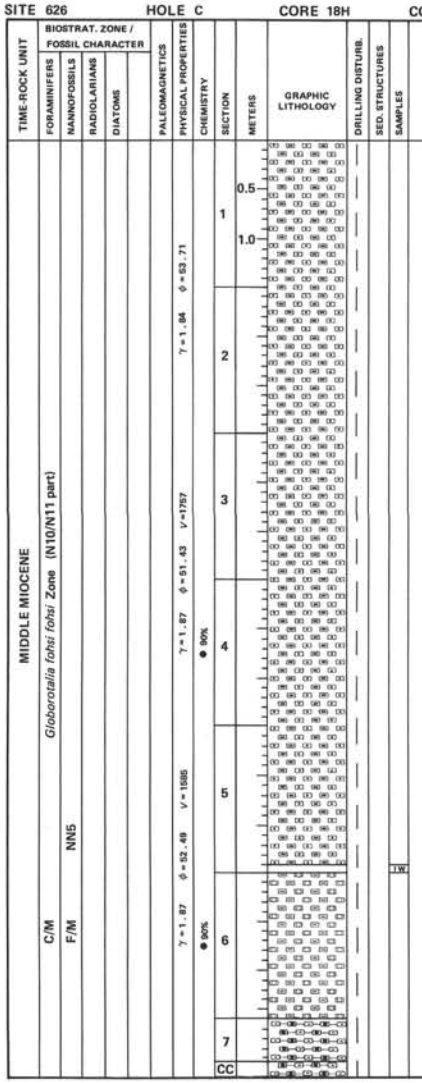

LITHOLOGIC DESCRIPTION

UNLITHIFIED PACKSTONE, UNLITHIFIED FLOATSTONE, and PARTIALLY LITHIFIED PACKSTONE

UNLITHIFIED PACKSTONE, light gray (5Y 7/2) to pale yellow (5Y 7/3), occurs from Section 1, 0 cm, to Section 5, 140 cm. Grains include foraminifers and skeletal fragments; the latter increase in abundance in Section 2, and clasts are also present. Clasts are mainly lithified skeletal packstones and grainstones. Glauconite makes up 1-5% and is especially abundant in Section 1. A large layer or clast of very porous foram skeletal grainstone containing shallow-water fossils occurs in Section 1, 10 cm.

UNLITHIFIED FLOATSTONE, pale yellow (5Y 7/3), occurs in Section 6, 0-150 cm. Contains large clasts (2-3 cm diameter), complete shells and fragments of lithified bioclastic foram PACKSTONE.

PARTIALLY LITHIFIED PACKSTONE, pale yellow (5Y 7/3), in Section 7, 0-19 cm, and in the CC; contains predominantly planktonic foraminifers and skeletal fragments as small clasts (1-2 cm).

SMEAR SLIDE SUMMARY (%):

	2,75 D	4,75 M	5,46 M	6,75 D
TEXTURE:				
Sand	50	—	25	30
Silt	25	—	20	30
Clay	25	—	55	40
COMPOSITION:				
Foraminifers	20	—	45	10
Nannofossils	Tr	5	20	Tr
Skeletal Fragments	30	—	15	20
Micrite	50	60	10	70
Clasts	—	35	—	—

SITE 626 HOLE C CORE 19H CORED INTERVAL 1014.1-1023.8 mbsl; 169.60-179.30 mbsf

TIME-ROCK UNIT	BIOSTRAT. ZONE / FOSSIL CHARACTER: FORAMINIFERS	NANNOFOSSILS	RADIOLARIANS	DIATOMS	PALEOMAGNETICS	PHYSICAL PROPERTIES	CHEMISTRY	SECTION	METERS	GRAPHIC LITHOLOGY	DRILLING DISTURB.	SED. STRUCTURES	SAMPLES	LITHOLOGIC DESCRIPTION
EARLY MIDDLE MIOCENE	C/M *Globorotalia peripheroronda/Praeorbulina glomerosa* Zone (N8 part/N9)	R/M NN4-5						1 CC	0.5					UNLITHIFIED PACKSTONE with minor UNLITHIFIED FLOATSTONE UNLITHIFIED PACKSTONE, light gray (2.5Y 7/2), in Section 1, 0-40 cm; alternating light brownish gray (2.5Y 6/2) and white (2.5Y 8/2) in Section 1, 40-74 cm. A large single layer or clast of foram skeletal LITHIFIED GRAINSTONE occurs in Section 1, 20 cm. UNLITHIFIED FLOATSTONE, light gray (10YR 7/2), in the CC; both matrix and large grains are clasts of very porous foram skeletal LITHIFIED GRAINSTONE.

SITE 626 HOLE D CORE 1R CORED INTERVAL 1022.9-1032.5 mbsl; 179.4-189.0 mbsf

TIME-ROCK UNIT	BIOSTRAT. ZONE / FOSSIL CHARACTER: FORAMINIFERS	NANNOFOSSILS	RADIOLARIANS	DIATOMS	PALEOMAGNETICS	PHYSICAL PROPERTIES	CHEMISTRY	SECTION	METERS	GRAPHIC LITHOLOGY	DRILLING DISTURB.	SED. STRUCTURES	SAMPLES	LITHOLOGIC DESCRIPTION
EARLY MIDDLE MIOCENE	Mixed Zones N8 to N11 (part) *Praeorbulina glomerosa/Globorotalia fohsi fohsi*	NN5	R/M					1, CC	0.5, 1.0				*	UNLITHIFIED PACKSTONE and minor LITHIFIED PACKSTONE, moderately deformed by drilling, hydrogen sulfide bubbled from upper part of core

UNLITHIFIED PACKSTONE, white (5Y 8/2), very deformed to soupy in Section 1, 0-107 cm. Medium to coarse grained, consists of planktonic foraminifers, clasts, skeletal debris (pteropods, *Halimeda*, red algae, bryozoans and echinoid spines).

LITHIFIED PACKSTONE, white to light gray (2.5Y 8/2 to 2.5Y 7/2), medium grained with rare coarse grains; inclusions of dead oil.

SMEAR SLIDE SUMMARY (%):

	1,70
	D
COMPOSITION:	
Glauconite	Tr
Skeletal Fragments	15
Foraminifers	35
Red Algae	5
Bryozoans	5
Clasts	40
Echinoid Spines	Tr
Halimeda	Tr
Pteropods	Tr

CORE 2 NO RECOVERY

SITE 626 HOLE D CORE 3R CORED INTERVAL 1042.1-1051.6 mbsl; 198.6-208.1 mbsf

TIME-ROCK UNIT	BIOSTRAT. ZONE / FOSSIL CHARACTER: FORAMINIFERS	NANNOFOSSILS	RADIOLARIANS	DIATOMS	PALEOMAGNETICS	PHYSICAL PROPERTIES	CHEMISTRY	SECTION	METERS	GRAPHIC LITHOLOGY	DRILLING DISTURB.	SED. STRUCTURES	SAMPLES	LITHOLOGIC DESCRIPTION
EARLY MIDDLE MIOCENE	Mixed Zones N8/N9 *Praeorbulina glomerosa/Globorotalia peripheroronda*	NN5	A/M					1, CC						UNLITHIFIED RUDSTONE to UNLITHIFIED GRAINSTONE

UNLITHIFIED RUDSTONE to UNLITHIFIED GRAINSTONE, light gray (10YR 7/2), in Section 1 and the CC. Contains clasts of planktonic foraminiferal PACKSTONE and shallow water shell fragments; contains material from overlying section (including Pleistocene fossils).

SITE 626 HOLE D CORE 4R CORED INTERVAL 1051.6-1061.2 mbsl; 208.1-217.7 mbsf

TIME-ROCK UNIT	BIOSTRAT. ZONE / FOSSIL CHARACTER: FORAMINIFERS	NANNOFOSSILS	RADIOLARIANS	DIATOMS	PALEOMAGNETICS	PHYSICAL PROPERTIES	CHEMISTRY	SECTION	METERS	GRAPHIC LITHOLOGY	DRILLING DISTURB.	SED. STRUCTURES	SAMPLES	LITHOLOGIC DESCRIPTION
EARLY MIDDLE MIOCENE	A/M *Praeorbulina glomerosa* Zone (N8/N9 part)	NN5	A/M					1, CC						UNLITHIFIED GRAINSTONE

UNLITHIFIED GRAINSTONE, light gray (2.5Y 7/2), in Section 1 and the CC. Consists of approximately 100% planktonic foraminifers (a few infilled with glauconite), with less than 1% nannofossils.

CORE 5 NO RECOVERY

SITE 626 HOLE D CORE 6R CORED INTERVAL 1070.8-1080.4 mbsl; 227.3-236.9 mbsf

TIME-ROCK UNIT	BIOSTRAT. ZONE / FOSSIL CHARACTER: FORAMINIFERS	NANNOFOSSILS	RADIOLARIANS	DIATOMS	PALEOMAGNETICS	PHYSICAL PROPERTIES	CHEMISTRY	SECTION	METERS	GRAPHIC LITHOLOGY	DRILLING DISTURB.	SED. STRUCTURES	SAMPLES	LITHOLOGIC DESCRIPTION
EARLY MIDDLE MIOCENE	A/M	B						CC			X			Empty core liner; LITHIFIED PACKSTONE occurs in the CC

Five fragments of LITHIFIED PACKSTONE, light gray (5Y 7/2), occur in the CC; contains planktonic foraminifers, approximately 1% glauconite.

CORE 7 NO RECOVERY CORE 8 NO RECOVERY CORE 9 NO RECOVERY

SITE 626 HOLE D CORE 10R CORED INTERVAL 1108.3-1117.9 mbsl; 264.8-274.4 mbsf

TIME-ROCK UNIT	BIOSTRAT. ZONE / FOSSIL CHARACTER: FORAMINIFERS	NANNOFOSSILS	RADIOLARIANS	DIATOMS	PALEOMAGNETICS	PHYSICAL PROPERTIES	CHEMISTRY	SECTION	METERS	GRAPHIC LITHOLOGY	DRILLING DISTURB.	SED. STRUCTURES	SAMPLES	LITHOLOGIC DESCRIPTION
(?) LATE EARLY MIOCENE	*Globigerinatella insueta* Zone? (N7/N8 part)	NN3	R/P					1, 2	0.5, 1.0					Empty core liner; a small sample for paleontological study was recovered from the CC

SITE 626 HOLE D CORE 11R CORED INTERVAL 1117.9-1127.2 mbsl; 274.4-283.7 mbsf

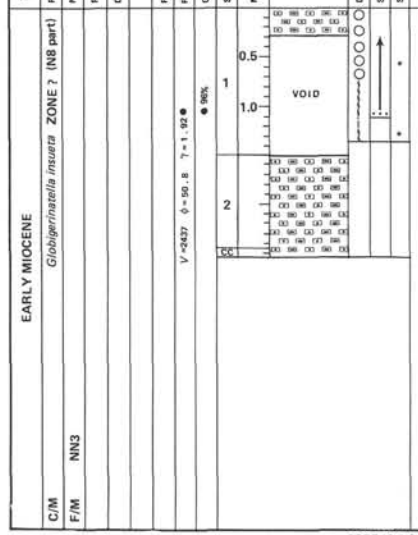

LITHOLOGIC DESCRIPTION

Entire core consists of UNLITHIFIED PACKSTONE

UNLITHIFIED PACKSTONE, white (5Y 8/2 to 2.5Y 8/2), throughout the core. Grades from fine, muddy sand in Section 1 to medium sand in Section 2, 80 cm. Coarse sand below this and in the CC is composed of planktonic foraminifers, clasts, skeletal debris, a few *Halimeda* fragments and echinoid spines.

SMEAR SLIDE SUMMARY (%):

	1,50 D	CC,10 D
TEXTURE:		
Sand	40	100
Silt	30	–
Clay	30	–
COMPOSITION:		
Cement	–	4
Accessory Minerals	–	Tr
Foraminifers	20	15
Nannofossils	5	–
Skeletal Fragments	50	58
Micrite/Skel. Debris	25	–
Echinoids	–	8
Spar Cement	–	14
Clasts	–	5

CORE 12 NO RECOVERY

SITE 626 HOLE D CORE 13R CORED INTERVAL 1136.7-1146.4 mbsl; 293.2-302.9 mbsf

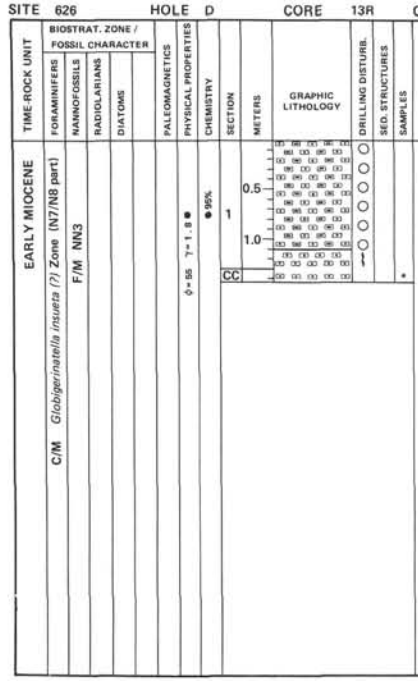

LITHOLOGIC DESCRIPTION

UNLITHIFIED PACKSTONE and UNLITHIFIED GRAINSTONE, graded (probably an artifact of drilling disturbance)

UNLITHIFIED PACKSTONE, white (2.5Y 8/2), occurs in Section 1, 0-110 cm, medium to fine grained, contains skeletal debris, foraminifers, spar cement, echinoid spines and clasts.

UNLITHIFIED GRAINSTONE, pale yellow (5Y 8/3), occurs in Section 1, 110-130 cm, and in the CC. Sediment is medium to coarse grained and well-sorted. Near its base, the CC contains rounded pebbles of lithified grainstone up to 2 cm diameter and skeletal material up to 1 cm in size near the base. Foraminifers in the unlithified, medium to coarse-grained matrix have overgrowths in many places. Cement spar and isolated large (4 mm) foraminifers are also observed.

SMEAR SLIDE SUMMARY (%):

	CC,10 D
TEXTURE:	
Sand	100
COMPOSITION:	
Glauconite	Tr
Foraminifers	20
Skeletal Fragments	50
Spar Cement	20
Echinoid Spines	10
Clasts	10

SITE 626 HOLE D CORE 14R CORED INTERVAL 1146.4-1156.1 mbsl; 302.9-312.6 mbsf

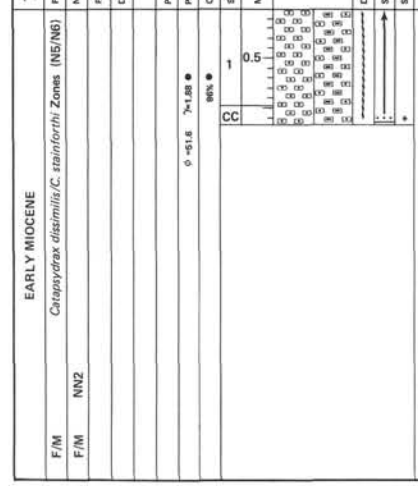

LITHOLOGIC DESCRIPTION

UNLITHIFIED GRAINSTONE to UNLITHIFIED PACKSTONE throughout the core, graded (probably an artifact of drilling disturbance)

UNLITHIFIED GRAINSTONE to UNLITHIFIED PACKSTONE, light gray (2.5Y 7/2) throughout the core. Contains unlithified skeletal fragments with subordinate planktonic foraminifers (poorly preserved), possible spar fragments and a small amount of carbonate mud. Large (2 mm size) skeletal fragments are near the base of the CC.

SMEAR SLIDE SUMMARY (%):

	CC,8 D
TEXTURE:	
Sand	60
Silt	30
Clay	10
COMPOSITION:	
Foraminifers	25
Nannofossils	Tr
Skeletal Frags.	30
Overgrowths	5
Micrite	40

SITE 626 HOLE D CORE 15R CORED INTERVAL 1156.1-1165.7 mbsl; 312.6-322.2 mbsf

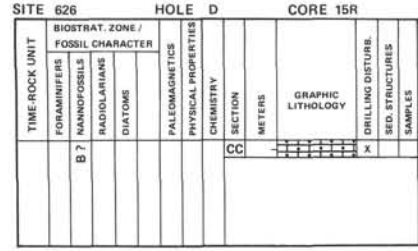

LITHOLOGIC DESCRIPTION

Empty core liner; LITHIFIED GRAINSTONE in CC

Several small (2-12 cm diameter) fragments and skeletal debris of LITHIFIED GRAINSTONE, pale yellow (5Y 7/3) and white (2.5Y 8/2 and 5Y 8/1), in the CC, fine grained; contains skeletal fragments.

SITE 626 HOLE D CORE 16R CORED INTERVAL 1165.7-1175.3 mbsl; 322.2-331.8 mbsf

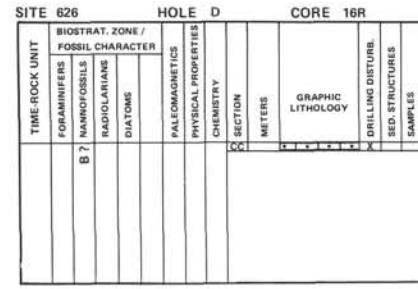

LITHOLOGIC DESCRIPTION

Empty core liner; LITHIFIED GRAINSTONE and minor CHERT in CC

Several small (less than 2 cm diameter) fragments of LITHIFIED GRAINSTONE, light gray (2.5Y 7/2), containing skeletal fragments and planktonic foraminifers. Also several small (2 mm diameter) fragments of CHERT, dark olive gray (5Y 3/2).

SITE 626 HOLE D CORE 17R CORED INTERVAL 1175.3-1184.8 mbsl; 331.8-341.3 mbsf

TIME-ROCK UNIT	BIOSTRAT. ZONE / FOSSIL CHARACTER: FORAMINIFERS	NANNOFOSSILS	RADIOLARIANS	DIATOMS	PALEOMAGNETICS	PHYSICAL PROPERTIES	CHEMISTRY	SECTION	METERS	GRAPHIC LITHOLOGY	DRILLING DISTURB.	SED. STRUCTURES	SAMPLES	LITHOLOGIC DESCRIPTION
NEOGENE		B						CC			X			Empty core liner. LITHIFIED GRAINSTONE and minor CHERT in CC Several small (2 cm diameter) fragments of LITHIFIED GRAINSTONE in the CC, light gray (2.5Y 7/2), containing planktonic foraminifers and skeletal fragments. Also several small (2-5 mm diameter) fragments of CHERT, dark olive gray (5Y 3/2).

SITE 626 HOLE D CORE 18R CORED INTERVAL 1184.8-1194.5 mbsl; 341.3-351.0 mbsf

TIME-ROCK UNIT	BIOSTRAT. ZONE / FOSSIL CHARACTER: FORAMINIFERS	NANNOFOSSILS	RADIOLARIANS	DIATOMS	PALEOMAGNETICS	PHYSICAL PROPERTIES	CHEMISTRY	SECTION	METERS	GRAPHIC LITHOLOGY	DRILLING DISTURB.	SED. STRUCTURES	SAMPLES	LITHOLOGIC DESCRIPTION
EARLY MIOCENE	R/M	NN2						1	0.5 1.0					Empty core liner; only a few grains in CC

SITE 626 HOLE D CORE 19R CORED INTERVAL 1194.5-1204.2 mbsl; 351.0-360.7 mbsf

TIME-ROCK UNIT	BIOSTRAT. ZONE / FOSSIL CHARACTER: FORAMINIFERS	NANNOFOSSILS	RADIOLARIANS	DIATOMS	PALEOMAGNETICS	PHYSICAL PROPERTIES	CHEMISTRY	SECTION	METERS	GRAPHIC LITHOLOGY	DRILLING DISTURB.	SED. STRUCTURES	SAMPLES	LITHOLOGIC DESCRIPTION
EARLY MIOCENE	A/M *Catapsydrax dissimilis/stainforthi* Zones (N5/N6)	R/M NN2						CC						Empty core liner; UNLITHIFIED PACKSTONE in CC. Sediment is highly disturbed as CC material was recovered by pouring the contents into a bucket UNLITHIFIED PACKSTONE, light gray (10YR 7/2), in CC. Medium to coarse-grained, contains lithoclasts, skeletal fragments, benthic and planktonic foraminifers with overgrowths, possible spar crystals, trace glauconite; approximately 1% chert fragments.

SITE 626 HOLE D CORE 20R CORED INTERVAL 1204.2-1213.9 mbsl; 360.7-370.4 mbsf

TIME-ROCK UNIT	BIOSTRAT. ZONE / FOSSIL CHARACTER: FORAMINIFERS	NANNOFOSSILS	RADIOLARIANS	DIATOMS	PALEOMAGNETICS	PHYSICAL PROPERTIES	CHEMISTRY	SECTION	METERS	GRAPHIC LITHOLOGY	DRILLING DISTURB.	SED. STRUCTURES	SAMPLES	LITHOLOGIC DESCRIPTION
EARLY MIOCENE	FM *Globorotalia kugleri* Zone (N4)	R/M ?					94% ●	1 CC	0.5				*	UNLITHIFIED PACKSTONE and GRAINSTONE UNLITHIFIED PACKSTONE, light gray (2.5Y 7/2), in Section 1 and the CC, 15-43 cm. Fine to medium grained in Section 1, and contains planktonic foraminifers (overgrown and infilled), skeletal fragments, clasts, echinoid spines, glauconite, and traces of chert. Material in the CC very highly disturbed during extrusion; fine to coarse grained, contains clasts, *Halimeda*, planktonic foraminifers with overgrowths, chert, and echinoid spines. UNLITHIFIED GRAINSTONE, light gray (2.5Y 7/2), in the CC, 0-15 cm. Contains coarse sand composed of clasts, traces of chert, *Halimeda*, bivalves, echinoid fragments, and gastropods. SMEAR SLIDE SUMMARY (%): CC,10 D COMPOSITION: Foraminifers 2 Altered Spar Cement 5 Skeletal Fragments 15 Clasts 49 *Halimeda* 7 Bivalves 3 Echinoids 1 Coral 1 Bryozoans Tr Gastropods Tr Chert 5 Pyrite Tr Unidentified 12

SITE 626 HOLE D CORE 21R CORED INTERVAL 1213.9-1223.6 mbsl 370.4-380.1 mbsf

TIME-ROCK UNIT	BIOSTRAT. ZONE / FOSSIL CHARACTER: FORAMINIFERS	NANNOFOSSILS	RADIOLARIANS	DIATOMS	PALEOMAGNETICS	PHYSICAL PROPERTIES	CHEMISTRY	SECTION	METERS	GRAPHIC LITHOLOGY	DRILLING DISTURB.	SED. STRUCTURES	SAMPLES	LITHOLOGIC DESCRIPTION
EARLY MIOCENE	C/M *Globorotalia kugleri* Zone (N4)	C/M NN1						1 CC	0.5				*	UNLITHIFIED PACKSTONE, soupy and very disturbed UNLITHIFIED PACKSTONE, white (2.5Y 8/2), fine to very fine grained; contains skeletal fragments, clasts, and planktonic foraminifers. SMEAR SLIDE SUMMARY (%): 1,70 D TEXTURE: Sand 50 Silt 25 Clay 25 COMPOSITION: Quartz 5 Foraminifers 10 Nannofossils 5 Bioclasts 10 Clasts 15 Micrite 55 Chert 5

SITE 626 HOLE D CORE 22R CORED INTERVAL 1223.6-1233.1 mbsl; 380.1-389.6 mbsf

TIME-ROCK UNIT	BIOSTRAT. ZONE / FOSSIL CHARACTER: FORAMINIFERS	NANNOFOSSILS	RADIOLARIANS	DIATOMS	PALEOMAGNETICS	PHYSICAL PROPERTIES	CHEMISTRY	SECTION	METERS	GRAPHIC LITHOLOGY	DRILLING DISTURB.	SED. STRUCTURES	SAMPLES	LITHOLOGIC DESCRIPTION
LATEST OLIGOCENE-EARLIEST MIOCENE	C/M *Globigerina ciperoensis/Globorotalia kugleri* Zones P22/N4	C/M NN1-NP25						1, 2, 3	0.5, 1.0					Empty core liner; only a few grains in the CC

SITE 626 HOLE D CORE 23R CORED INTERVAL 1233.1-1242.8 mbsl; 389.6-399.3 mbsf

TIME-ROCK UNIT	BIOSTRAT. ZONE / FOSSIL CHARACTER: FORAMINIFERS	NANNOFOSSILS	RADIOLARIANS	DIATOMS	PALEOMAGNETICS	PHYSICAL PROPERTIES	CHEMISTRY	SECTION	METERS	GRAPHIC LITHOLOGY	DRILLING DISTURB.	SED. STRUCTURES	SAMPLES	LITHOLOGIC DESCRIPTION
LATE OLIGOCENE	C/M *Globigerina ciperoensis* Zone (P22)	C/P NP25					γ = 1.7 - 1.9	1, CC	0.5				•	UNLITHIFIED PACKSTONE UNLITHIFIED PACKSTONE, white (2.5Y 8/2), fine to medium in Section 1, coarse in the CC. Consists of clasts, planktonic foraminifers, and skeletal fragments. Traces of black iron oxide flakes in the CC. SMEAR SLIDE SUMMARY (%): CC,7 M COMPOSITION: Quartz 20 Carbonate 30 Iron Oxides 50 Biotite Tr

SITE 626 HOLE D CORE 24R CORED INTERVAL 1242.8-1252.4 mbsl; 399.3-408.9 mbsf

TIME-ROCK UNIT	BIOSTRAT. ZONE / FOSSIL CHARACTER: FORAMINIFERS	NANNOFOSSILS	RADIOLARIANS	DIATOMS	PALEOMAGNETICS	PHYSICAL PROPERTIES	CHEMISTRY	SECTION	METERS	GRAPHIC LITHOLOGY	DRILLING DISTURB.	SED. STRUCTURES	SAMPLES	LITHOLOGIC DESCRIPTION
LATE OLIGOCENE	F/M *Globigerina ciperoensis* Zone (P22)	F/M NP25						1, 2	0.5, 1.0					Empty core liner; only a few grains in the CC

SITE 626 HOLE D CORE 25R CORED INTERVAL 1252.4-1262.0 mbsl; 408.9-418.5 msbf

TIME-ROCK UNIT	BIOSTRAT. ZONE / FOSSIL CHARACTER: FORAMINIFERS	NANNOFOSSILS	RADIOLARIANS	DIATOMS	PALEOMAGNETICS	PHYSICAL PROPERTIES	CHEMISTRY	SECTION	METERS	GRAPHIC LITHOLOGY	DRILLING DISTURB.	SED. STRUCTURES	SAMPLES	LITHOLOGIC DESCRIPTION
								1	0.5, 1.0					Empty core liner; a few grains of LITHIFIED GRAINSTONE in the CC GRAINSTONE is composed of planktonic foraminifers with spar cement.

CORE 26 NO RECOVERY

SITE 626 HOLE D CORE 27R CORED INTERVAL 1271.2-1280.8 mbsl, 427.7-437.3 mbsf

TIME-ROCK UNIT	BIOSTRAT. ZONE / FOSSIL CHARACTER: FORAMINIFERS	NANNOFOSSILS	RADIOLARIANS	DIATOMS	PALEOMAGNETICS	PHYSICAL PROPERTIES	CHEMISTRY	SECTION	METERS	GRAPHIC LITHOLOGY	DRILLING DISTURB.	SED. STRUCTURES	SAMPLES	LITHOLOGIC DESCRIPTION
LATE OLIGOCENE	*Globigerina ciperoensis* Zone (P22)	NP25 F/M				γ = 1.8-2.0		1 CC			○ ○		*	UNLITHIFIED PACKSTONE and UNLITHIFIED GRAINSTONE, very soupy and disturbed by drilling

UNLITHIFIED PACKSTONE, white (2.5Y 8/2), fine grained, composed of small clasts, foraminifers, bioclasts and skeletal fragments.

UNLITHIFIED GRAINSTONE, light gray (2.5Y 7/2), medium to coarse grained, composed of skeletal debris, foraminifers, intraclasts (up to 2 cm in size) composed of well-cemented LITHIFIED GRAINSTONE and chert.

SMEAR SLIDE SUMMARY (%):

	1,20 D
TEXTURE:	
Sand	40
Silt	30
Clay	30
COMPOSITION:	
Foraminifers	20
Nannofossils	5
Skeletal Fragments	10
Clasts	20
Sparitic Cement	5
Micrite	40

SITE 626 HOLE D CORE 28R CORED INTERVAL 1280.8-1290.3 mbsl; 437.3-446.8 mbsf

TIME-ROCK UNIT	BIOSTRAT. ZONE / FOSSIL CHARACTER: FORAMINIFERS	NANNOFOSSILS	RADIOLARIANS	DIATOMS	PALEOMAGNETICS	PHYSICAL PROPERTIES	CHEMISTRY	SECTION	METERS	GRAPHIC LITHOLOGY	DRILLING DISTURB.	SED. STRUCTURES	SAMPLES	LITHOLOGIC DESCRIPTION
		B				γ = 2.469		CC						Empty core liner; LITHIFIED GRAINSTONE in the CC

Two small (4-5 cm diameter) fragments of LITHIFIED GRAINSTONE, light gray (2.5Y 7/2), in the CC; well indurated planktonic foraminiferal GRAINSTONES, spar cement.

SITE 626 (HOLE A)

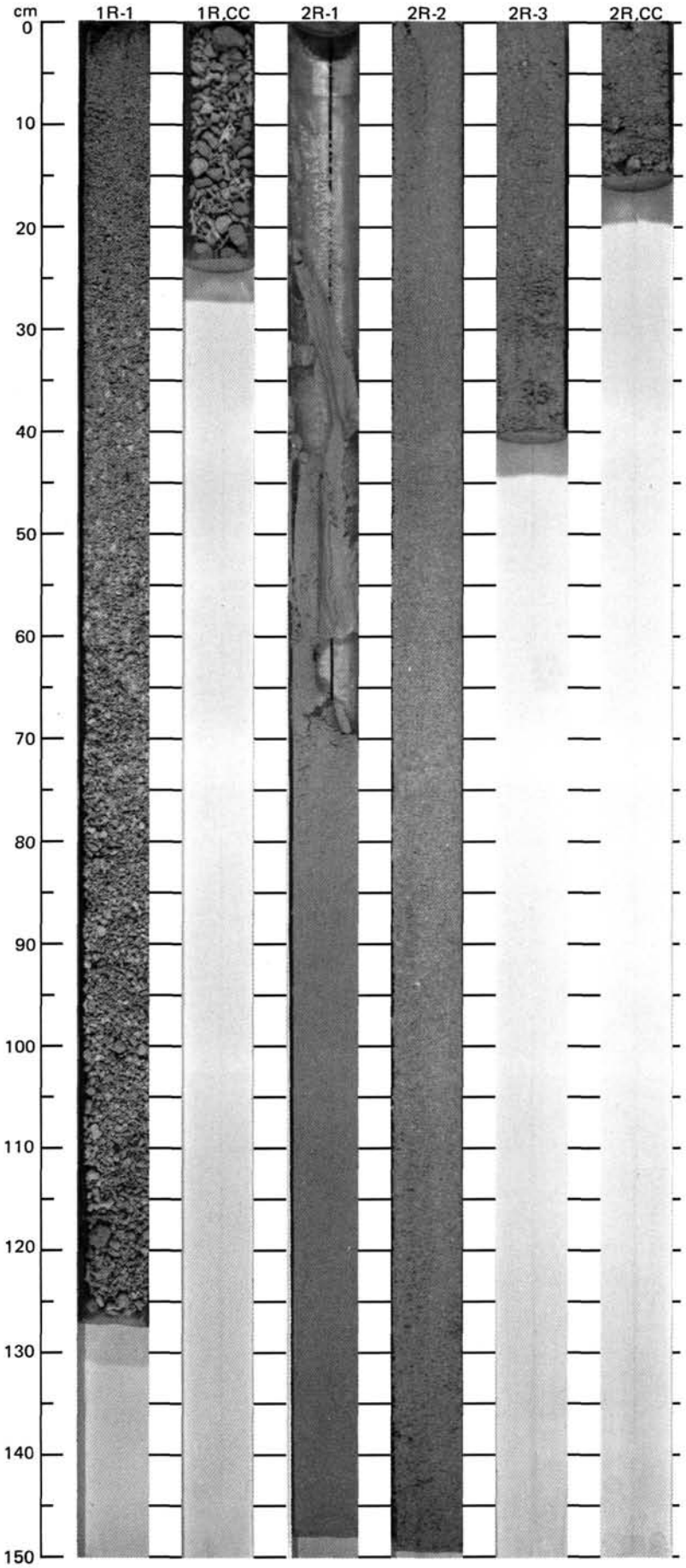

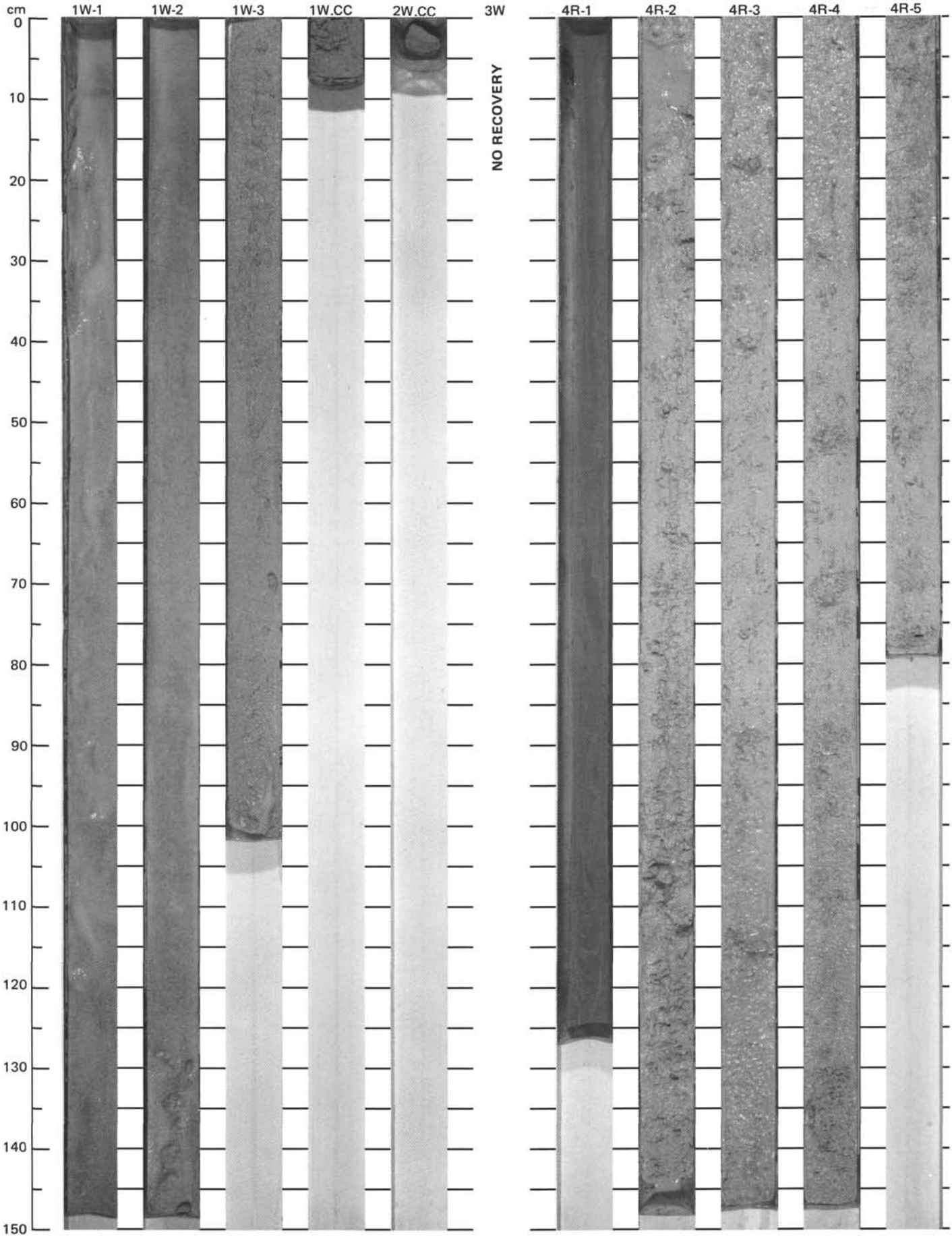
cm
1W-1
1W-2
1W-3
1W.CC
2W.CC
3W
NO RECOVERY
4R-1
4R-2
4R-3
4R-4
4R-5
0
10
20
30
40
50
60
70
80
90
100
110
120
130
140
150

SITE 626 (HOLE B)

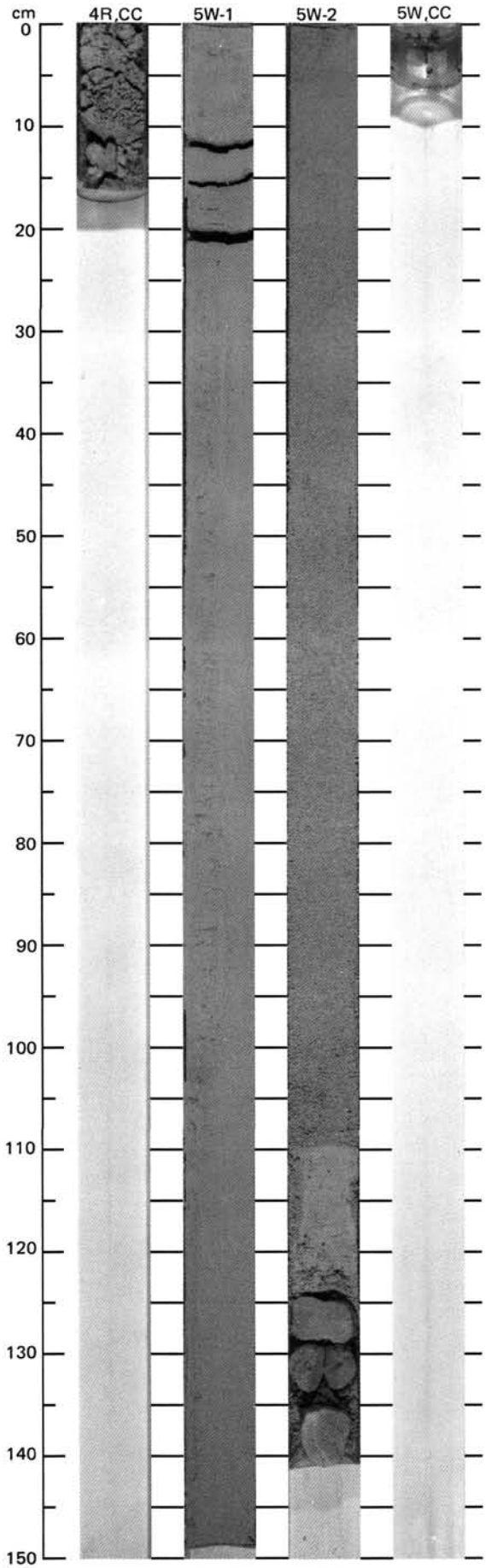

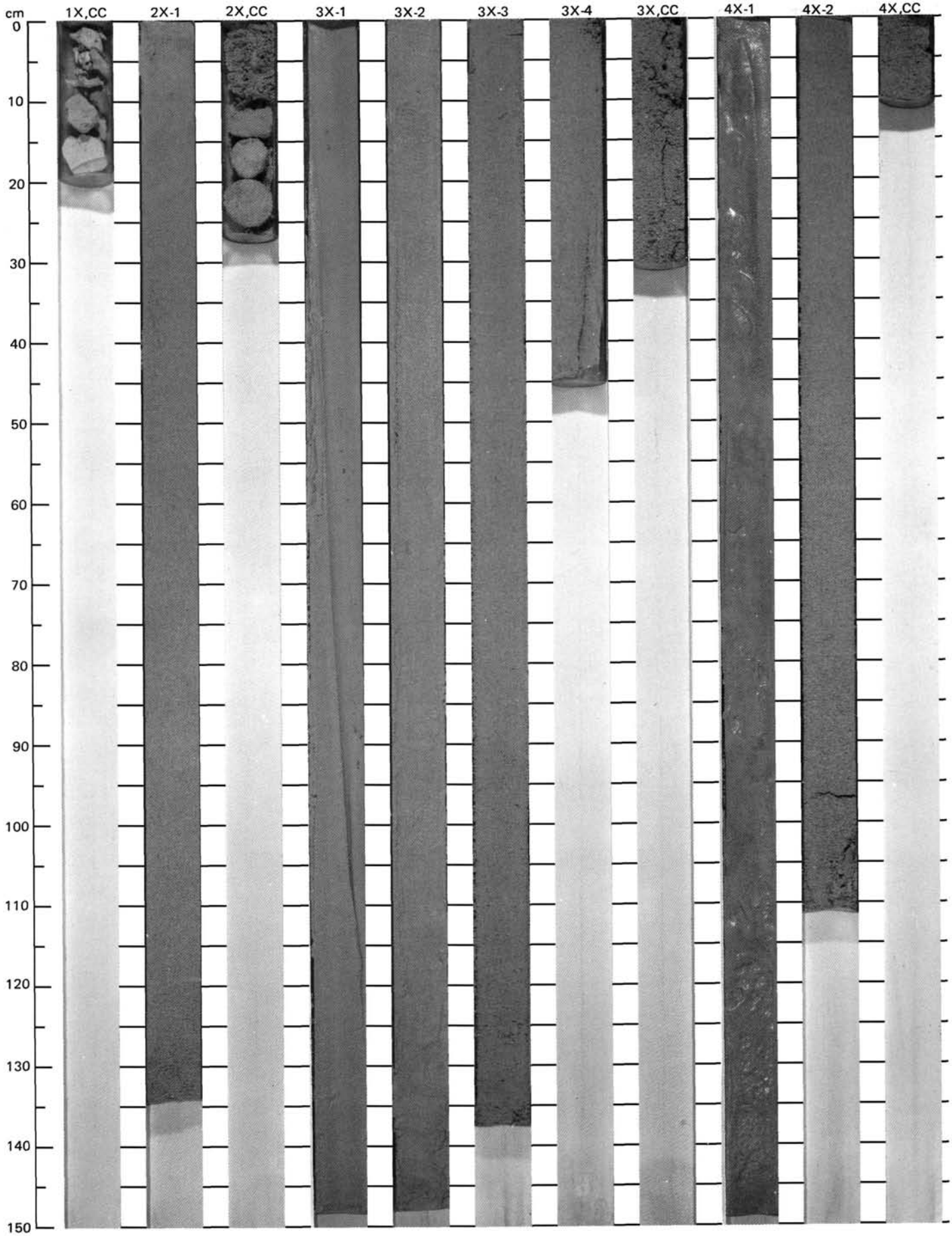
cm
1X,CC
2X-1
2X,CC
3X-1
3X-2
3X-3
3X-4
3X,CC
4X-1
4X-2
4X,CC
0
10
20
30
40
50
60
70
80
90
100
110
120
130
140
150

SITE 626 (HOLE C)

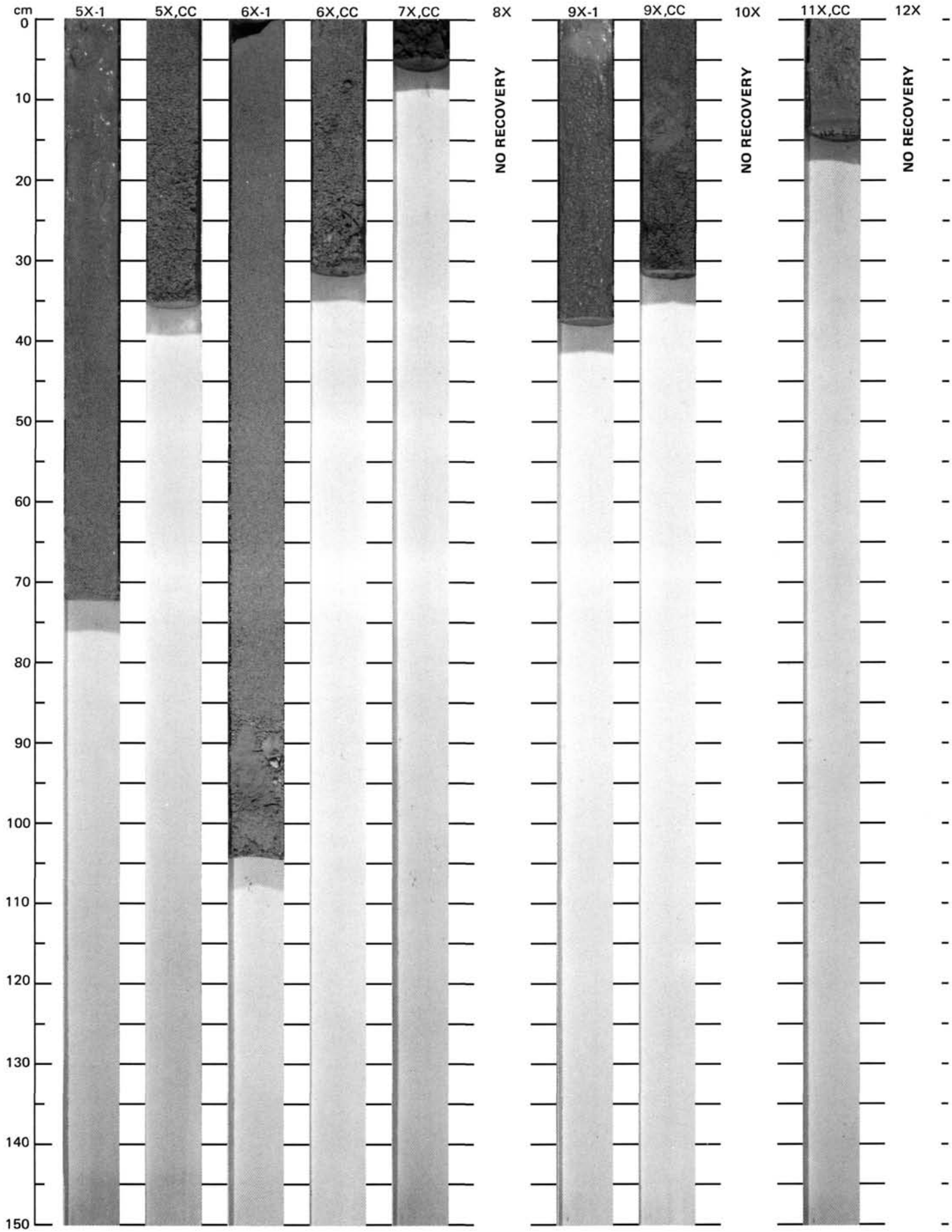

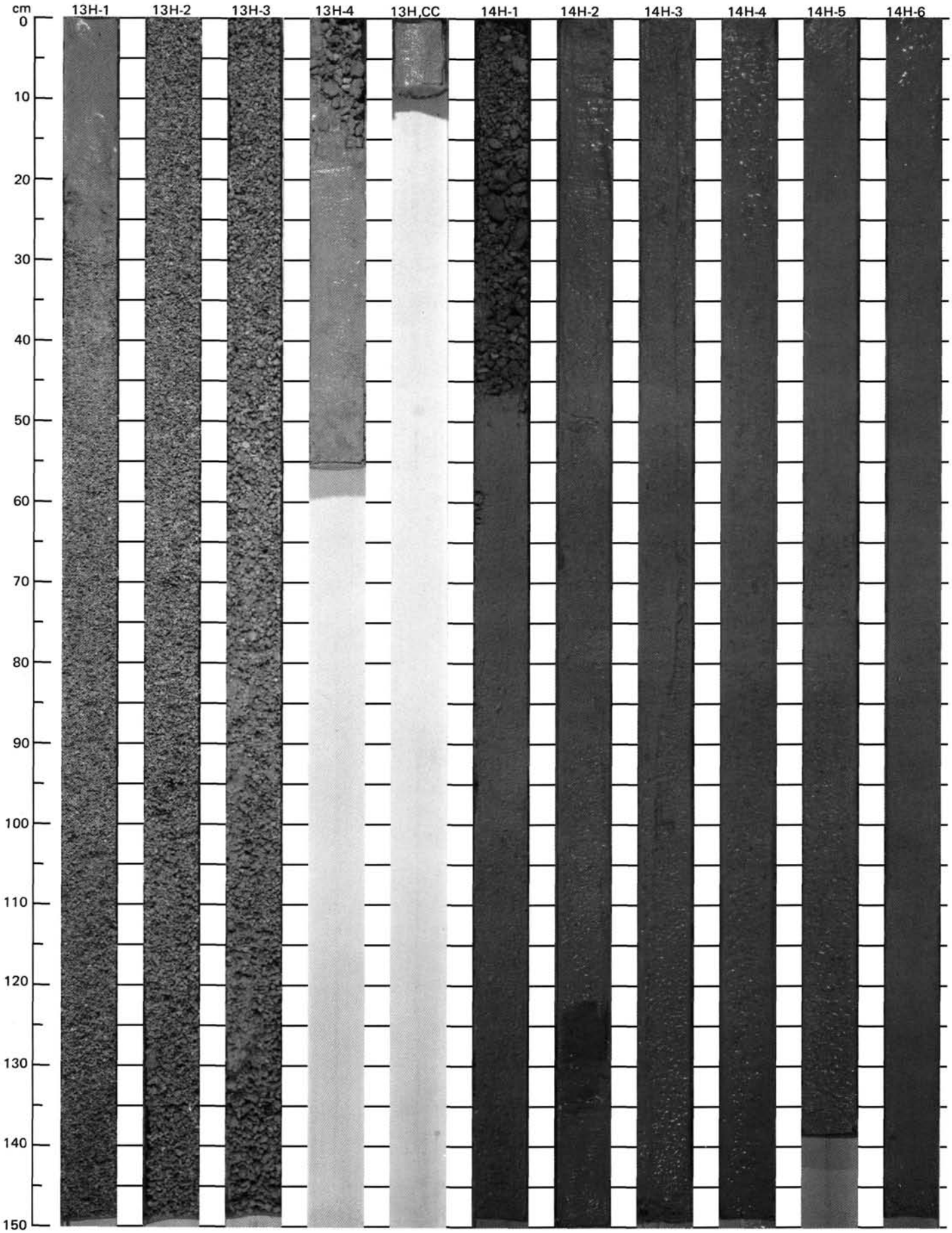
cm
13H-1
13H-2
13H-3
13H-4
13H,CC
14H-1
14H-2
14H-3
14H-4
14H-5
14H-6
0
10
20
30
40
50
60
70
80
90
100
110
120
130
140
150

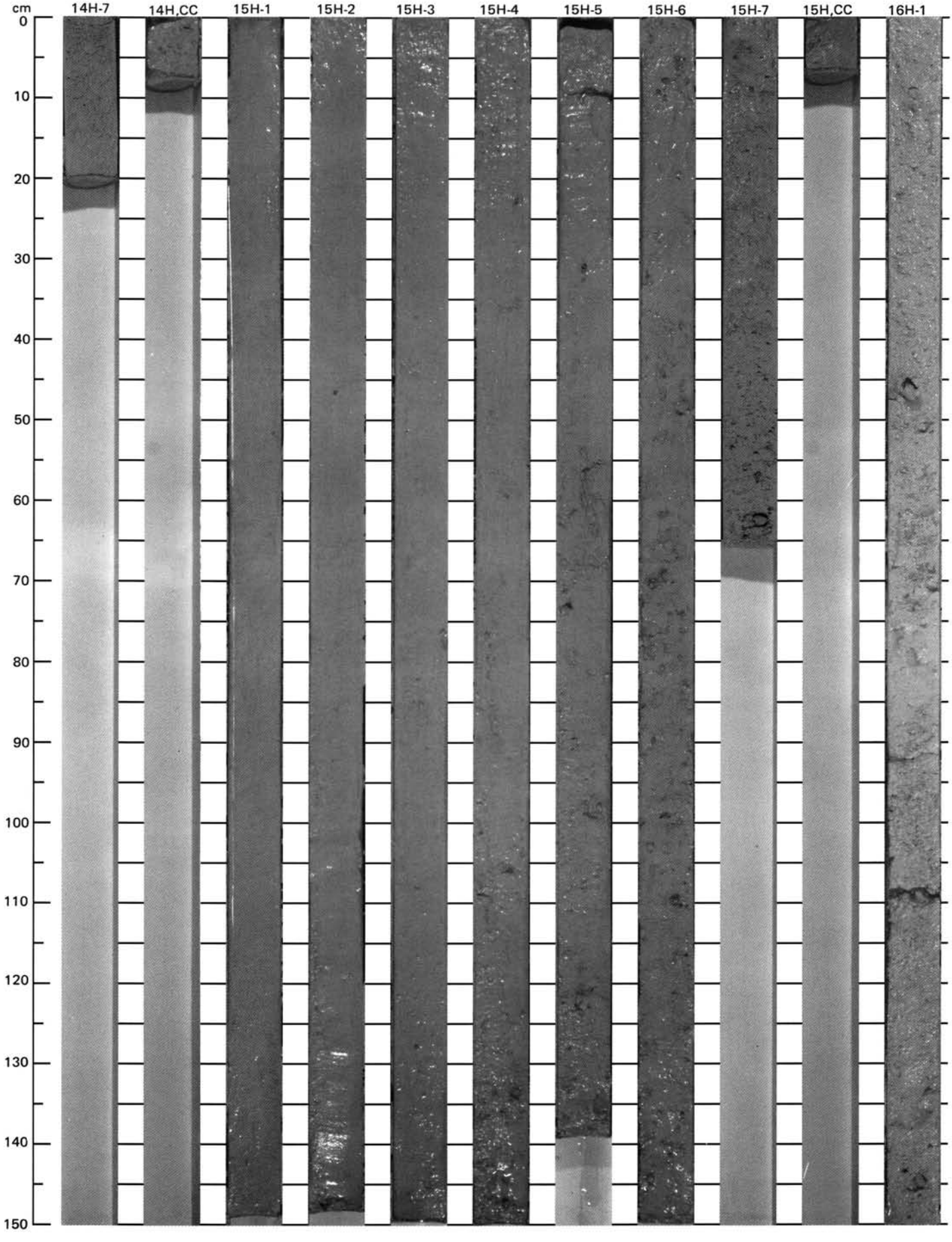
cm
14H-7
14H,CC
15H-1
15H-2
15H-3
15H-4
15H-5
15H-6
15H-7
15H,CC
16H-1
0
10
20
30
40
50
60
70
80
90
100
110
120
130
140
150

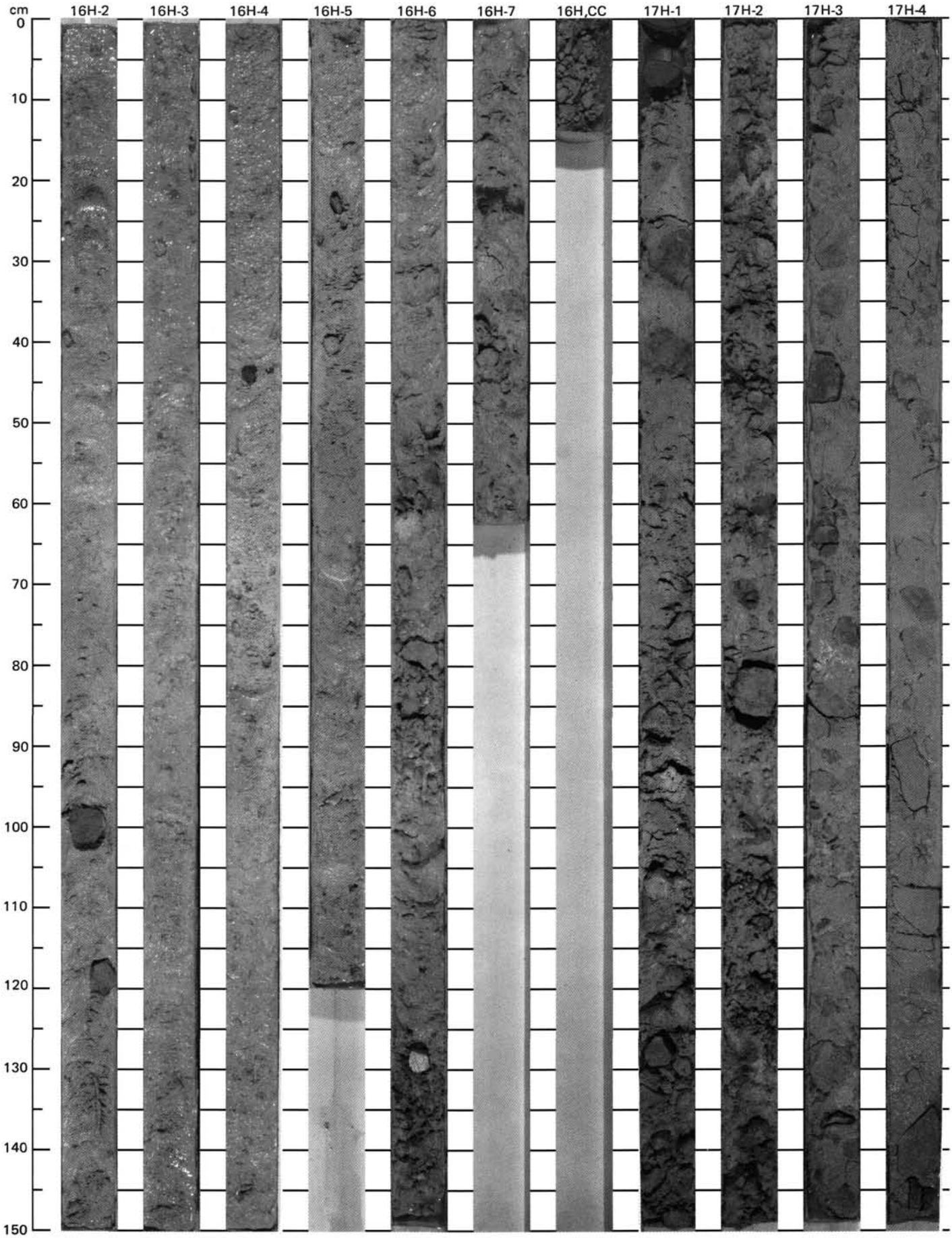
cm
16H-2
16H-3
16H-4
16H-5
16H-6
16H-7
16H,CC
17H-1
17H-2
17H-3
17H-4
0
10
20
30
40
50
60
70
80
90
100
110
120
130
140
150

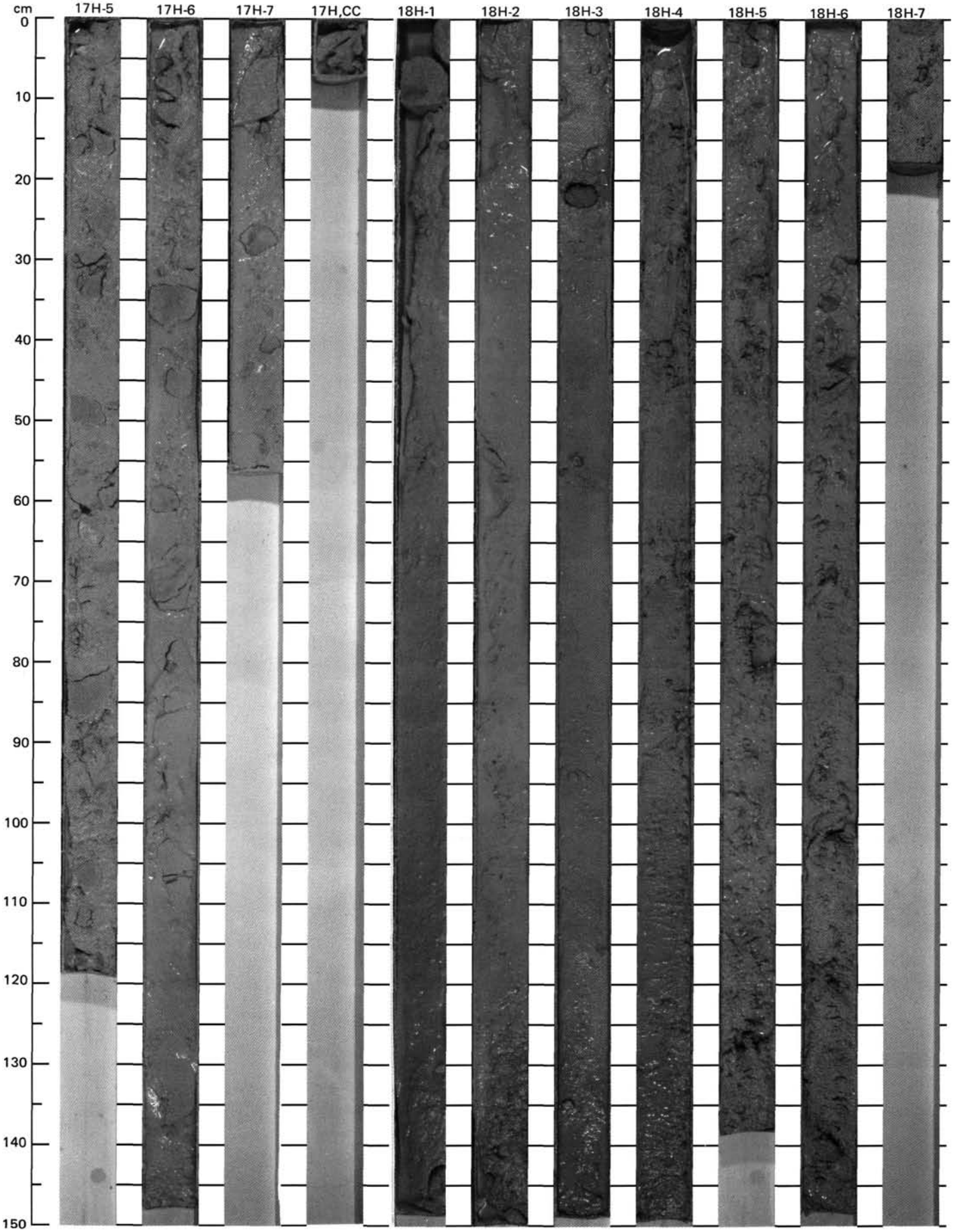
cm
17H-5
17H-6
17H-7
17H,CC
18H-1
18H-2
18H-3
18H-4
18H-5
18H-6
18H-7
0
10
20
30
40
50
60
70
80
90
100
110
120
130
140
150

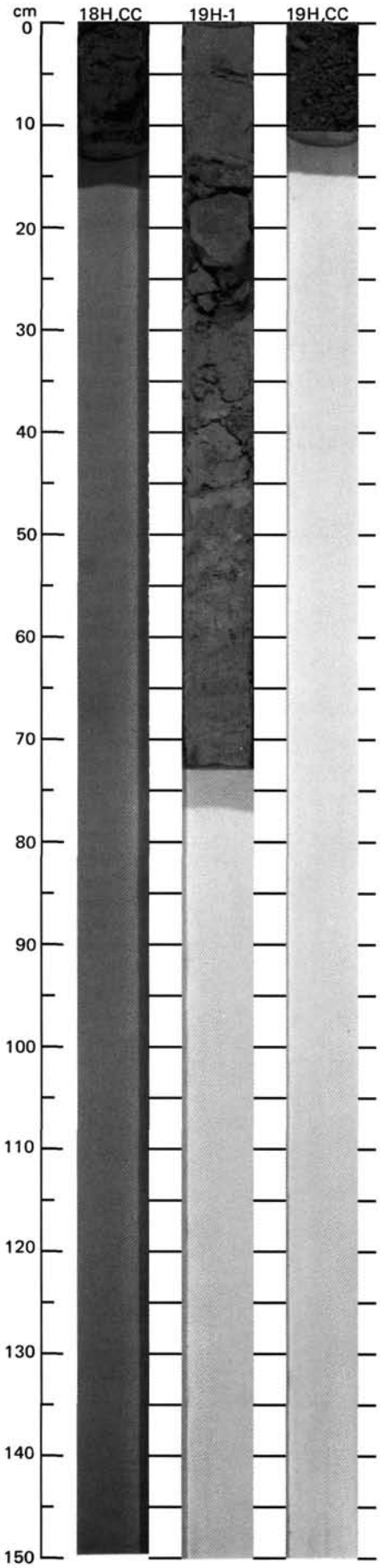
cm
18H,CC
19H-1
19H,CC
0
10
20
30
40
50
60
70
80
90
100
110
120
130
140
150

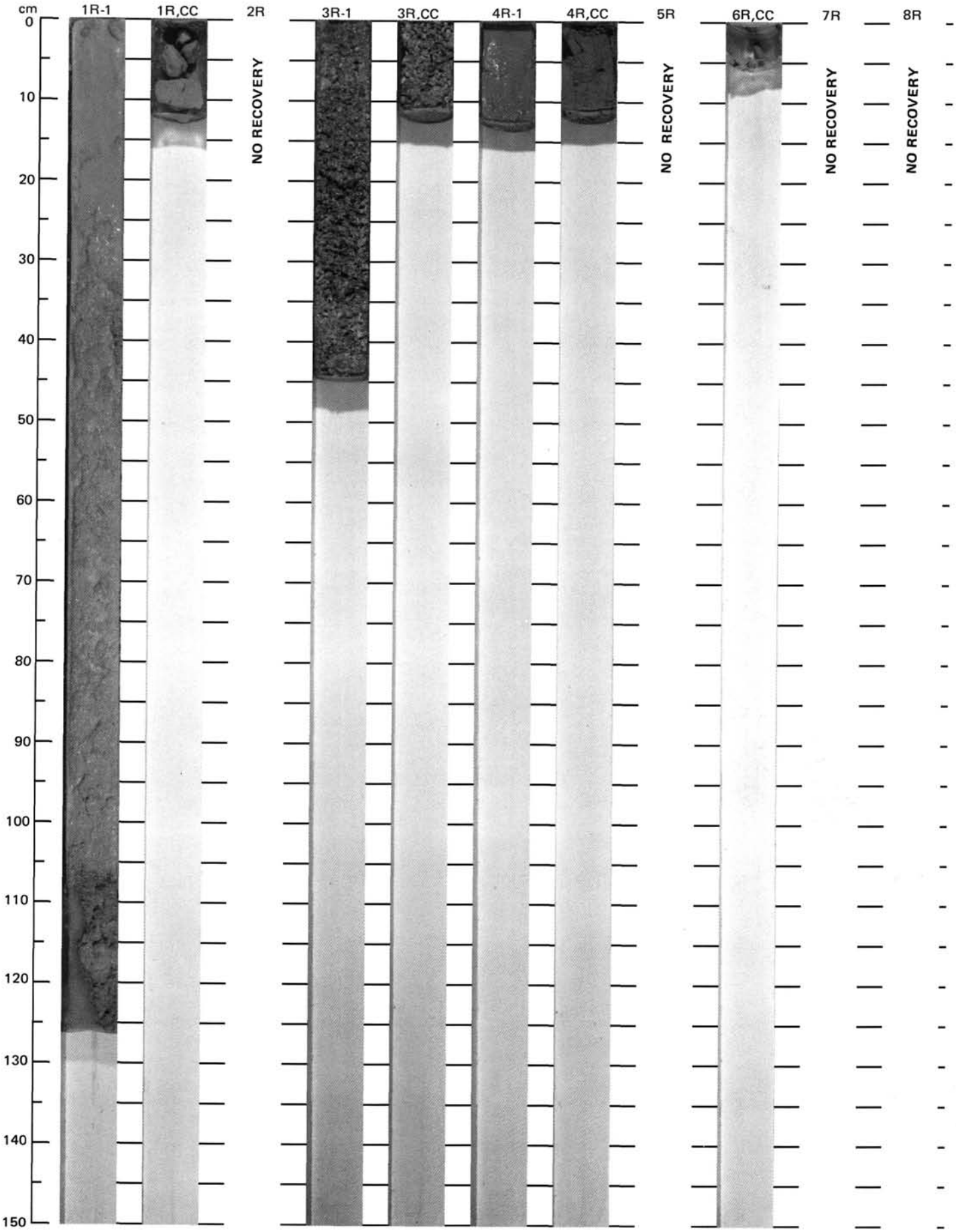
cm
0
10
20
30
40
50
60
70
80
90
100
110
120
130
140
150
1R-1
1R,CC
2R
NO RECOVERY
3R-1
3R,CC
4R-1
4R,CC
5R
NO RECOVERY
6R,CC
7R
NO RECOVERY
8R
NO RECOVERY

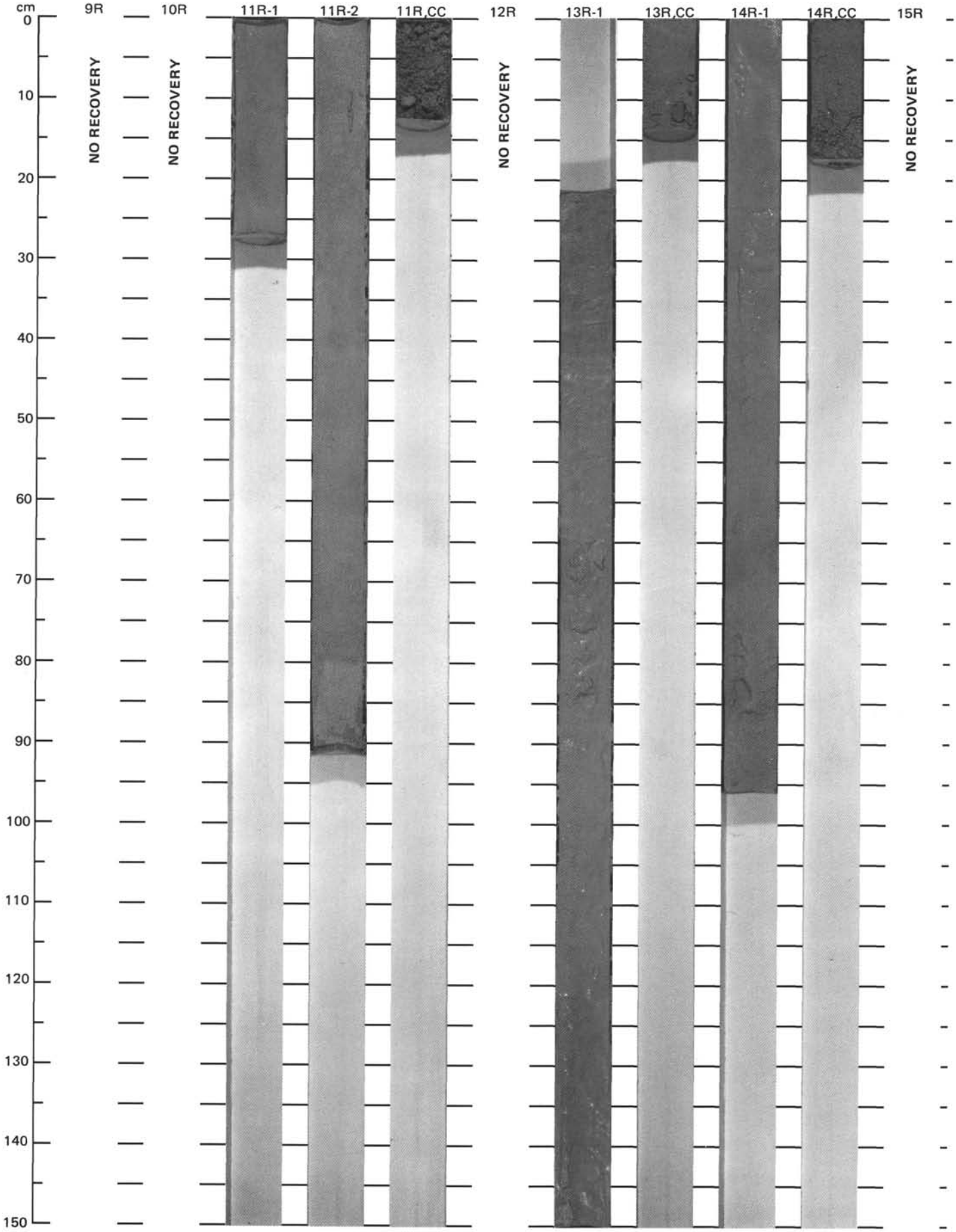
cm
0
10
20
30
40
50
60
70
80
90
100
110
120
130
140
150
9R
NO RECOVERY
10R
NO RECOVERY
11R-1
11R-2
11R,CC
12R
NO RECOVERY
13R-1
13R,CC
14R-1
14R,CC
15R
NO RECOVERY

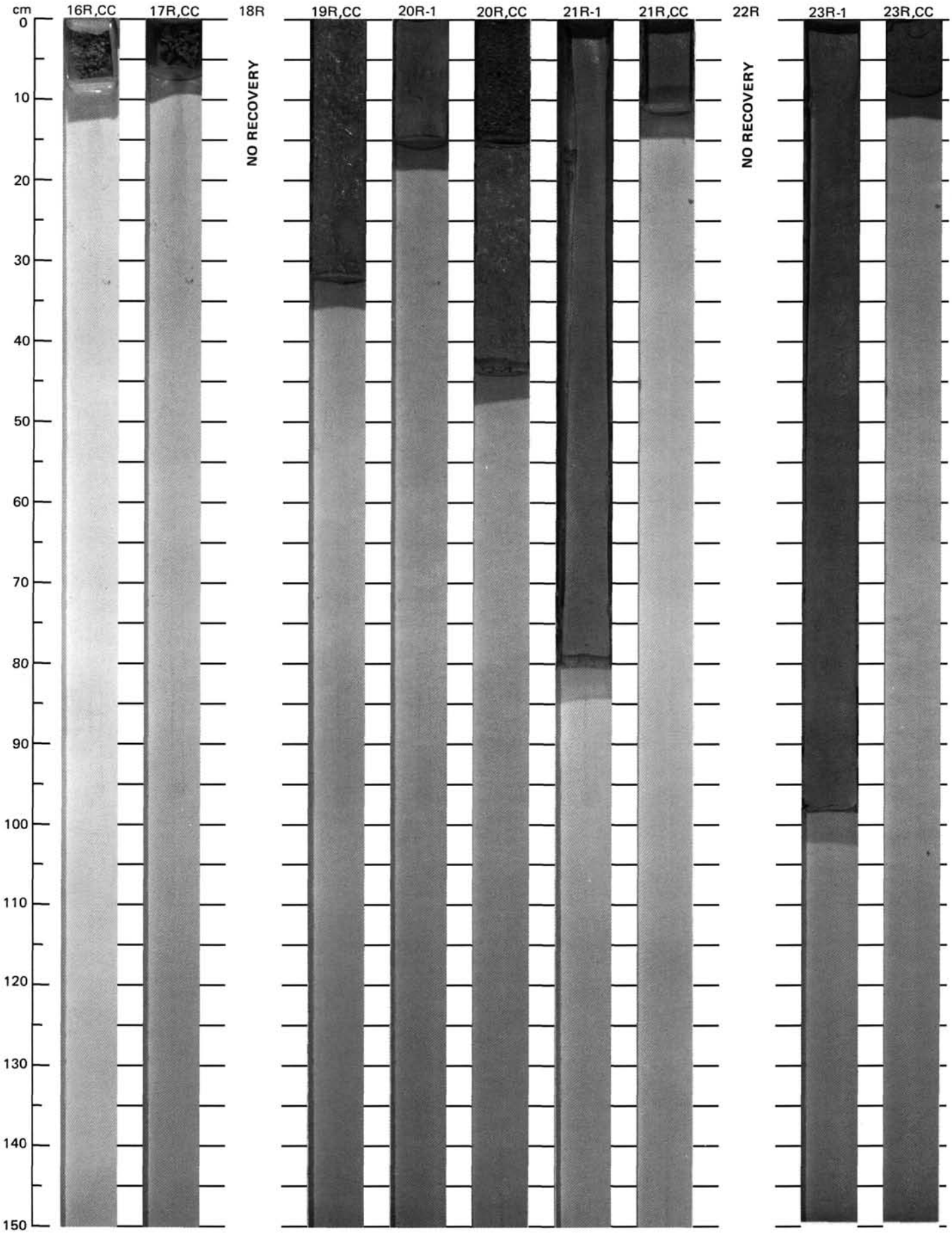
cm
16R,CC
17R,CC
18R
NO RECOVERY
19R,CC
20R-1
20R,CC
21R-1
21R,CC
22R
NO RECOVERY
23R-1
23R,CC
0
10
20
30
40
50
60
70
80
90
100
110
120
130
140
150

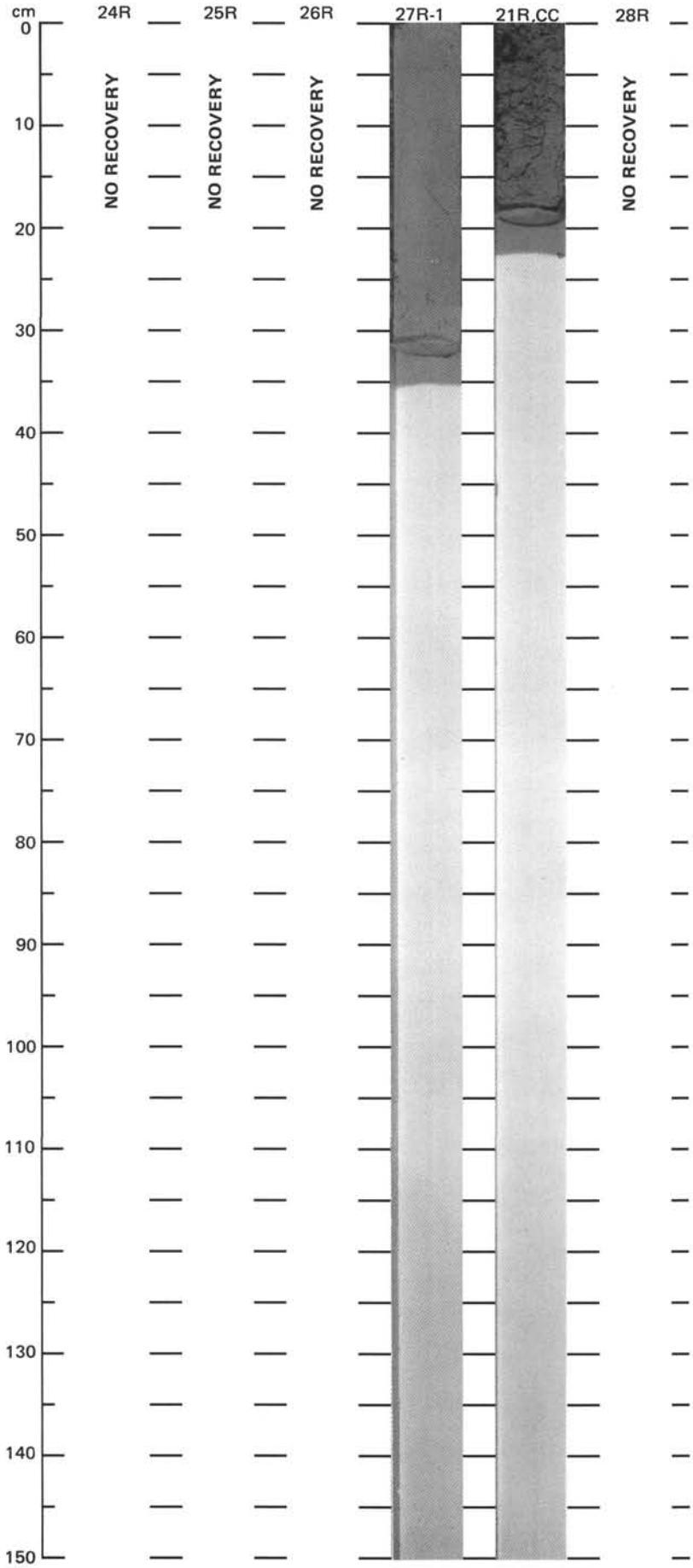
cm
24R
25R
26R
27R-1
21R,CC
28R
NO RECOVERY
NO RECOVERY
NO RECOVERY
NO RECOVERY
0
10
20
30
40
50
60
70
80
90
100
110
120
130
140
150